PETERSBURG NUCLEAR PHYSICS INSTITUTE
NAMED BY B.P. KONSTANTINOV
OF NATIONAL RESEARCH CENTER “KURCHATOV INSTITUTE”

50 YEARS

International Workshop

“Dzyaloshinskii-Moriya Interaction and Exotic Spin Structures”

Abstracts and programme

6–10 September 2021
Vyborg, Russia

DMI 2021 WORKSHOP

https://oiks.pnpi.spb.ru/events/DMI-2021

International Workshop

Dzyaloshinskii-Moriya Interaction and Exotic Spin Structures

TOPICS

* Monoaxial chiral helimagnets.
* DMI effect on the magnetic structure.
* Exotic spin structures (skyrmions, etc.).
* Topological defects and spintronics.
* Spin excitations in helimagnets.
* Frustrated magnetic systems.
* Thin films and surface effects.
* Chirality in optics, acoustics and magnetoacoustics.
* DMI in molecular magnets.
* Magnetism and polarized neutron scattering (Maleyev's approach to science).

Organizers

Petersburg Nuclear Physics Institute named by B.P. Konstantinov of National Research Center "Kurchatov Institute" (NRC «Kurchatov Institute» - PNPI) http://www.pnpi.nrcki.ru/

Russian Neutron scattering Society (ROSNEUTRO) http://rosneutro.ru/

Scientific Committee

Co-Chairman: **Vladimir Voronin** (NRC «Kurchatov Institute» - Petersburg Nuclear Physics Institute, Gatchina, Russia)

Co-Chairman: **Jun-ichiro Kishine** (The Open University of Japan, Chiba, Japan)

Dmitry Aristov (NRC «Kurchatov Institute» - Petersburg Nuclear Physics Institute, Gatchina, Russia)

Javier Campo (Faculty of Sciences, University of Zaragoza, Zaragoza, Spain)

Nadezhda Chubova (NRC «Kurchatov Institute», Moscow, Russia)

Vladimir Dmitrienko (Institute of Crystallography RAS, Moscow, Russia)

Vyacheslav Em (NRC «Kurchatov Institute», Moscow, Russia)

Markus Garst (Institute of Theoretical Solid State Physics, Karlsruhe, Germany)

Igor Golosovsky (NRC «Kurchatov Institute» - Petersburg Nuclear Physics Institute, Gatchina, Russia)

Christopher Marrows (School of Physics and Astronomy, University of Leeds, Leeds, UK)

Stephen McVitie (School of Physics and Astronomy, University of Glasgow, Glasgow,UK)

Theodore Monchesky (Department of Physics and Atmospheric Science, Dalhousie University, Halifax, Nova Scotia, Canada)

Alexander Ovchinnikov (Ural State University, Ekaterinburg, Russia)

Catherine Pappas (Delft University of Technology, Delft, The Netherlands)

Ulrich Rossler (Leibniz Institute for Solid State and Materials Research, Dresden, Germany)

Arseny Syromyatnikov (NRC «Kurchatov Institute» - Petersburg Nuclear Physics Institute, Gatchina, Russia)

Yoshihiko Togawa (Osaka University, Osaka, Japan)

Oleg Utesov (NRC «Kurchatov Institute» - Petersburg Nuclear Physics Institute, Gatchina, Russia)

Andrey Yashenkin (NRC «Kurchatov Institute» - Petersburg Nuclear Physics Institute, Gatchina, Russia)

Organizing Committee

NRC «Kurchatov Institute» - Petersburg Nuclear Physics Institute, Gatchina, Russia

Co-Chairperson: **Elena Likholetova**

Co-Chairman: **Vladimir Voronin**

Technical support: **Ekaterina Utkina**, **Kirill Pshenichnyi**

Financial support: **Svetlana Smelyagina**, **Irina Vlasova**, **Olga Travina**, **Natalia Kuga**

Public relations: **Natalia Bush**

Visa support: **Natalia Nikitina**, **Rimma Zheronkina**

Contact

E-mail: rno-secretary@lns.pnpi.spb.ru

https://oiks.pnpi.spb.ru/events/DMI-2021

PROGRAMME

*Moscow time UTC+3:00

Monday. 6 September 2021		
12.00 - 13.00	**Check in**	
13.00 - 14.00	**Lunch**	
14:00 - 14.15	**Opening ceremony**	
Session 1: Magnetism and polarized neutron scattering (In memory of Sergey Maleyev). Chair: Andrey G. Yashenkin		
14.15 - 14.45	**Dmitry N. Aristov** NRC KI - PNPI, Gatchina, Russia	Dynamics of the skyrmion crystal in the stereographic projection method.
14.45 - 15.15	**Vladimir P. Mineev** L.D. Landau Institute for Theoretical Physics RAS, Chernogolovka, Russia	Piezomagnetism in ferromagnetic superconductors.
15.15 - 15.45	**Arseny V. Syromyatnikov** NRC KI - PNPI, Gatchina, Russia	New short-wavelength spin excitations in triangular antiferromagnets.
15.45 - 16.15	**Coffee break**	
16.15 - 16.40	**Igor A. Zobkalo** NRC KI - PNPI, Gatchina, Russia	Unexpected discovery of a new way to control DM interaction.
16.40 - 17.10	**Alexandre Ivanov** Institut Laue-Langevin, Grenoble, France	Pseudodipolar interactions in antiferromagnetic relatives of electron doped cuprate superconductors.
17.10 - 17.35	**Catherine Pappas** Delft University of Technology, Delft, The Netherlands	Helimagnetic correlations close to the Quantum Critical Points of MnSi under mechanical and chemical pressure.
17.35 - 18.00	**Sergey V. Grigoryev** NRC KI - PNPI, Gatchina, Russia	Critical fluctuations beyond the quantum phase transition in Dzyaloshinskii-Moriya helimagnets $Mn_{1-x}Fe_xSi$.
18.30	**Film about Sergey Maleyev**	
19.00 - 22.00	**Welcome Party**	

Tuesday. 7 September 2021		
Session 2: Monoaxial chiral helimagnets. Chair: Alexander S. Ovchinnikov		
09.30 - 10.00	**Jun-ichiro Kishine** The Open University of Japan, Chiba, Japan	Chirality-induced phonon dispersion in a noncentrosymmetric micropolar crystal.
10.00 - 10.30	**Yoshihiko Togawa** Osaka Prefecture University, Osaka, Japan	Spin selection effect in $CrNbS_2$.
10.30 - 11.00	**Alexander S. Ovchinnikov** Ural Federal University, Ekaterinburg, Russia	Magnetic response of a highly nonlinear soliton lattice in a monoaxial chiral helimagnet.
11.00 - 11.30	**Coffee break**	
11.30 - 12.00	**Alexey A. Tereshchenko** Ural Federal University, Ekaterinburg, Russia	Investigation of a deformation of the magnetic soliton lattice under tensile stress by lorentz electron microscopy.
12.00 - 12.30	**Vladimir E. Sinitsyn** Ural Federal University, Ekaterinburg, Russia	Discrete magnetic breathers in monoaxial chiral helimagnet.
13.00 - 14.00	**Lunch**	
14.00 - 17.00	**Excursion through the downtown Vyborg**	
Wednesday. 8 September 2021		
Session 3: DMI effect on the magnetic structure: part I. Chair: Evgeny V. Altynbaev		
09.30 - 10.00	**Viacheslav A. Chizhikov** A.V. Shubnikov Institute of Crystallography RAS, Moscow, Russia	Anisotropy of the magnetic phases of cubic helimagnets.
10.00 - 10.30	**Vladimir A. Sidorov** Vereshchagin Institute of High Pressure Physics RAS, Troitsk, Moscow, Russia	New high-entropy alloys with cubic non-centrosymmetric B20 structure: high-pressure synthesis, magnetic properties and ab-initio calculations.

10.30 - 10.45	**Denis Salamatin** Vereshchagin Institute of High Pressure Physics RAS, Troitsk, Moscow, Russia	Pressure influence on the valence and magnetic state of Yb in noncentrosymmetric heavy-fermion $YbNiC_2$.
10.45 - 11.00	**Ravil A. Sadykov** Institute For Nuclear Research RAS, Troitsk, Moscow, Russia	Nonmagnetic high pressure clamp cell for neutron scattering.
11.00 - 11.30	**Coffee break**	
11.30 - 12.00	**Javier Campo** Instituto de Ciencia de Materiales de Aragón – Universidad de Zaragoza, Zaragoza, Spain	A new magnetic intermediate state, “B-Phase”, in MnSi probed by small-angle neutron scattering and muon spin rotation.
12.00 - 12.20	**Vladimir Krasnorussky** Vereshchagin Institute of High Pressure Physics RAS, Troitsk, Moscow, Russia	Magnetization of MnSi in small fields: magnetic helixes rotation study.
12.20 - 12.40	**Daria O. Skanchenko** NRC KI - PNPI, Gatchina, Russia	Split of the magnetic and crystallographic states in $Fe_{1-x}Rh_xGe$.
13.00 - 14.00	**Lunch**	
Session 3: DMI effect on the magnetic structure: part II. Chair: Viacheslav A. Chizhikov		
14:00 - 14.30	**Alexander S. Moskvin** Ural Federal University, Ekaterinburg, Russia	Dzyaloshinskii's interaction and exchange-relativistic effects in orthoferrites.
14.30 - 15.00	**Igor V. Golosovsky** NRC KI - PNPI, Gatchina, Russia	Detection of weak distortions of the magnetic structure due to the Dzyaloshinsky-Moriya interaction in multiferroics-ferroborates revealed by the single-crystal neutron diffraction.
15.00 - 15.30	**Mikhail A. Semkin** M. N. Miheev Institute of Metal Physics Ural Branch of RAS, Ekaterinburg, Russia	Magnetic structures of $LiNi_{1-x}Co_xPO_4$ solid state.

15.30 - 16.00	**Coffee break**	
Session 4: Spin excitations in helimagnets. Chair: Dmitry N. Aristov		
16.00 - 16.30	**Alexander I. Smirnov** Kapitza Institute for Physical Problems, RAS, Moscow, Russia	Electron spin resonance of an interacting spinon liquid with uniform Dzyaloshinski-Moriya interaction.
16.30 - 17.00	**Markus Garst** Karlsruhe Institute of Technology, Karlsruhe, Germany	Spin waves of the conical helix in cubic chiral magnets.
17.00 - 17.15	**Kirill A. Pshenichnyi** NRC KI - PNPI, Gatchina, Russia	Non-trivial temperature variation of spin wave dynamics in $Co_8Zn_8Mn_4$.
17.15 - 17.45	**Sebastian Bustingorry** Instituto de Nanociencia y Nanotecnología, CNEA-CONICET, Centro Atómico Bariloche, Bariloche, Argentina	Dynamics of chiral solitons driven by polarized currents.
Thursday. 9 September 2021		
Session 5: Exotic spin structures (skyrmions, etc.): part I. Chair: Dmitry N. Aristov		
09.30 - 10.00	**Oleg I. Utesov** NRC KI - PNPI, Gatchina, Russia	Mean-field approach for square skyrmion lattice in centrosymmetric tetragonal magnets.
10.00 - 10.30	**Max Hirschberger** The University of Tokyo, Tokyo, Japan; RIKEN CEMS, Wako, Japan	Spirals and skyrmions in magnets and their emergent electromagnetism.
10.30 - 11.00	**Jan Masell** The University of Tokyo, Tokyo, Japan; RIKEN CEMS, Wako, Japan	Helitronics and (anti-)skyrmions in magnets with DMI.
11.00 - 11.30	**Coffee break**	
11.30 - 12.30	**On-line Poster Session**	

13.00 - 14.00	**Lunch**	
Session 5: Exotic spin structures (skyrmions, etc.): part II. Chair: Oleg I. Utesov		
14.00 - 14.30	**Victor Laliena** Instituto de Ciencia de Materiales de Aragón – Universidad de Zaragoza, Zaragoza, Spain	Magnonic goos-hänchen effect induced by one dimensional solitons.
14.30 - 14.50	**Evgeny V. Altynbaev** NRC KI - PNPI, Gatchina, Russia	Evolution of the skyrmion lattice in MnGe-based compounds under high pressure
14.50 - 15.10	**Victor A. Ukleev** Paul Scherrer Institute, Canton Aargau, Switzerland	Frustration-driven magnetic fluctuations as the origin of the low-temperature skyrmion phase in $Co_7Zn_7Mn_6$.
15.10 - 15.30	**Viktor E. Timofeev** NRC KI - PNPI, Gatchina, Russia; St. Petersburg Electrotechnical University “LETI”, St. Petersburg, Russia	Triple helix versus skyrmion lattice in two-dimensional noncentrosymmetric magnets.
15.30 - 16.00	**Coffee break**	
16.00 - 16.20	**Sergii Grytsiuk** Forschungszentrum Jülich, Germany	Spin spiral twist caused by Dzyaloshinskii-Moriya Interaction in B20 chiral magnets.
16.20 - 16.40	**Sebastian Diaz** University of Duisburg-Essen, Duisburg, Germany	Majorana bound states induced by antiferromagnetic skyrmion textures.
16.40 - 17.00	**Santiago Antonio Osorio** Instituto de Nanociencia y Nanotecnología, CNEA-CONICET, Centro Atómico Bariloche, Bariloche, Argentina	Metastability and creation of single chiral soliton states in monoaxial helimagnets.
17.00 - 17.30	**Vladimir E. Dmitrienko** A.V. Shubnikov Institute of Crystallography RAS, Moscow, Russia	Exotic spin structure in the pseudogap phase of high-T_c superconductor $HgBa_2CuO_4$.

17.30 - 18.00	**Andre Cano** Université Grenoble Alpes, Grenoble, France	Nickelate superconductors: an ongoing dialog between theory and experiments.
Friday. 10 September 2021		
Session 6: Thin films and surface effects. Chair: Igor V. Golosovsky		
09.30 - 10.00	**Giovanni Carlotti** University of Perugia, Perugia, Italy	Spin waves non reciprocity in magnetic ultrathin films, magnonic crystals and nanostructures as a tool to quantify interfacial Dzyaloshinskii-Moriya interaction.
10.00 - 10.20	**Dmitry A. Tatarskiy** Institute for physics of microstructures RAS, Nizhny Novgorod, Russia	Effect of interfacial Dzyaloshinskii-Moriya interaction on polarized neutrons reflection.
10.20 - 10.40	**Maxim V. Sapozhnikov** Institute for physics of microstructures RAS, Nizhny Novgorod, Russia	Direct observation of topological Hall effect in Co/Pt nanostructured films.
10.40 - 11.00	**Oleg G. Udalov** Institute for physics of microstructures RAS, Nizhny Novgorod, Russia	Control of DMI with strain in artificial multilayer structures.
11.00 - 11.30	**Alexander P. Pyatakov** M.V. Lomonosov Moscow State University, Moscow, Russia	Dzyaloshinskii-Moria interaction in multiferroic and magnetoelectric materials: the cases of $BiFeO_3$, magnetic films and interfaces.
11.30 - 12.00	**Coffee break**	
Session 7: DMI in molecular magnets. Chair: Igor A. Zobkalo		
12.00 - 12.30	**Alexey I. Aleksandrov** Institute of Synthetic Polymeric Materials named after N.S. Enikolopov RAS, Moscow, Russia	Multiferroics - polymer composites based on organometallic dimers with the Dzyaloshinsky-Moria effect.

12.30 - 12.45	**Oksana V. Koplak** Institute of Problems of Chemical Physics of RAS, Moscow, Russia	Time resolved FORC analysis and magnetic anisotropy in molecular based magnets.
12.45 - 13.15	**Dmitry A. Pshenay-Severin** Ioffe Institute, St. Petersburg, Russia	Effect of deformation on topological properties of cobalt monosilicide.
13.15 - 13.30	**Concluding session**	
13.30 - 14.30	**Lunch**	
14.30 - 15.00	**Check out from the hotel**	

On-line poster session	
Alexey I. Aleksandrov Institute of Synthetic Polymeric Materials named after N.S. Enikolopov RAS, Moscow, Russia	Radio-frequency superradiance upon mechanical activation of polymer composites based on organometallic dimers with the Dzyaloshinsky-Moria effect.
Vladimir D. Bessonov M. N. Miheev Institute of Metal Physics Ural Branch of RAS, Ekaterinburg, Russia	Brillouin spectroscopy of the interfacial Dzyaloshinskii–Moriya interactions in alloy embedded Pt-Co nanostructures.
Alexander V. Bokov Vereshchagin Institute of High Pressure Physics RAS, Troitsk, Moscow, Russia	Study of positron annihilation lifetime in non-symmetric monosilicides (B20) by ^{48}V source.
Nikolay M. Chtchelkatchev Vereshchagin Institute of High Pressure Physics RAS, Troitsk, Moscow, Russia	On an ab initio theory of the temperature dependence of hyperfine quadrupole interaction in metals: application to hexagonal Zn and Cd.
Marta Crisanti Delft University of Technology, Delft, The Netherlands	Position Dependent Stability and Metastability of the Skyrmion state in Ni substituted Cu_2OSeO_3.
Vasiliy N. Glazkov P.Kapitza Institute for Physical Problems RAS, Moscow, Russia	Anisotropy-induced soliton excitation in magnetized strong-rung spin ladders.
Kyosuke Ishito Tokyo Institute of Technology, Tokyo, Japan	Chiral phonons in helical single crystal Te by circularly polarized Raman spectroscopy.
Hiroshi Katsumoto Forschungszentrum Jülich, Jülich, Germany	Revisit of Dzyaloshinskii-Moriya interaction with symmetry.

Shizeng Lin Los Alamos National Laboratory, Washington, USA	Topological spin texture in centrosymmetric magnets.
Maria V. Magnitskaya Vereshchagin Institute of High Pressure Physics RAS, Troitsk, Moscow, Russia	The magnetic and electronic properties of the $FeRhGe_2$ compound (B20).
Olga V. Nemytova M. N. Miheev Institute of Metal Physics Ural Branch of RAS, Ekaterinburg, Russia	Magnetic Properties of Frustrated Ytterbium and Holmium Rare Earth Titanates Doped With Yttrium and Bismuth.
Shun Okumura The University of Tokyo, Tokyo, Japan	Magnetic hedgehog lattice in a centrosymmetric cubic metal.
Miguel Pardo Instituto de Nanociencia y Materiales de Aragón, CSIC-Universidad de Zaragoza, Zaragoza, Spain	Incommensurate magnetic phases of the multiferroic compound $MnCr2O_4$ described with the superspace formalism.
Md. Abu Jafar Pikul Khulna University, Khulna, Bangladesh	Fast magnetization reversal of a magnetic nanoparticle driven by a down-chirp microwave field pulse at finite temperature.
Alexander Sadovnikov Saratov State University, Saratov, Russia	Spin wave propagation in strain mediated magnonic waveguides.
Yusuke Shimamoto Osaka Prefecture University, Sakai, Osaka, Japan	Observation of phonon modes in a chiral spin soliton lattice.
Kotaro Shimizu The University of Tokyo, Tokyo, Japan	Phase degree of freedom in multiple-Q topological spin textures.

Hiroaki Shishido Osaka Prefecture University, Sakai, Osaka, Japan	Thin film growth of a chiral magnet $YbNi_3Al_9$.
Sergey V. Solovyov Moscow Institute of Physics and Technology, Moscow, Russia	Sperimagnetic phase transitions in ferrimagnetic amorphous alloy GdFeCo.
Filipp Timkovskii NRC KI - PNPI, Gatchina, Russia	Antiferromagnets with random vacancies and substitutional spins on triangular lattice.
Hirosawa Tomoki University of Basel, Basel, Switzerland	Magnonic quadrupole topological insulator in antiskyrmion crystals.
Anatoly V. Tsvyaschenko Vereshchagin Institute of High Pressure Physics RAS, Troitsk, Moscow, Russia	Low-temperature transition in non-centrosymmetric CoGe: the influence of the quadrupole transition on the occurrence of an incommensurate phase.
Oleg I. Utesov NRC KI - PNPI, Gatchina, Russia	Phase competition in anisotropic frustrated antiferromagnets.

SESSION 1. MAGNETISM AND POLARIZED NEUTRON SCATTERING (IN MEMORY OF SERGEY MALEYEV).

Dynamics of the skyrmion crystal in the stereographic projection method

V. Timofeev[1,2], D. Aristov[1,3]

[1] *Konstantinov Petersburg Nuclear Physics Institute of National Research Centre «Kurchatov Institute», Gatchina, Russia*
[2] *Saint-Petersburg Electrotechnical University LETI, Saint-Petersburg, Russia*
[3] *Saint-Petersburg State University, Saint Petersburg, Russia*

Corresponding Author's Email: aristov@thd.pnpi.spb.ru

Dzyaloshinskii-Moriya interaction (DMI) is the key ingredient for obtaining topologically non-trivial magnetization configurations in ordered magnets. One such configuration, the skyrmion crystal, is a regular ordering of magnetic knots. [1] The magnetic dynamics of this structure is rather unusual and is described by a number of bands in the appearing magnetic superlattice. [2]

We study the basic model of the SkX appearing in 2D system with ferromagnetic exchange, DMI and uniform magnetic field, *B*, perpendicular to the plane. We employ the stereographic projection method in the continuum model, describing the fluctuating magnetization vector in terms of complex-valued field. The static SkX configuration is modeled by a sum of the fields, referred to individual skyrmions on the triangular superlattice. [3] The dynamics is then found from second variation of the Lagrangian. The appearing equations allow rather straightforward analysis of magnon dispersion and its evolution with *B*.

The topological nature of the ground state leads to non-trivial gauge field, *A,* in the magnon Hamiltonian. The emerging band structure consists of two groups of bands. One group is topologically trivial, with flat dispersion and rapidly evolving with *B*. Another group consists of bands with non-zero Chern numbers, rather robustly coupled to each other and only weakly sensitive to *B*. Berry curvature for the second group is sign-reversal within the Brillouin zone and peaked near symmetry points there. Two groups of bands almost do not hybridize. In the region of stability of SkX we do not observe the closing and re-opening phenomenon for spectral gaps reported elsewhere [4].

References

[1] P. Huang, T. Schönenberger, M. Cantoni, et al., Nature Nanotechnology **15**, 761 (2020).
[2] Markus Garst et al, J. Phys. D: Appl. Phys. **50,** 293002 (2017).
[3] V.E. Timofeev, A.O. Sorokin, and D. N. Aristov, Phys. Rev. B **103**, 094402 (2021).
[4] S.A. Díaz, T.Hirosawa, J. Klinovaja, D. Loss, Phys. Rev. Res. **2**, 013231 (2020).

Piezomagnetism in ferromagnetic superconductors

V.P. Mineev

Universite Grenoble Alpes, CEA, IRIG, PHELIQS, Grenoble, France
Landau Institute for Theoretical Physics, Chernogolovka, Russia

Corresponding Author's Email: vladimir.mineev@cea.fr

The appearance of magnetization during the application of mechanical stress and the creation of elastic deformation during the application of a magnetic field are two fundamental properties of piezomagnetic materials. The symmetry of superconducting ferromagnets UGe_2, URhGe, UCoGe allows piezomagnetism. In addition to conventional piezomagnetic properties occurring in both normal and superconducting states, superconducting state of these piezomagnets has its own specificity. Unlike conventional superconductors, in uranium ferromagnets, the critical transition temperature to the superconducting state changes its value when the direction of the field changes to the opposite [1].

References

[1] V.P. Mineev, Zh.Eksp.Teor.Fiz. 159, 653 (2021) [JETP 132, 556 (2021)].

New short-wavelength spin excitations in non-collinear spin-1/2 antiferromagnets

A.V. Syromyatnikov

Konstantinov Petersburg Nuclear Physics Institute
of National Research Centre «Kurchatov Institute», Gatchina, Russia

Corresponding Author's Email: asyromyatnikov@yandex.ru

We discuss spin-1/2 Heisenberg antiferromagnet on simple square lattice in magnetic field H using the recently proposed bond-operator technique (BOT). It is well known that magnetically ordered phases of quantum magnets are well described at least qualitatively by the conventional spin-wave theory (SWT) that only introduces quantum corrections into the classical solution of the problem. We observe that quantum fluctuations change drastically dynamical properties of the considered model at H close to its saturation value: the dynamical structure factor shows anomalies corresponding to Green's function poles which have no counterparts in the SWT. That is, quantum fluctuations produce multiple short-wavelength magnon modes not changing qualitatively the long-wavelength spin dynamics. Our results are in agreement with previous quantum Monte-Carlo simulations and exact diagonalization of finite clusters.

We discuss also spin-1/2 Heisenberg antiferromagnet on the triangular lattice using BOT. We use the variant of BOT which takes into account all spin degrees of freedom in the magnetic unit cell containing three spins. Apart from conventional magnons known from the SWT, there are novel high-energy collective excitations in BOT which are built from high-energy excitations of the magnetic unit cell. We obtain also another novel high-energy quasiparticle which has no counterpart not only in the SWT but also in the harmonic approximation of BOT. All observed elementary excitations produce visible anomalies in dynamical spin correlators. We show that quantum fluctuations considerably change properties of conventional magnons predicted by the SWT. The effect of a small easy-plane anisotropy is discussed. The anomalous spin dynamics with multiple peaks in the dynamical structure factor is explained that was observed recently experimentally in $Ba_3CoSb_2O_9$ and which the SWT could not describe even qualitatively.

Unexpected discovery of a new way to control DM interaction

$\boxed{\text{S.V. Maleyev}}$, A.G. Gukasov[1,2], V.P. Plakhty[1], I.A. Zobkalo[1,3]

[1] *Konstantinov Petersburg Nuclear Physics Institute of National Research Centre «Kurchatov Institute», Gatchina, Russia*
[2] *Laboratoire Léon Brillouin, Gif sur Yvette Cedex, France*
[3] *National Research Centre «Kurchatov Institute», Moscow, Russia*

Corresponding Author's Email: zobkalo_ia@pnpi.nrcki.ru

In the beginning of eighties of last century, the experiment inspired by theoreticians from Novosibirsk [1] was prepared and performed by our research team at WWR-M reactor (PNPI). It was supposed that P-parity non-conservations effect in small interactions could be observed by the neutron scattering on the compounds with helix magnetic structures. According to [1] this effect should manifest itself in the difference of populations of domains with different handedness in helix magnetic structures. The idea of that study was to search for the difference of left/right helices in metal Ho below T_N. For this search the special experimental set-up was prepared which allowed to measure Bragg scattering by multidetector unit from zeroth magnetic satellite on "white" thermal beam. Neutron polarization was maintained along or opposite to scattering vector, which was directed perpendicular to the incident beam for zero satellites. The intensity of helicoid satellite is proportional to the difference of domains population with different helix handedness, therefore asymmetry of the scattering p $p(\pm\boldsymbol{k})$ will be proportional to this difference:

$$p(\pm\boldsymbol{k}) = [I^+(\pm\boldsymbol{k}) - I^-(\pm\boldsymbol{k})] / [I^+(\pm\boldsymbol{k}) + I^-(\pm\boldsymbol{k})] \sim (n_r - n_l) \qquad (1)$$

where $I^{\pm}$ - intensity of magnetic satellite for incident neutron polarization along (+) or opposite (-) to the scattering vector, n_r, n_l – portions of right or left helices. For the sample we used the sawdust of metal holmium, obtained with a file from an ingot. In the performed experiments we observed the difference between "right" and "left" domains, which we first took for the desired effect of non-parity conservation. But afterword we discovered, that the sign of the effect depends on the method of sample preparation, namely from the sense of mechanical action. This effect we considered just as some experimental imperfection, preventing to obtain subject of a study, coming from the P-parity non-conservation only. All that we could do in this case – to make an upper estimate that expected effect not higher than 1.6×10^{-4} in Ho [2]. This was not very optimistic result which we considered to be not worthy of much attention and we haven't thought about it for more than 10 years.

At the middle of nineties S.V. Maleyev put his attention on the ideas of Kawamura [3], who clamed that magnets with non-collinear magnetic structure belongs to the new class of universality of second order phase transitions – chiral class. The experimental difficulty in the studies of such new universality class connected with the fact that in the experiment neutrons feel average chirality, i.e. difference between "right" and "left" domains. In order to make the experimental investigation of Kawamura's hypothesis, it is necessary to obtain difference between chiral domains, detectable by the neutrons. At this time S.V. Maleyev, who kept in mind our results with Ho [2], proposes to use elastic torsion to control the spin chirality, that in turn permits to study the new class of universality. At the same time, he develops the theory of the interaction of the elastic torsion and spin chirality [4-5]. According to Maleyev, chiral field interaction with of the crystal lattice in a case of elastic torsion around axis z can be written in the expression:

$$W = -2[\boldsymbol{m}_1 \times \boldsymbol{m}_2]_z \tau N_m \Sigma\, z g(\boldsymbol{R}) \sin(\boldsymbol{kR}) \qquad (2)$$

where $\tau = -d\varphi/dz$ - torsion angle, N_m – number of magnetic atoms in the sample, g(***R***) determines the strength of interaction. This expression connects directly the torsion angle τ with chirality.

Then a new polarized neutron studies of Ho, aimed to find the difference in the chiral and magnetization critical exponents were performed [6]. In these studies, non equal chiral domain population was created purposefully by the torsion device. As a result, difference between "right" and "left" domains of about 3% was achieved. This difference was enough to obtain chiral critical exponent for metal Ho, which appeared to be independent on the staggered magnetization. The wise and timely consideration by S.V. Maleyev of experiments, which gave the impression of being unsuccessful, gave impact to very impressive findings in the new scientific field.

References

[1] O.L. Zhizhimov and I.B. Khriplovich, *Zh. Exp. Theor. Fiz.* ***84***, 342 (1983).
[2] A.G. Gukasov, I.A. Zobkalo, V.I. Kozlov and V.P. Plakhty, *Preprint LNPI* ***896*** (1983).
[3] H. Kawamura, *J. Phys. Soc. Japan* ***61***, 1299 (1991).
[4] V.P. Plakhty, S.V. Maleyev, J. Wosnitza, B.K. Kremer, D. Visser, J. Kulda, O.P. Smirnov, A.G. Gukasov, I.A. Zobkalo and E. Moskvin, *Physica B* ***267-268***, 259 (1999);
[5] V.I. Fedorov, A.G. Gukasov, V. Kozlov, S.V. Maleyev, V.P. Plakhty and I.A. Zobkalo, *Physics Letters A* ***224***, 372 (1997).
[6] V.P. Plahty, W. Schweika, Th. Bruckel, J. Kulda, S.V. Gavrilov, L.-P. Regnault and D. Visser, *Phys. Rev. B* ***64***, 100402 (2001).

Helimagnetic correlations close to the Quantum Critical Points of MnSi under pressure and of $Mn_{1-x}Fe_xSi$

C. Pappas[1], A.O Leonov[2], L.J. Bannenberg[1], R. Sadykov[3,4], R.M. Dalgliesh[5], C. Goodway[5], D.L. Schlagel[6], T.A. Lograsso[6] , E. Lelièvre-Berna, Eddy[7], P. Falus[7], P. Fouquet[7], T. Wolf[8], F. Weber[8]

[1] Delft University of Technology, Delft, The Netherlands
[2] Chiral Research Center, Hiroshima Daigaku, Hiroshima, Japan
[3] Institute for Nuclear Research, Moscow, Russia
[4] Institute of High Pressure Physics RAS, Troitsk, Moscow, Russia
[5] ISIS, Harwell Oxford, UK
[6] Ames Laboratory, Ames, USA
[7] Institute Laue-Langevin, Grenoble, France
[8] Karlsruhe Institute of Technology, Karlsruhe, Germany

Corresponding Author's Email: c.pappas@tudelft.nl

The archetype cubic chiral magnet MnSi is home to some of the most fascinating states in condensed matter from the stabilisation of exotic states like chiral skyrmions [1] or the interplay between localised and itinerant magnetism. Under mechanical pressure, or chemical pressure in the form of Fe doping in $Mn_{1-x}Fe_xSi$, a non-Fermi liquid behavior sets-in which has been attributed to a chiral spin liquid and quantum fluctuations [2-4]. The origin and nature of these phenomena are still an open question, which we have addressed by combining small angle neutron scattering (SANS) and neutron spin echo spectroscopy [5-7].

At intermediate pressures the helical propagation vector of MnSi smoothly reorients from ⟨111⟩ to ⟨100⟩. At higher pressures, around the critical pressure $p_C \sim 1.4$ GPa, magnetic fields stabilize conical spirals and skyrmion lattices even in the absence of helimagnetic correlations at zero field, thus even above p_C as illustrated by Fig. 1. This occurs in a part of the phase diagram where previous studies reported non-Fermi liquid and topological Hall effect behavior. This unexpected observation can be attributed to a softening of the magnetic moment reflecting an enhancement of the itinerant electron character of the magnetism in MnSi with increasing pressure. We argue that this enhancement could be a driver in the destabilization of the long-range helical order at p_C.

Under chemical pressure, our results show that the destabilisation of the helical periodicity in on $Mn_{1-x}Fe_xSi$ (fig. 2) is also driven by the modification of the electronic state but with a different specific microscopic mechanism. An analysis of our results, using the Dzyaloshinskii model for cubic non-centrosymmetric ferromagnets, shows that the effect of pressure on the helical pitch ℓ is very different from that of doping (Fig. 3). This indicates that in contrast to MnSi under pressure, frustration possibly due to achiral Ruderman-Kittel-Kasuya-Yosida (RKKY) interactions is important in $Mn_{1-x}Fe_xSi$. This frustration increases with increasing Fe doping. We argue that this effect explains both the expansion of the precursor phase with increasing x and the abrupt disappearance of long range helimagnetic periodicity at $x^* \sim 0.11$ (see Fig. 2).

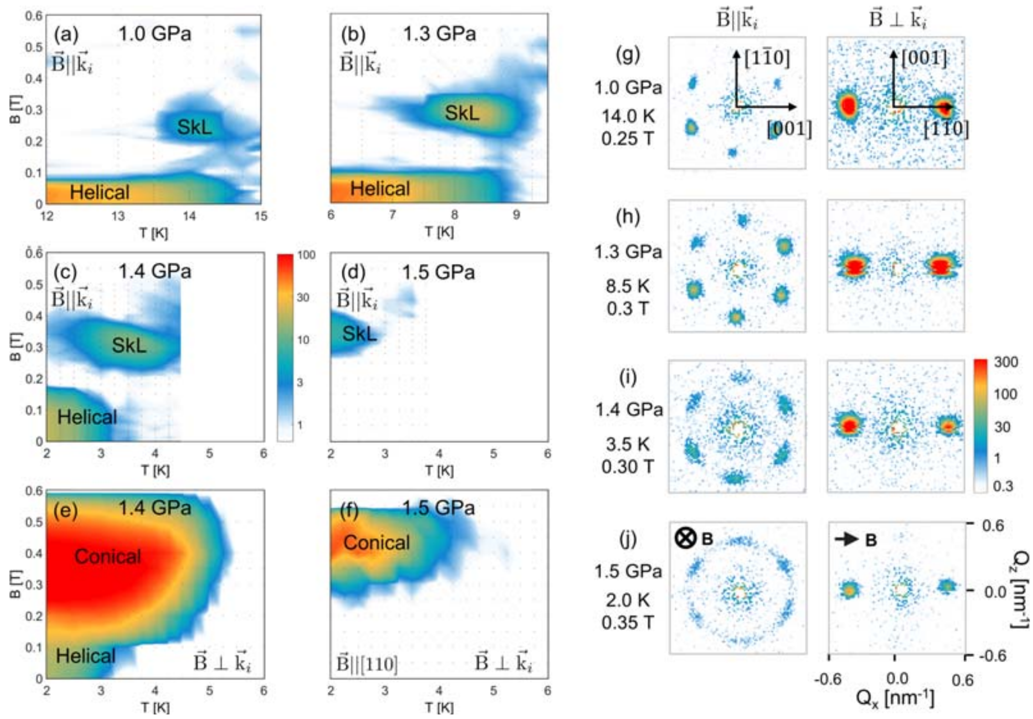

Fig.1 (after [5]): Small angle neutron scattering (SANS) results of MnSi under pressure and under magnetic field. (a)–(f) display contour plots of the total scattered SANS intensity, as obtained from summing the intensity of the SANS patterns outside the direct beam, as a function of temperature and magnetic field and for the different pressures indicated. In (a)–(d), the magnetic field $\vec{B}$ was applied parallel to the incoming neutron beam designated by $\vec{k}$ $(\vec{B}||\vec{k})$, and in (e) and (f) it was applied perpendicular to it $(\vec{B} \perp \vec{k})$. The gray dots indicate the points at which the measurements were performed. (g)–(j) display characteristic SANS patterns for the indicated pressures, temperatures, and magnetic fields, and for the two experimental configurations. The measurements were performed after zero field cooling the sample and by stepwise increasing the magnetic field.

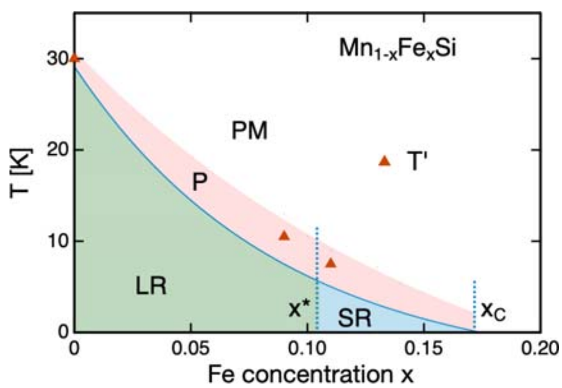

Fig.2 (after [7]): Phase diagram of $Mn_{1-x}Fe_xSi$ deduced from SANS and susceptibility measurements [6-8]. The pink shaded area indicates the precursor phase, P, and PM stands for the paramagnetic phase. The blue line indicates the transition to the ordered helimagnetic phase with long (LR) and short (SR) range periodicity respectively. The temperatures T' have been determined with polarised SANS and for T < T' the scattering is fully chiral.

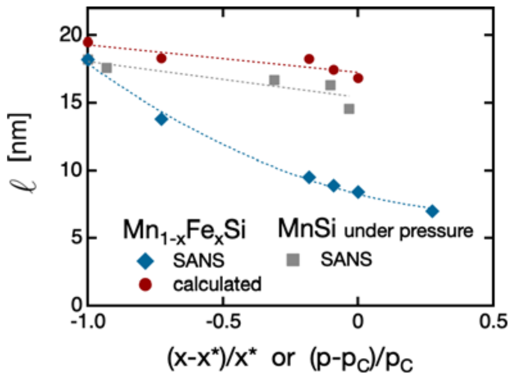

Fig.3 (after [7]): Evolution of the helical pitch as a function of Fe doping, in the case of Mn1−xFexSi, or as a function of pressure, in the case of MnSi (base temperature data from [3,4]). For the sake of comparison, the abscissa is either the relative doping (x − x)/x* for $Mn_{1-x}Fe_xSi$ or the relative pressure (p − pC)/pC for MnSi. The red dots have been calculated for Mn1−xFexSi using the Dzyaloshinskii model for cubic noncentrosymmetric ferromagnets.*

References

[1] S. Mühlbauer et al., Science 323, 915 (2009).
[2] C. Pfleiderer, et al., Nature 414, 427 (2001).
[3] S.V. Demishev et al., JETP Lett. 100, 28 (2014) and JETP Lett. 104, 116 (2016).
[4] V.V. Glushkov et al., Phys. Rev. Lett. 115, 256601.
[5] L.J. Bannenberg et al., Phys. Rev B 100, 054447 (2019).
[6] L.J. Bannenberg, et al., Phys. Rev. B 98, 184431 (2018).
[7] C. Pappas et al., Phys. Rev. Res. 3, 013019 (2021).
[8] L.J. Bannenberg, et al., Phys. Rev. B 98, 184431 (2018).

Critical fluctuations beyond the quantum phase transition in Dzyaloshinskii-Moriya helimagnets $Mn_{1-x}Fe_xSi$

S.V. Grigoriev[1,2,3], O.I. Utesov[1,2], N.M. Chubova[3], C.D. Dewhurst[4], D. Menzel[5]

[1] *Konstantinov Petersburg Nuclear Physics Institute of National Research Centre «Kurchatov Institute», Gatchina, Russia*
[2] *Saint-Petersburg State University, Saint Petersburg, Russia*
[3] *National Research Centre «Kurchatov Institute», Moscow, Russia*
[4] *Institute Laue-Langevin, Grenoble, France*
[5] *Technische Universitat Braunschweig, Braunschweig, Germany*

Corresponding Author's Email: grigoryev_sv@pnpi.nrcki.ru

Polarized small-angle neutron scattering was used for studying of critical fluctuations in the Dzyaloshinskii-Moriya helimagnets $Mn_{1-x}Fe_xSi$ with x = 0.10, 0.15, 0.20. $Mn_{1-x}Fe_xSi$ compounds are helically ordered below Tc and show a helical fluctuation regime above Tc in a wide range up to T_{DM}. The critical temperatures Tc and T_{DM} decrease with x and tend to 0 at x = 0.11 and 0.17, respectively. It was shown experimentally that three samples reveal properties of fluctuations in different regimes. The sample with x=0.10 provides sharp narrow peak in polarized SANS maps for temperatures near Tc and in the ordered phase, whereas in the one with x=0.15 critical fluctuations are suppressed by the disorder which destroys long-range magnetic order, corresponding scattering peaks being substantially wider than for x=0.10. For the sample with x=0.20 even at lowest temperatures only traces of the half-moon scattering patterns are visible. The degree of the scattering polarization is close to 1 for all three samples meaning that the corresponding helical fluctuations are chiral. $Mn_{1-x}Fe_xSi$ compounds represent an example of the system where ferromagnetic exchange approaches zero but Dzyaloshinskii-Moriya interaction is finite and provides chiral rotation of spins in magnetic fluctuations. We argue at the qualitative level that observed peculiarities can be attributed to defect antiferromagnetic bonds which are added to the system by Fe ions and lead to finite correlation length of the spiral at small temperatures for x > xc.

It is known that the magnetic structure of these compounds is a spin spiral with a large period from 30 to 3000 Å, which is formed as a result of the balance of two interactions - symmetric ferromagnetic exchange and antisymmetric Dzyaloshinsky-Moriya interaction. $Mn_{1-x}Fe_xSi$ compounds are an example of systems in which ferromagnetic exchange tends to zero with increasing x, but the Dzyaloshinsky – Moriya interaction remains constant and provides 100% chiral spin rotation in magnetic fluctuations [1]. On the contrary, $Mn_{1-x}Fe_xGe$ compounds provide an example of a system where ferromagnetic exchange remains practically constant with a change in x, but the Dzyaloshinsky – Moriya interaction tends to zero at x = 0.70, which leads to a transition from the helical to the ferromagnetic state of the system [2]. It can be concluded that two interactions - ferromagnetic exchange and the Dzyaloshinsky-Moriya interaction - turn out to be independent and their magnitude can be separately controlled by changing the concentration of chemical elements in the quasi-binary compounds $Mn_{1-x}Fe_xSi$ and $Mn_{1-x}Fe_xGe$.

Authors thank for support the Russian Scientific Foundation (Grant No 17-12-01050).

References

[1] S.V. Grigoriev, O.I. Utesov, N.M. Chubova, C.D. Dewhurst, D. Menzel, S.V. Maleyev, ZhETF, Vol. 159, No. 4, p. 690. 690–695 (2021).
[2] S.V. Grigoriev, N.M. Potapova, S.-A. Siegfried, V.A. Dyadkin, E.V. Moskvin, V. Dmitriev, D. Menzel, C.D. Dewhurst, D. Chernyshov, R.A. Sadykov, L.N. Fomicheva, and A.V. Tsvyashchenko, Phys. Rev. Lett. 110, 207201 (2013).

SESSION 2. MONOAXIAL CHIRAL HELIMAGNETS.

Chirality-induced phonon dispersion in a noncentrosymmetric micropolar crystal

J. Kishine[1,2], A.S. Ovchinnikov[3,4], A.A. Tereshchenko[3]

[1] Division of Natural and Environmental Sciences, The Open University of Japan, Chiba, Japan
[2] Institute for Molecular Science, Okazaki, Aichi, Japan
[3] Institute of Natural Sciences and Mathematics, Ural Federal University, Ekaterinburg, Russia
[4] Institute of Metal Physics of Ural Division, RAS, Ekaterinburg, Russia

Corresponding Author's Email: kishine@ouj.ac.jp

In this presentation, I report our recent progress on "chiral phonon" [1]. Features of the phonon spectrum of a chiral crystal are examined within the micropolar elasticity theory [2]. This formalism accounts for not only translational micromotions of a medium but also rotational ones. It is found that there appears the phonon band splitting depending on the left- and right-circular polarization in a purely phonon sector without invoking any outside subsystem. The phonon spectrum reveals parity breaking while preserving time-reversal symmetry, i.e., it possesses true chirality. We find that hybridization of the microrotational and translational modes gives rise to the acoustic phonon branch with a "roton" minimum reminiscent of the elementary excitations in the superfluid helium-4. We argue that a mechanism of this phenomena is in line with Nozi`eres' reinterpretation of the rotons as a manifestation of an incipient crystallization instability [3]. We discuss a close analogy between the translational and rotational micromotions in the micropolar elastic medium and the Bogoliubov quasiparticles and gapful density fluctuations in 4He.

References

[1] J. Kishine, A.S. Ovchinnikov, and A.A. Tereshchenko, Phys.Rev. Lett. 125, 245302 (2020).
[2] A.C. Eringen, Microcontinuum Field Theories: I. Foundations and Solids (Springer, New York, 1999).
[3] Nozi`eres, J. Low Temp. Phys. 137, 45 (2004).

Spin selection effect in chiral inorganic crystals

Yo. Togawa

Osaka Prefecture University, Osaka, Japan

Corresponding Author's Email: y-togawa@pe.osakafu-u.ac.jp

The concept of chirality is widely found in many phenomena in nature and governs the symmetry properties of the chiral system. The original meaning of chirality is provided by a geometrical relationship of handedness [1]: a pair of objects that correspond to their mirrored images but cannot be superimposed on each other. They are distinguishable from their counterparts and contain only the symmetry operation of pure rotation. Furthermore, a dynamical aspect of chirality [2], which could be referred to as dynamical chirality, has increased its importance, motivated by a variety of chirality-induced responses discovered in many research fields such as biochemistry [3], nano-optics [4], condensed matter physics [5], and magnetism [6]. An interplay between structural and dynamical chirality should play a key role in the mechanism underlying chirality-induced phenomena.

In this talk, we will focus on a role of chirality in crystals in terms of an emergence of macroscopic spin response, being inspired by recent works on chiral magnetism and chiralityinduced spin polarization. These viewpoints may bring us to a new frontier of chiral spin material science.

One of the good examples enlightening the importance of chirality in crystals is a chiral magnetic crystal [7]. Crystalline and magnetic chirality in such crystals play an important role in inducing a variety of striking physical responses through a coupling with conduction electrons or electromagnetic fields. A microscopic effect, associated with a symmetry breaking of chiral magnetic crystals, spreads over the whole crystal and the physical responses emerge on macroscopic length scales. Indeed, an antisymmetric (Dzyaloshinskii-Moriya) exchange interaction [8-9] works throughout a monoaxial CrNb3S6 crystal and consequently induces nontrivial electrical transport phenomena [10-11] and collective dynamics of chiral magnetic orders [12-13].

Moreover, it is found that a chiral crystal exhibits a spin-polarized state when the charge current is injected into the crystal [14-16]. A spin-polarized transport occurs in a linear regime of the current-voltage characteristics. Importantly, a robust protection of the spin polarization enables a nonlocal spin transport over micrometers. Such a spin polarization has also been demonstrated in chiral molecules via spin-polarized photocurrent emission [17] and tunneling transport experiments [18, 19]. The phenomena, where electrons flowing through a chiral material become spin polarized, are frequently called chirality-induced spin selectivity (CISS). Importantly, while the CISS phenomena occur at a nanometer scale in chiral molecules, the same effect happens at macroscopic length scales over micrometers or longer in chiral crystals. A comprehensive understanding of the CISS remains an important issue and may clarify the interplay between structural and dynamical chirality.

References

[1] Lord Kelvin, *Baltimore Lectures on Molecular Dynamics and the Wave Theory of Light* (C.J. Clay and Sons, London, 1904), p.619.
[2] L.D. Barron, *Molecular Light Scattering and Optical Activity* (2nd edn., Cambridge University Press, Cambridge, U.K., 2004).
[3] E. Hendry *et al*., Nat. Nanotechnol. **5**, 783 (2010).
[4] C. Kelly *et al*., Nat. Commun. **11**, 5169 (2020).
[5] J. Kishine *et al*., Phys. Rev. Lett. **125**, 245302 (2020).
[6] Y. Togawa *et al*., Phys. Rev. Lett. **108**, 107202 (2012).

[7] For a review, Y. Togawa *et al*., J. Phys. Soc. Jpn. **85**, 112001 (2016).
[8] I. E. Dzyaloshinskii, J. Phys. Chem. Solids **4**, 241 (1958).
[9] T. Moriya, Phys. Rev. **120**, 91 (1960).
[10] Y. Togawa *et al*., Phys. Rev. B **92**, 220412(R) (2015).
[11] R. Aoki, Y. Kousaka, and Y. Togawa, Phys. Rev. Lett. **122**, 057206 (2019).
[12] F. Goncalves *et al*., Phys. Rev. B **95**, 104415 (2017).
[13] Y. Shimamoto *et al*., submitted.
[14] A. Inui *et al*., Phys. Rev. Lett. **124**, 166602 (2020).
[15] Y. Nabei *et al*., Appl. Phys. Lett. **117**, 052408 (2020).
[16] K. Shiota *et al*., to appear in Phys. Rev. Lett.
[17] B. Göhler *et al*., Science **331**, 894 (2011).
[18] Z. Xie *et al*., Nano Lett. **11**, 4652 (2011).
[19] M. Suda *et al*., Nat. Commun. **10**, 2455 (2019).

Magnetic response of a highly nonlinear soliton lattice in a monoaxial chiral helimagnet

A.S. Ovchinnikov[1,2], J. Kishine[3,4]

[1] *Institute of Natural Science and Mathematics, Ural Federal University, Ekaterinburg, Russia*
[2] *Institute of Metal Physics of Ural Division, RAS, Ekaterinburg, Russia*
[3] *Division of Natural and Environmental Sciences, The Open University of Japan, Chiba, Japan*
[4] *Institute for Molecular Science, Okazaki, Aichi, Japan*

Corresponding Author's Email: alexander.ovchinnikov@urfu.ru

Measurements of dynamical magnetic response in $CrNb_3S_6$ provide exciting challenges that need to be addressed theoretically. One area of research is focused on spin resonance measurements [1,2] that find an explanation within the theory of standing spin waves in a finite-size chiral soliton lattice [3]. Other area of these studies involves oscillating magnetic susceptibility measurements, which reveal a strong presence of higher-order harmonic components of magnetization near the incommensurate-commensurate phase transition and which still remain unexplained [4,5]. Low frequencies of the ac field used in these experiments, 10–104 Hz, lie far below the spin resonance frequencies of the order of 10 GHz that unites this task with a general issue of emergence of slow dynamics from high-energy processes. Another difference is that the spin resonance theory invokes Bloch wave collective excitations propagating over the CSL originated from periodicity of this configuration. However, near the IC-C phase transition the spectrum is undergoing serious changes that are linked to representation of the periodic Lamé potential of the CSL as the sum of Pöschl-Teller potentials localized in space. This necessitates altering the description of spin fluctuations in this regime. More importantly, differential equations of spin dynamics used in the theory of spin resonance [3] describe only linear response of magnetization. To explain the appearance of higher-order harmonics in the magnetic response an another integration scheme of spin dynamics equations should be applied.

In the recent work [6] we developed a formalism to describe features of the nonlinear responses revealed in $CrNb_3S_6$ in the vicinity of the IC-C phase transition. We assume that crossover identified experimentally from the weakly nonlinear CSL regime, where the higher-order magnetization harmonics are absent, to the highly nonlinear CSL regime, where they were detected, may be associated with the changing balance between Fourier transforms that make up the static CSL configuration. Another assumption we made is that each of the Pöschl-Teller potentials constituent in the periodic potential of the highly nonlinear CSL covers only a home unit cell of the length L. The problem is then reduced to search of a spectrum of spin fluctuations for each individual potential and concomitant nonlinear response. A result for the entire system is the sum of these individual contributions.

To implement this approach, we used a Lagrangian description of spin dynamics based on the collective coordinates method, where two dynamical variables are relevant, i.e., one describes a shift in the kink position and the other does a deformation of the kink under such a motion. Interaction between these coordinates and the oscillating magnetic field applied perpendicularly to the chiral axis does determine nonlinear nature of magnetic responses. Employing a well-developed algorithm for finding periodic solutions of the spin dynamics, we solve the equations of motion in a perturbative manner with respect to the oscillating field. We obtain the higher-order harmonic components of magnetization and concomitant phase shifts originating from higher-order powers of the ac field. The comparison of hierarchy of these contributions with experimental values provides a measure of the kink potential localization L. Thus, we demonstrate that the emergence of higher-order harmonics takes place in a narrow range of steady magnetic fields when there is an optimal distance between the kinks. Moreover, at lower distances, which corresponds to the weakly nonlinear CSL regime, our perturbative scheme is no longer valid. At larger distances (or equivalently, for lower kink density) contributions of the higher-order harmonics become negligible, which confirms restoring of linear response prior to the transition into the ferromagnetic phase [4].

The authors acknowledge JSPS Bilateral Joint Research Projects (JSPS-RFBR), the Russian Foundation for Basic Research (RFBR), Grant No. 20-52-50005.

References

[1] F.J.T. Goncalves, T. Sogo, Y. Shimamoto, Y. Shimamoto, Y. Kousaka, J. Akimitsu, S. Nishihara, K. Inoue, D. Yoshizawa, M. Hagiwara, M. Mito, R.L. Stamps, I.G. Bostrem, V.E. Sinitsyn, A.S. Ovchinnikov, J. Kishine, and Y. Togawa, *Phys. Rev. B* 95, 104415 (2017).
[2] F.J.T. Goncalves, T. Sogo, Y. Shimamoto, I. Proskurin, V.E. Sinitsyn, Y. Kousaka, I. G. Bostrem, J. Kishine, A.S. Ovchinnikov, and Y. Togawa, *Phys. Rev. B* 98, 144407 (2018).
[3] J. Kishine, V.E. Sinitsyn, I.G. Bostrem, I. Proskurin, F.J.T. Gonsalves, Y. Togawa, and A.S. Ovchinnikov, *Phys. Rev. B* 100, 024411 (2019).
[4] E.M. Clements, R. Das, M.-H. Phan, L. Li, V. Keppens, D. Mandrus, M. Osofsky, and H. Srikanth, *Phys. Rev. B* 97, 214438 (2018).
[5] K. Tsuruta, M. Mito, H. Deguchi, J. Kishine, Y. Kousaka, J. Akimitsu and K. Inoue, *Phys. Rev. B* 93, 104402 (2016).
[6] J. Kishine and A.S. Ovchinnikov, *Phys. Rev. B* 101, 184425 (2020).

Investigation of a deformation of the magnetic soliton lattice under tensile stress by Lorentz electron microscopy

G.W. Paterson[1], A.A. Tereshchenko[2], S. Nakayama[3], Y. Kousaka[3], J. Kishine[4,5], S. McVitie[1], A.S. Ovchinnikov[2,6], I. Proskurin[2,7], Y. Togawa[3]

[1] *School of Physics and Astronomy, University of Glasgow, Glasgow, United Kingdom*
[2] *Institute of Natural Science and Mathematics, Ural Federal University, Ekaterinburg, Russia*
[3] *Department of Physics and Electronics, Osaka Prefecture University, Sakai, Japan*
[4] *Division of Natural and Environmental Sciences, The Open University of Japan, Chiba, Japan*
[5] *Institute for Molecular Science, Okazaki, Aichi, Japan*
[6] *Institute of Metal Physics of Ural Division, RAS, Ekaterinburg, Russia*
[7] *Department of Physics and Astronomy, University of Manitoba, Winnipeg, Canada*

Corresponding Author's Email: alexey.tereshchenko@urfu.ru

We investigate the effect of an external tensile force on the monoaxial helimagnet $CrNb_3S_6$, which has a magnetic order in the form of the soliton lattice without elastic deformations [1]. The problem turns out to be equivalent to a search of magnetic configurations formed simultaneously by the external magnetic field b_1 and the single-ion magnetic anisotropy b_2 caused by the mechanical stress (Fig.1). The treatment of this problem may be formulated via the double sine-Gordon model [2,3]. In earlier studies, to identify different phases of the double sine-Gordon model, the technique of the elastic neutron scattering has been proposed [4]. We suggest the Lorentz transmission electron microscopy to identify the possible incommensurate phases (Fig.2).

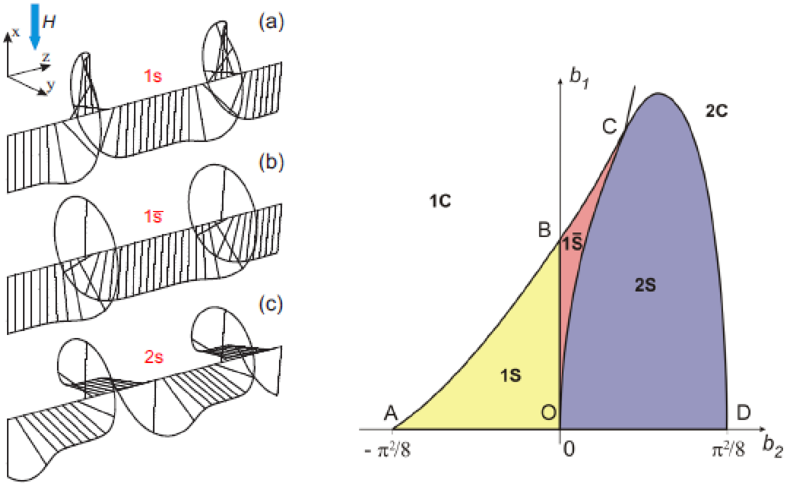

Fig.1 Profiles of the magnetization distribution of incommensurate phases of the double sine-Gordon model: (a, b) 1s phase, (c) 2s phase. Phases 1s and $1\bar{s}$ differ by the existence in the 1s phase of a ferromagnetic region inside each kink. (d) Phase diagram of the model in the plane (b_1-b_2).

Calculation of the corresponding Aharonov-Bohm shifts of the electronic phase reconstructs a complete picture of images of incommensurate magnetic structures of the model, obtained by the transmission electron microscopy, and enables to trace their evolution under change of the magnetic field and mechanical stress. Comparison of the experimental Fresnel contrasts of the Lorentz microscopy probed on the mechanically stretched $CrNb_3S_6$ sample (Fig.3), with appropriate theoretical results enables to identify the so-called incommensurate 1*s* phase predicted theoretically in Ref. [2].

This work was supported by a grant from the Russian Foundation for Basic Research (project No. 20-52-50005).

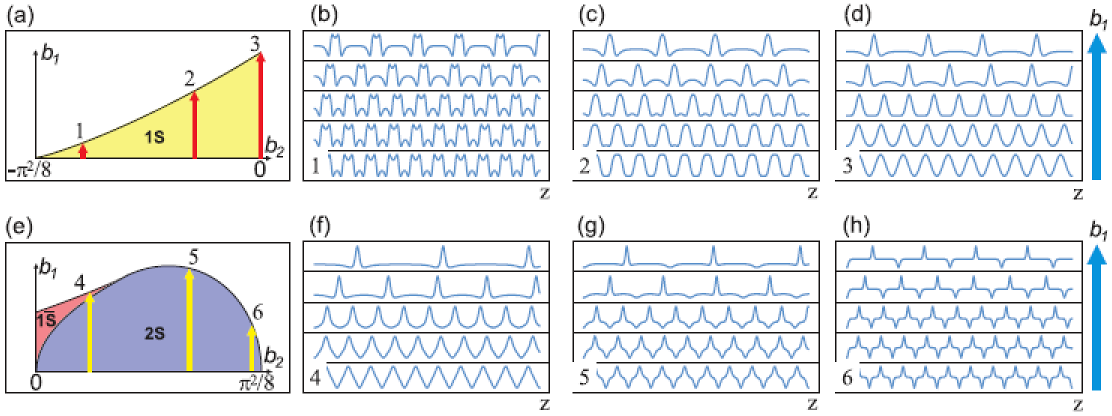

Fig.2 Upper panel: the profile of the evolution of the Fresnel signal intensity with a change in the external magnetic field (b_1) along the selected directions in the 1s phase diagram (red arrows). Cases of large (b), small (c) and zero (d) deformations are shown. Bottom panel: similar graphs for 1$\bar{s}$ and 2s phases (e). Cases of small (f), medium (g) and large (h) deformations are shown.

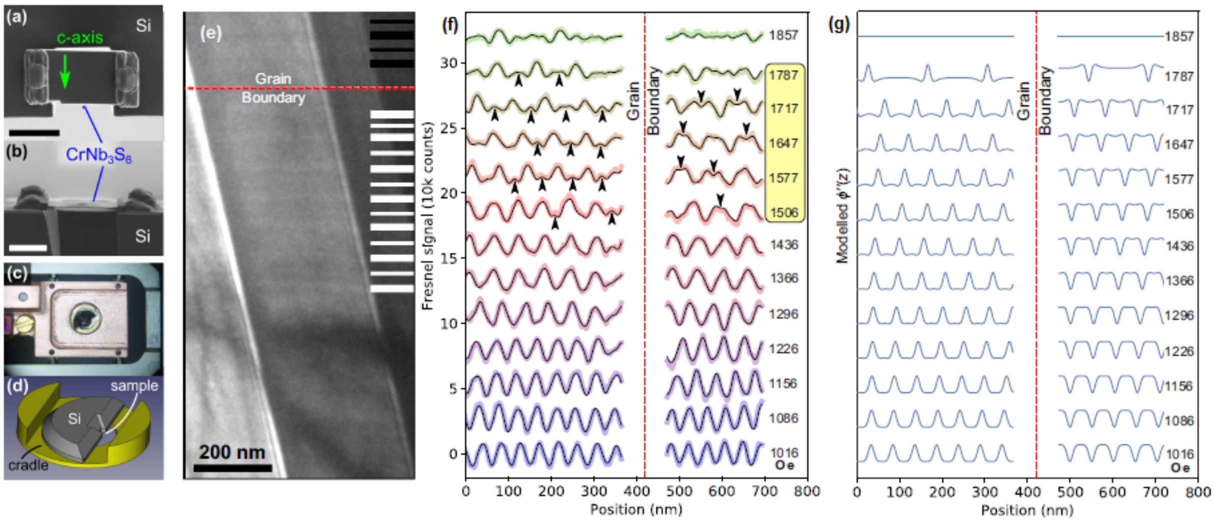

Fig.3 Top (a) and side (b) views of the $CrNb_3S_6$ sample on a silicon substrate. Schematic of the setup for measuring the effects of elastic stress (c, d). Lorentz diffraction pattern of $CrNb_3S_6$ sample subjected to tensile stress (e). Comparison of the experimental Fresnel contrast (f) with the model calculation (g).

References

[1] G.W. Paterson, A.A. Tereshchenko, S. Nakayama, Y. Kousaka, J. Kishine, S. McVitie, A.S. Ovchinnikov, I. Proskurin, Y. Togawa, *Physical Review B* **101**, 184424 (2020).
[2] S. Iwabuchi, *Prog. Theor. Phys.* **70**, 941 (1983).
[3] V.A. Golovko, D.G. Sannikov, *JETP* **55**, 562 (1982).
[4] Yu.A. Izyumov, V.M. Laptev, *JETP* **58**, 1267 (1983).

Discrete magnetic breathers in monoaxial chiral helimagnet

V.E. Sinitsyn[1], E.G. Ekomasov[2], I.G. Bostrem[1], A.S. Ovchinnikov[1,3], J. Kishine[4,5]

[1] *Institute of Natural Science and Mathematics, Ural Federal University, Ekaterinburg, Russia*
[2] *Bashkir State University, Ufa, Russia*
[3] *Institute of Metal Physics of Ural Division, RAS, Ekaterinburg, Russia*
[4] *Division of Natural and Environmental Sciences, The Open University of Japan, Chiba, Japan*
[5] *Institute for Molecular Science, Okazaki, Aichi, Japan*

Corresponding Author's Email: vladimir.sinitsyn@urfu.ru

The study of nonlinear spin dynamics in magnetic materials remains essential research area in modern magnetism. Discrete breathers (DB), or intrinsic localized modes, that periodic in time and localized in space arise in discrete systems with translational invariance owing to interplay between nonlinearity and discreteness. In present work, we consider discrete magnetic breathers similar to the discovered in ferro- and antiferromagnetic spin chains with easy-plane single-ion anisotropy [1-3].

We have previously shown that, even though the antisymmetric exchange interaction significantly lowers the symmetry, magnetic breathers also can exist in monoaxial chiral helimagnets [4].

The model Hamiltonian of the chiral monoaxial helimagnet is of the form

$$\mathcal{H} = -2J\sum_n \vec{S}_n\cdot\vec{S}_{n+1} + A\sum_n (S_n^z)^2 + D\sum_n [\vec{S}_n\times\vec{S}_{n+1}]_z - H\sum_n S_n^z,$$

where the first term is the exchange coupling along the chiral axis (*z*-axis) with *J*>0. The second describes the single-ion anisotropy with the constant *A*, while the third does Dzyaloshinskii-Moriya interaction of the strength *D*. The last term denotes Zeeman coupling with an external magnetic field *H* directed along the *z* axis. The magnetic field is assumed to be strong enough, so that in the ground state all spins are ordered along the external field direction. This forced ferromagnetic arrangement requires $H > 2S\left(\sqrt{4J^2+D^2} - J + A\right)$ [5].

The appropriate spin variables $s_n^{\pm} = (S_n^x \pm iS_n^y)/S$ and $s_n^z = S_n^z/S$ describe spin deviations from the ground state, where *S* is the magnitude of spin.

The equations of motion for these variables become

$$\frac{i\hbar}{2JS}\frac{d}{dt}s_n^+ = s_n^+(s_{n+1}^z + s_{n-1}^z) - s_n^z(s_{n-1}^+ + s_{n+1}^+) - 2Bs_n^+s_n^z +$$
$$+i\frac{D}{2J}s_n^z(s_{n-1}^+ - s_{n+1}^+) + \frac{H}{2JS}s_n^+,$$

Where $s_n^z = \sqrt{1-|s_n^+|^2}$ and $B = A/2J$.

Time-periodic solutions of the form $s_n^+ = s(t)\exp(ikna - i\omega t)$ are to be found the equations

$$\Omega s_n = s_n\left(\sqrt{1-s_{n+1}^2} + \sqrt{1-s_{n-1}^2}\right) - 2Bs_n\sqrt{1-s_n^2} - \sqrt{1-s_n^2}(s_{n-1}+s_{n+1})\sqrt{1+\frac{D^2}{4J^2}}$$

Intrinsic localized spin wave modes are expected to exist in perfect discrete magnetic chains due to salient nonlinearity in the exchange and anisotropy interactions. These intrinsic modes may lie inside the linear wave band and splitting off from its upper or lower edges, so-called ILSM of the dark type [1]. On the contrary, the bright type modes can appear at frequencies either just above the upper band edge or just below the lower edge of the linear spin wave spectrum.

Using the numerical algorithm [6] we obtain all mentioned types of breathers. One of the most interesting case is the dark bottom breather (Fig. 1), because this is the only type of breathers that could be excited in a chiral helimagnet with a small value of easy-plane anisotropy.

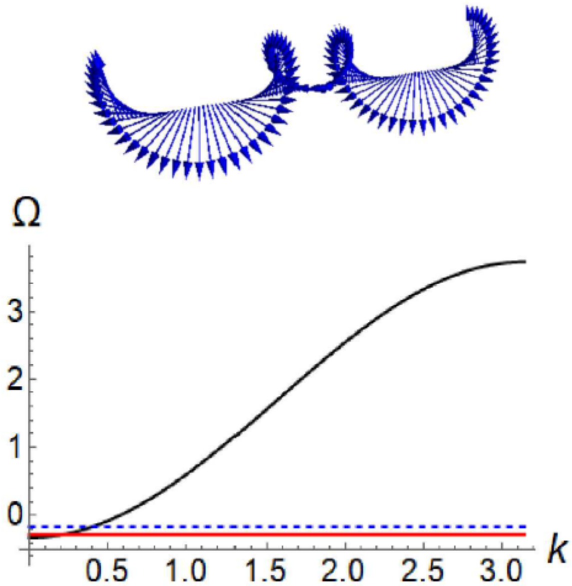

Fig.1 The bottom dark breather mode (upper panel). Transversal spin components (relative to the chain axis) are shown with a factor 20 expansion. Lower panel: The spin-wave spectrum at the easy-plane anisotropy B=0.15 (soild black). The breather frequency $\Omega = -0.28$ *(red solid) is upper bounded by blue dashed* $\Omega_u = 1 - B - \sqrt{1+(D/2J)^2}$.

We also obtained analytical formulas for all types of breathers in the continuum limit.

It should be mentioned that in case of the magnetic breathers in a chiral system the spin deviations form a spatial spiral with a step value of $\delta = \tan^{-1}(D/2J)$, (Fig. 1) and therefore they have a topological charge.

The authors acknowledge the Russian Foundation for Basic Research (RFBR), Grant No. 20-02-00213.

References

[1] S.V. Rakhmanova, and A.V. Shchegrov, Phys. Rev. B 57, R14012 (1998).
[2] S. Rakhmanova, and D.L. Mills, Phys. Rev. B 54, 9225 (1996).
[3] R. Lai, and A.J. Sievers, Phys. Rep. 314, 147 (1999).
[4] I.G. Bostrem, Vl.E. Sinitsyn, A.S. Ovchinnikov, E.G. Ekomasov and J. Kishine, AIP Advances, vol. 11, Id. 015208 (2021).
[5] J. Kishine and A.S. Ovchinnikov, Theory of Monoaxial Chiral Helimagnet in Solid State Physics, vol. 66, R.E. Camley and R.L. Stamps (Academic Press, New York, 2015).
[6] I.G. Bostrem, V.E. Sinitsyn, A.S. Ovchinnikov, M.I. Fakhretdinov and E.G. Ekomasov, Lett. Mater., vol. 11, pp. 109-114, (2021).

SESSION 3. DMI EFFECT ON THE MAGNETIC STRUCTURE.

Anisotropy of the magnetic phases of cubic helimagnets

V.A. Chizhikov

A.V. Shubnikov Institute of Crystallography, Federal Scientific Research Center "Crystallography and Photonics", RAS, Moscow, Russia

Corresponding Author's Email: chizhikov@crys.ras.ru

In cubic magnetic crystals such as MnSi and Cu_2OSeO_3, the coexistence of high point symmetry and structural chirality leads to an interesting phase diversity (Fig. 1). At temperatures well below the Curie point, three phases, namely, helical, conical, and polarized ferromagnetic ones, are distinguished with phase transitions in a magnetic field between them. These phases are structurally very similar and differ mainly in the behavior of magnetic susceptibility.

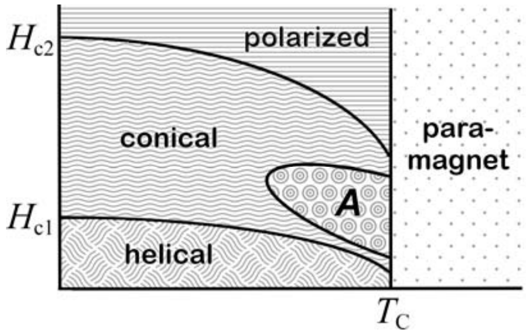

Fig.1. Phase diagram of a cubic chiral ferromagnet. Below critical temperature T_C, there are a number of magnetic-field-dependent phases. Critical fields H_{c1} and H_{c2} separate the helical, conical, and polarized ferromagnetic phases. The region of existence of the mysterious double twist A phase exists near the Curie temperature.

The most intriguing phase is certainly the so-called A phase, which appears near the Curie point in intermediate magnetic fields [1]. It is now generally accepted that the A phase is a triangular lattice of field-stabilized linear topological defects, namely, skyrmions (Fig. 2) [2]. The magnetization in the A phase rotates about skyrmion cores oriented along a magnetic field and is turned over against the field at the cores. The obvious energy disadvantage of this turn-over is compensated by the advantage of a double twist of the magnetization field.

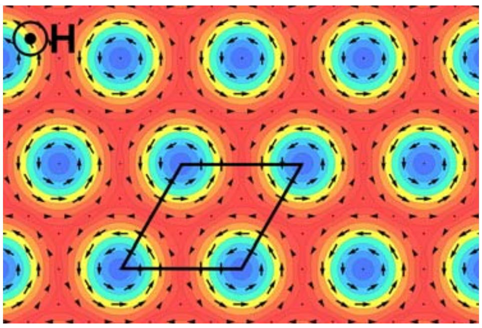

Fig.2. The A phase of a cubic chiral ferromagnet. The color gradient indicates the projection of magnetization onto the magnetic field direction: (red) along field and (blue) opposite to field. The arrows are the projections of the magnetization field onto the plane perpendicular to the field.

In [3], to describe the magnetic structure of cubic chiral ferromagnets in terms of a phenomenological approach, we used the approximation $|\mathbf{M}(\mathbf{r})| = \text{const}$, which is well applicable at temperatures well below the temperature of transition from a paramagnetic to an ordered phase. In this approximation, the dimensionless Landau–Lifshitz energy

$$E = (\partial\boldsymbol{\mu}/\partial r_\alpha)\cdot(\partial\boldsymbol{\mu}/\partial r_\alpha)/2 + \boldsymbol{\mu}\cdot[\nabla\times\boldsymbol{\mu}] - \mathbf{h}\cdot\boldsymbol{\mu}, \quad (1)$$

contains external magnetic field $\mathbf{h} = \mathbf{H}/H_{c2}$ as a single parameter, and all nontrivial magnetic phases, namely, helical, conical, and A phase, exist in the range $0 \leq h < 1$. Here, $\boldsymbol{\mu} = \mathbf{M}/M$. Using this model, we showed that the helical phase in a weak magnetic field is well described by conical–elliptical helices. The magnetic susceptibility depends on the angle between magnetic field and helix direction. Thus, for the field parallel/perpendicular to the helix, $\chi_{\|} = 2\chi_{\perp}$. The form of the magnetic susceptibility tensor is consistent with both the experimental data [4] and the results obtained using other theoretical approaches [5].

The A phase has been simulated as a function of the magnetic field and the wavenumber k_0 of the main helices. The results of calculations showed that the A phase is most energetically favorable at $H \approx 0.41H_{c2}$, and $k_0 \approx 97.8\%$ of the wavenumber of the conical-phase helices (Fig. 3). Nevertheless, in terms of this approximation, the A phase energy does not fall below the conical-phase energy at the same field. The most probable explanation of the fact that the A phase is more favorable than the conical phase under certain conditions is that the condition $|\mathbf{M}(\mathbf{r})| = \text{const}$ in the A phase region near the Curie point T_C is only approximately met because of thermal fluctuations of a magnetic order, which are strong near the transition temperature.

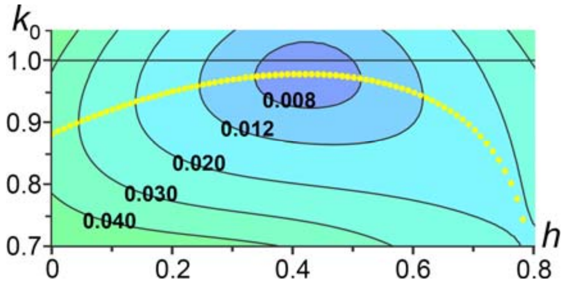

Fig.3. Difference $\langle E_A \rangle - E_c$ between the average energy densities of the A phase (simulation) and the conical phase as a function of magnetic field h and the wavenumber of the main helices k_0. The yellow points correspond to the global energy minimum of the A phase at a given field.

The interaction of spins with a local crystal field was considered as the cause of the cubic anisotropy of the magnetic properties of the crystals under study. In this case, the Landau–Lifshitz energy (1) should be supplemented by the anisotropic term $\alpha(\mu_x^4+\mu_y^4+\mu_z^4)$. The sign of α is determined by the crystallographic directions along which helices are arranged in the helical phase: $\alpha > 0$ corresponds to the ‹111› directions and $\alpha < 0$, to the ‹100› directions. The absolute value of α can be estimated from the critical field H_{c1} that separates the helical and conical phases, $|\alpha| \approx (H_{c1}/H_{c2})^2$.

Cubic anisotropy was shown to affect the stability of the A phase depending on the magnetic field direction; however, this effect alone is too weak to explain the existence of the phase. For example, the A phase becomes more stable if a field is applied along the ‹111› directions at $\alpha > 0$ and along ‹100› at $\alpha < 0$. Some experimental observations demonstrate the opposite picture. For example, the A phase in an MnSi crystal exists in a wider temperature range if a field is applied along the ‹100› directions [6], and the A phase in Cu_2OSeO_3 is more stable if a field is parallel to ‹111› [7]. This discrepancy can serve as an argument in favor of another microscopic cause for the appearance of cubic anisotropy in these crystals. Such a cause can be, e.g., the DM interaction between the spins ordered in a lattice with cubic symmetry. In this case, anisotropic terms with spatial derivatives of magnetization should appear in the Landau–Lifshitz energy.

References

[1] S.V. Grigoriev, S.V. Maleyev, A.I. Okorokov, et al., *Phys. Rev. B 74*, 214414 (2006).
[2] U.K. Rößler, A.A. Leonov, and A.N. Bogdanov, *J. Phys.: Conf. Ser. 303*, 012105 (2011).
[3] V.A. Chizhikov, *J. Exp. Theor. Phys. 132*, 559 (2021).
[4] V.N. Narozhnyi and V.N. Krasnorussky, *Phys. Rev. B 91*, 134403 (2015).
[5] M. Janoschek, M. Garst, A. Bauer, et al., *Phys. Rev. B 87*, 134407 (2013).
[6] A. Bauer and C. Pfleiderer, *Phys. Rev. B 85*, 214418 (2012).
[7] T. Adams, A. Chacon, M. Wagner, et al., *Phys. Rev. Lett. 108*, 237204 (2012).

New high-entropy alloys with cubic non-centrosymmetric B20 structure: high pressure synthesis, magnetic properties and *ab-initio* calculations

A.V. Tsvyashchenko[1,2], V.A. Sidorov[1,2], A.V. Bokov[1,2], D.A Salamatin[1,2], V.N. Krasnorussky[1], A.V. Semeno[1,3], N.M. Chtchelkachev[1], M.V. Magnitskaya[1,2], V.V. Brazhkin[1]

[1] *Vereshchagin Institute of High Pressure Physics RAS, Troitsk, Moscow, Russia*
[2] *Lebedev Physical Institute RAS, Moscow, Russia*
[3] *Prokhorov General Physics Institute RAS, Moscow, Russia*

Corresponding Author's Email: sidorov@hppi.troitsk.ru

Binary transition metal compounds TMX (where TM = Rh, Mn, Fe, Co and X = Si, Ge) form cubic non-centrosymmetric B20 structure and exhibit many interesting properties: skyrmion lattices, pressure induced quantum phase transitions, the existence of massless electronic excitations like Weil fermions, coexistence of superconductivity and weak ferromagnetism. For Ge containing compounds high pressure is generally required for synthesis. The unit cell of B20 structure consists of four TM atoms and four Si or Ge atoms which form mutually penetrating tetrahedrons. We have synthesized at high pressure multi-component compounds $RhMnFeCoSi_4$, $RhMnFeCoGe_4$, $RhMnFeCoSi_2Ge_2$, $RhMnFeCoSi_3Ge$ and $RhMnFeCoSiGe_3$ which may be regarded as high entropy alloys. All of them crystallize in cubic B20 structure and exhibit magnetic ordering. We have measured their magnetic properties in the range 2-400 K and magnetic fields up to 9 T at ambient pressure and magnetic susceptibility in the range 4.2-300 K at high pressure up to 5.5 GPa and follow the evolution of magnetic transition temperatures with pressure. All synthesized compounds exhibit semimetallic electric properties. We also made *ab initio* calculations of $RhMnFeCo(Si,Ge)_4$ in nonmagnetic and magnetic states using the PAW pseudopotential method as implemented in the VASP package [1], with the PBE–GGA version of the exchange-correlation potential. The difference in the band structures and density of states upon changing the metalloid constituent from Si to Ge is discussed. The results are compared with our experimental data.

This work was supported by Russian Science Foundation under Grants No. 17-12-01050, No. 18-12-00438 and No. 19-12-00111.

References

[1] G. Kresse, J. Furthmuller, *Phys. Rev. B* ***54***, 11169 (1996).

Pressure influence on the valence and magnetic state of Yb in noncentrosymmetric heavy-fermion $YbNiC_2$

D.A. Salamatin[1,2,3], V.A. Sidorov[1,3], N.M. Chtchelkatchev[1], M.V. Magnitskaya[1,3], N. Martin[4], A.E. Petrova[1,3], J. Guo[5], C. Huang[5], Y. Zhou[5], L. Sun[5], A.V. Tsvyashchenko[1,3]

[1] Institute for High Pressure Physics, RAS, Troitsk, Moscow, Russia
[2] Joint Institute for Nuclear Research, Dubna, Russia
[3] P.N. Lebedev Physical Institute of the RAS, Moscow, Russia
[4] Université Paris-Saclay, CNRS, CEA, LLB, Gif-sur-Yvette, France
[5] Institute of Physics, ChAS, Beijing, China

Corresponding Author's Email: dasalam@gmail.com

In work, we present studies of neutron diffraction, electrical resistivity, magnetic susceptibility, magnetization and specific heat of noncentrosymmetric $YbNiC_2$. At normal pressure, $YbNiC_2$ is a moderate heavy-fermion compound with Kondo lattice. At 16 K, we observe an anomaly in the temperature dependence of specific heat ascribed to an abrupt valence change of Yb ions. At pressures above 7 GPa, the valence change and the Kondo lattice state are suppressed, and near a temperature of 10 K we detect the appearance of magnetic order. Above 5 GPa, the temperature dependence of the resistivity behaves similarly to other compounds of the $CeNiC_2$-type family, indicating the formation of charge density waves. This is attributed to the nesting properties of the Fermi surface found within the DFT+DMFT treatment. Our *ab initio* calculations also show that the valence of Yb in $YbNiC_2$ at normal conditions is 2.85, which increases with temperature and pressure. The Fermi surface of $YbNiC_2$ is quite simple in shape in comparison with the one of $YbCoC_2$. Also, it implies a lower (and more anisotropic) conductivity of $YbNiC_2$ than that of $YbCoC_2$. As the result of performed investigations, the *P-T* phase diagram of the $YbNiC_2$ compound has been obtained (Fig. 1).

This work was supported by Russian Science Foundation: D.A.S., V.A.S., A.E.P. and A.V.T. acknowledge the support of their experimental work (Grant RSF 17-12-01050); N.M.C. and M.V.M. are grateful for the support of their theoretical work (Grant RSF 18-12-00438). The numerical calculations were carried out using computing resources of the federal collective usage center Complex for Simulation and Data Processing for Mega-science Facilities at NRC "Kurchatov Institute" (http://ckp.nrcki.ru/), the "Govorun" supercomputer of the Multifunctional Information and Computing Complex at LIT JINR (Dubna), and supercomputers at Joint Supercomputer Center of RAS (JSCC RAS).

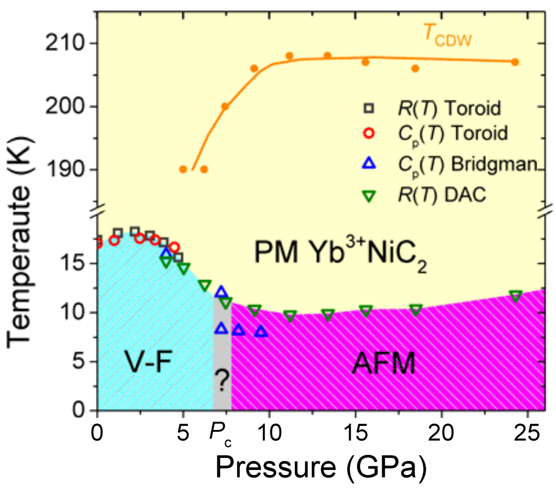

Fig.1 The pressure-temperature phase diagram of $YbNiC_2$. Yellow region (PM) - paramagnetic state with Yb^{3+}, blue region (V-F) - valence-fluctuating state of Yb ions with enhanced spin-fluctuations, magenta region (AFM) - antiferromagnetic Yb, grey region (?) - a possible coexistence of V-F and AFM phases, orange points (T_{CDW}) – charge density wave transition temperature (the orange line is a guide to the eye). Grey squares, red circles, blue and green triangles are the temperatures of anomalies deduced from the measurements of resistance and specific heat.

A new magnetic intermediate state, “B-phase”, in MnSi probed by small-angle neutron scattering and muon spin rotation

K. Ohishi[1], M. Ohkuma[2], M. Mito[2], M. Pardo-Sainz[3], S. Iwasaki[4], J. Akimitsu[4], Y. Cai[5,6], S. Yoon[6], K.M. Kojima[5,6], Y. Kousaka[4,7], K. Inoue[8], V. Laliena[4], J. Campo[2]

[1] *Neutron Science and Technology Center, Comprehensive Research Organization for Science and Society (CROSS), Tokai, Ibaraki, Japan*
[2] *Graduate School of Engineering, Kyushu Institute of Technology, Kitakyushu, Japan*
[3] *Aragón Nanoscience and Materials Institute (CSIC - University of Zaragoza), Zaragoza, Spain*
[4] *Research Institute for Interdisciplinary Science, Okayama University, Okayama, Japan*
[5] *TRIUMF, Vancouver, British Columbia, Canada*
[6] *University of British Columbia, Vancouver, British Columbia, Canada*
[7] *Department of Physics and Electronics, Osaka Prefecture University, Sakai, Osaka, Japan*
[8] *Chirality Research Center, Hiroshima University, Higashihiroshima, Japan*

Corresponding Author’s Email: Javier.Campo@csic.es

A violation of space-inversion symmetry entails a Dzyaloshinskii-Moriya interaction originating from the spin-orbit interaction, which stabilizes a chiral helimagnetic spin alignment. The chiral helimagnetic structures, forming only one-handed screw magnetic structures, have attracted attention because of the emergence of unique topological magnetic textures such as magnetic skyrmion lattices (SkL) [1] and chiral magnetic soliton lattices [2].

Recently, we suggested theoretically, that at low T the conical (CH) and forced-ferromagnetic (FFM) phases in cubic helimagnets, are not connected but are separated by another SkL, which could be metastable, and a new phase of unknown nature (*B-phase*) just below the critical field H_c at low T [3]. The theoretical prediction of the new SkL phase at low T is in good agreement with the experiments reported in ref [4,5]. On the other hand, by using careful ac susceptibility measurements at low temperature, we determined the magnetic phase diagrams of oriented crystals of MnSi [6]. It is consistent with the theoretical prediction for the new unknown low temperature phase.

In order to clarify the nature of this new phase at low T near critical field, we performed small-angle neutron scattering (SANS) measurements at TAIKAN in J-PARC and muon spin rotation (μSR) measurements at M15 in TRIUMF. Figure 1 shows the magnetic field dependence of the SANS patterns at 2 K [7]. At both 0.3 T (CH phase) and 0.5 T (*B-phase*), the SANS patterns show two peaks along the horizontal axis in Fig. 1(a) and (b) for $H \perp$ in coming neutron beam wave vector $\boldsymbol{k}_i$. These are the magnetic Bragg peaks of the conical state. On the other hand, as shown in Fig. 1(c) and (d), no diffraction peaks were observed for H // $\boldsymbol{k}_i$, in which, for example, a six-fold-symmetric diffraction pattern due to a formation of SkL is observed in *A*-phase (SkL). These results suggest the CH phase exists in *B-phase* and *B-phase* is different from *A*-phase near T_c. According to the μSR results, we found the internal magnetic field distribution in *B-phase* is apparently different from

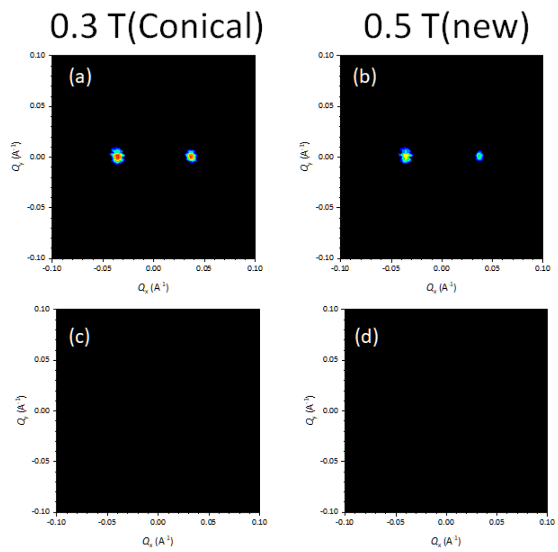

Fig.1 H dependence of the SANS patterns at 2 K (a,b) with the condition of H // [111] $\perp$ $\boldsymbol{k}_i$, and (c,d) that of H // [111] // $\boldsymbol{k}_i$ [7].

that in CH and FFM phases, consistent with the SANS results.

In the presentation, we will talk about the results of both SANS and μSR in detail, and discuss a spin texture in *B-phase*.

References

[1] S. Muhlbauer et al., Science 323, 915 (2009).
[2] T. Togawa et al., Phys. Rev. Lett. 108, 107202 (2012).
[3] V. Laliena and J. Campo, Phys. Rev. B 96, 134420 (2017).
[4] H. Oike et al., Nat. Phys. 10, 62 (2016).
[5] T. Nakajima et al., Phys. Rev. B 98, 014424 (2018).
[6] M. Ohkuma et al., in preparation.
[7] K. Ohishi et al., JPS Conf. Proc. 33, 011060 (2021).

Magnetization of MnSi in small fields: magnetic helixes rotation study

V.N. Krasnorussky[1], V.N. Narozhnyi[2]

[1] *Vereshchagin Institute for High Pressure Physics, RAS, Moscow, Russia*
[2] *10 Central Ave., Troitsk, Moscow, Russia*

Corresponding Author's Email: krasnorussky@mail.ru

Details of low magnetic field magnetization of MnSi single crystal were investigated below magnetic domains reorientation field H_{C1}. Static magnetization was measured for $H \parallel [0,0,1]$, [1,1,1] and [1,1,0] using vibrating sample magnetometer.

Clear magnetic anisotropy of magnetic behavior of MnSi at $H < H_{C1}(T)$ was found. Analysis of the obtained data has shown that the observed anisotropy is connected with at least two factors: (1) pronounced anisotropy of $H_{C1}(T)$, ($H_{C1}^{[001]}/H_{C1}^{[111]}$ varies from ~3 at $T = 5.5$ K to ~10 at $T \rightarrow T_N = 28.8$ K [1]); (2) different character of magnetic helixes rotation from virgin magnetic multi domains state (MDS) to the state with helix wave vector parallel to magnetic field, for $H \parallel [1,1,1]$ on one side, and $H \parallel [0,0,1]$ and [1,1,0] on the other.

Experimentally determined (for different directions of applied field) characters of magnetic helixes rotation were compared with the model proposed by Plumer and Walker [3]. Three parameters were used to fit the data: H_{C1}, $[\partial M/\partial H]_{MDS}$ and $[\partial M/\partial H]_{SDS}$. H_{C1} corresponds to maximum of experimentally determined magnetic susceptibility $\partial M(H)/\partial H$ in MDS. $[\partial M/\partial H]_{MDS}$ denotes initial magnetic susceptibility determined at $H \rightarrow 0$ in MDS. $[\partial M/\partial H]_{SDS}$ corresponds to magnetic susceptibility in magnetic single domain state (SDS) and can be obtained, e.g., from $M(H)$ curves at $H > H_{C1}(T)$ [1,2].

For initial virgin state for $H \parallel [0,0,1]$ and [1,1,0] an increase of magnetic field up to H_{C1} leads to gradual increase of magnetic susceptibility. Experimental curves $M(H)$ and $\partial M(H)/\partial H$ are rather well represented by dependencies proposed in [3]. At the same time for $H \parallel [1,1,1]$ magnetic susceptibility remains practically constant up to $H \sim H_{C1}/2$ (at least for $T = 5.5$ K). Only for $H_{C1}(T)/2 < H < H_{C1}(T)$ an increase of $\partial M(H)/\partial H$ was observed which corresponds to the rotation of magnetic helixes of all magnetic domains along H. $M(H)$ and $\partial M(H)/\partial H$ curves can be fitted by formulas [3] only roughly. Difference in character of magnetic helixes rotation for different directions of magnetic field described above was not reported earlier for MnSi.

Additionally $M(H)$ was measured for $H \parallel [1,1,0]$ when the sample was initially transformed to magnetic SDS by varying $H \parallel [1,1,1]$ from 0 up to 11 kOe and then back to 0 [1,2]. Then the sample was rotated to $H \parallel [1,1,0]$ at the same temperature. An estimation of the expected value of ratio of $M(H)$ slopes in the initial and final single domain states can be easely obtained taking into account that $\chi_\parallel / \chi_\perp \approx 0.56$ at $T = 5.5$ K [2], [$\chi_\perp$ and $\chi_\parallel$ correspond to $H\perp$ and $H \parallel (111)$-planes, containing magnetic moments, respectively]. It equals ≈ 0.85. Experimentally the value of ≈ 0.84 was observed for this case. This is in good agreement with the expectation described above and thus can be considered as one more confirmation of a possibility to preserve a magnetic SDS in MnSi even in zero field.

Our results for MnSi have been compared with the magnetization data reported for $Fe_{0.8}Co_{0.2}Si$ [4,5]. For $Fe_{0.8}Co_{0.2}Si$ a step-like increase of $\partial M(H)/\partial H$ was observed at $H \approx H_{C1}$ [4] (in cases when the sample was initially magnetized in magnetic fields perpendicular to the direction of H in which $M(H)$ then was measured). At the same time $M(H)$ curves with more gradual increase of $\partial M(H)/\partial H$ were reported for magnetization from magnetic virgin state [4,5]. Difference with the behavior observed for MnSi may be related with slightly higher value of magnetic anisotropy in $Fe_{0.8}Co_{0.2}Si$.

We thank S.M. Stishov for the possibility of using MnSi sample for experiments.

This investigation was performed in Vereshchagin Institute for High Pressure Physics RAS.

References

[1] V.N. Narozhnyi and V.N. Krasnorussky, *Zh. Eksp. Teor. Fiz. 143*, 900 (2013), *Sov. Phys. JETP*, *116*, No. 5 (2013).
[2] V.N. Narozhnyi and V.N. Krasnorussky, *Phys. Rev. B*. 91, 134403 (2015).
[3] M.L. Plumer and M.B. Walker, *J. Phys. C: Solid State Phys. 14*, 4689 (1981).
[4] K. Ishimoto, H. Yamauchi, M. Ohashi, et. al., *Jpn. J. Appl. Phys. 32 Suppl. 3,* 287 (1993).
[5] S.V. Grigoriev, V.A. Dyadkin, D. Menzel, et. al., *Phys. Rev. B 76,* 224424 (2007).

Split of the magnetic and crystallographic states in $Fe_{1-x}Rh_xGe$

D.O. Skanchenko[1,5], E.V. Altunbaev[1,2,5], A.V. Sidorov[2,5], G. Chaboussant[3], N. Martin[3], A.E. Petrova[5], D.A Salamatin[2,5], S.V. Grigoriev[1,4], A.V. Tsvyashchenko[2,5]

[1] *Konstantinov Petersburg Nuclear Physics Institute of National Research Centre «Kurchatov Institute», Gatchina, Russia*
[2] *Vereshchagin Institute of High Pressure Physics RAS, Troitsk, Moscow, Russia*
[3] *Laboratoire Leon Brillouin, CEA Saclay, Cedex, France*
[4] *Saint-Petersburg State University, Saint Petersburg, Russia*
[5] *Lebedev Physical Institute, RAS, Moscow, Russia*

Corresponding Author's Email: skanchenko_do@pnpi.nrcki.ru

The temperature evolution of the magnetic structure of $Fe_{1-x}Rh_xGe$ compounds was investigated by small-angle neutron scattering (SANS) and SQUID-magnetometry. These compounds, synthesized at high pressure, crystallize into a B20 noncentrosymmetric cubic structure [1]. The absence of an inversion symmetry in the arrangement of the magnetic atoms leads to the appearance of an antisymmetric Dzyaloshinskii – Moriya (DM) interaction and the formation of a magnetic spiral [2, 3]. In particular, the magnetic system of the FeGe compound is ordered into a magnetic spiral at temperatures below T_C = 278 K [4]. Nevertheless, it is known that the B20 binary compound RhGe exhibits weak ferromagnetism below T_m = 140 K and goes into a superconducting state at T_C = 4.5 K [5].

The data obtained by powder X-ray diffraction showed the split of the diffraction peaks of the diffraction patterns of $Fe_{1-x}Rh_xGe$ compounds in a wide concentration range, x ϵ [0.25–0.9]. In this case, no additional peaks are observed, which indicates the existence of identical structures with close cell parameters. In this case, the ratio of the intensities of the split peaks depends on x, while the splitting width remains practically unchanged. These facts, together with the performed theoretical analysis of the stability of the two detected phases, indicate that the structural splitting occurs within one crystallite, and is not a consequence of the crystallization of compounds with close values of the Rh(Fe)-concentration.

The SQUID magnetometry method also indicates the coexistence of two magnetic structures in each of the studied samples in the indicated concentration range with unique temperatures of magnetic ordering. To determine the types of magnetic structures, SANS measurements were carried out.

Based on the results of the studies, it was possible to establish that, in the concentration range x < 0.25 of $Fe_{1-x}Rh_xGe$ compounds, a helical structure is observed. The ordering temperature of the helical structure, as well as the wave vector of the magnetic helix, decreases with increase of x. A further increase in the Rh-concentration leads to the separation of the system into two structural and, as a consequence, magnetic phases. One of them, with a large cell parameter, corresponds to a ferromagnetic state at temperatures below T_C = 280 K for x = 0.25. The magnetic ordering temperature of the ferromagnetic phase drops to zero at x = 0.95. A structure with a smaller cell parameter is characterized by a helical magnetic ordering at a temperature T_C = 260 K for x = 0.25, which vanishes at x = 0.9. The magnitude of the wave vector of the helical structure decreases with increase of x from $k_s = 0.09 \pm 0.005$ nm^{-1} at x = 0 to zero at x = 0.5. This indicates the transition of the magnetic structure to the ferromagnetic state. A further increase in the parameter x leads to an increase of the wave vector value of the magnetic spiral. A similar behavior of the wave vector was found earlier for $Fe_{1-x}Mn_xGe$ and $Fe_{1-x}Co_xGe$ compounds [6, 7]. This phenomenon was interpreted as a flip of the magnetic chirality with a change in the concentration x and was later confirmed by theoretical calculations [8].

The authors are grateful for the support of the Russian Science Foundation (grant no. 17 12 01050).

References

[1] A.V. Tsvyashchenko, J. Less-Common Met. 99, L9 (1984).
[2] I.E. Dzyaloshinskii, Zh. Eksp. Teor. Fiz. 46 1420 (1964).
[3] P. Bak, M.H. Jensen, J. Phys. C13 L881 (1980).
[4] B. Lebech, et. al., Journal of Physics: Condensed Matter **1**, 6105 (1989).
[5] A.V. Tsvyashchenko et al., J. of All. and Comp., vol. 686, pp. 431–437 (2016).
[6] S.V. Grigoriev et al., Phys. Rev. Lett. 110, 207201 (2013).
[7] S.V. Grigoriev, S.-A. Siegfried et al., Phys. Rev. B 90, 174414 (2014).
[8] T. Koretsune, N. Nagaosa, and R. Arita, Sci. Rep. 5, 13302 (2015).

Complex magnetic order in the Nd(Tb)$Fe_3(BO_3)_4$ multiferroic revealed by the single crystal neutron diffraction

I.V. Golosovsky[1], A.I. Vasilev[1], A.A. Mukhin[2], E. Ressouche[3], V. Skumryev[4], I. Urcelay-Olabarria[5], I.A. Gudim[6] and L.N. Bezmaternykh[6]

[1] Konstantinov Petersburg Nuclear Physics Institute of National Research Centre «Kurchatov Institute», Gatchina, Russia
[2] Prokhvorov General Physics Institute, RAS, Moscow, Russia
[3] Université Grenoble Alpes, CEA, INAC-MEM, Grenoble, France
[4]Institució Catalana de Recerca i Estudis Avancats, Barcelona, Spain
[5] Fisika Aplikatua II, Zientzia eta Teknologia Fakultatea, Universidad del Pais Vasco, UPV/EHU, Bilbao, Spain
[6] Kirenskii Institute of Physics, Siberian Division of RAS, Krasnoyarsk, Russia

Corresponding Author's Email: golosovsky_iv@pnpi.nrcki.ru

The magnetic structure of the substituted multiferroic-ferroborates (Nd,Tb)$Fe_3(BO_3)_4$ was determined within the framework of a self-consistent refinement of the single-crystal neutron diffraction data [1]. In the refinement, strict restrictions were used, implied by the fact that the Fe sublattice induces a magnetic order in the sublattice of rare earth elements.

A small replacement of Nd by Tb leads to a reorientation of the main antiferromagnetic vector L from the basal plane towards the hexagonal axis. The refinement at 2 K shows the existence of distortions in the collinear antiferromagnetic spin arrangement of Fe. Therefore, in addition to the main antiferromagnetic vector L, the magnetic structure must be described by the additional combinations of spin components, allowed by symmetry. They coexist with certain components of the vector L and originate from the Fe-Fe exchange interactions of Dzyaloshinsky-Moriya. Based on the diffraction experiment, the values of these combinations as well as the main antiferromagnetic vector L were evaluated.

References

[1] I.V. Golosovsky et al., PRB, **99**, 134439, 2019.

Magnetic structures of $LiNi_{1-x}Co_xPO_4$ solid state

M.A. Semkin[1,2], N.V. Urusova[2,3], A.N. Pirogov[1,2]

[1] *M.N. Miheev Institute of Metal Physics, Ural Branch, RAS, Ekaterinburg, Russia*
[2] *Institute of Natural Sciences and Mathematics, Ural Federal University, Ekaterinburg, Russia*
[3] *Institute of Solid State Chemistry, Ural Branch, RAS, Ekaterinburg, Russia*

Corresponding Author's Email: semkin@imp.uran.ru

The Dzyaloshinskii-Moriya interaction has proved a key ingredient in explaining an induced or spontaneous electric polarization in several systems. A noncollinear incommensurate order of the magnetic moments results in a displacement of the oxygen ions situated between neighboring moments. A net displacement of charge is generated. Noncollinear order may appear as a consequence of competing interactions, so-called spin frustration. Such systems are associated with large magnetoelectric effects [1].

The lithium orthophosphate family Li*M*PO_4 (*M* = Mn, Fe, Co, Ni) is an excellent model system for studying the magnetoelectric effect in many ways. All family members exhibit commensurate near-collinear antiferromagnetic order as well as the magnetoelectric effect in their low-temperature and low-field ground state [2].

An incommensurate – commensurate antiferromagnetic transition has been found in the $LiNiPO_4$. The incommensurate phase occurs over a narrow range of intermediate temperatures (20.8–21.8) K between the C magnetic structure and a paramagnetic phase [3]. The transition to the paramagnetic state for $LiCoPO_4$ occurs without the incommensurate phase [4].

The aim of our work is to study the effect of replacement of nickel ions by cobalt ions on magnetic structures in the $LiNi_{1-x}Co_xPO_4$ solid state synthesized by a glycerol-nitrate method. The $LiNi_{1-x}Co_xPO_4$ samples with x = (0-0.5) were studied by MPMS, X-ray and neutron diffraction measurements.

The temperatures of magnetic phase transitions are decrease with increasing the cobalt concentration. Such the behavior of the magnetic phase transitions is explained by a magnetic ordering competition. In the $LiNi_{1-x}Co_xPO_4$ solid state with x = 0.5 the spin components of magnetic structure are oriented along the *c*- and *b*-axis. The partial doping of $LiNi_{1-x}Co_xPO_4$ by cobalt ions leads to a narrowing of the temperature interval where the incommensurate phase is established.

The reported study was funded by RFBR (project No. 19-32-60011).

References

[1] E. Fogh, O. Zaharko, J. Schefer, C. Niedermayer, S. Holm-Dahlin, M.K. Sorensen, A.B. Kristensen, N.H. Andersen, D. Vaknin, N.B. Christensen, and R. Toft-Petersen, *Physical Review B* ***99***, 104421 (2019).
[2] T.B.S. Jensen, N.B. Christensen, M. Kenzelmann, H.M. Rønnow, C. Niedermayer, J. Schefer, N.H. Andersen, K. Lefmann, M. Zimmermann, J. Li, J.L. Zarestky, and D. Vaknin, *Physical Review B* ***79***, 092412 (2009).
[3] R. Toft-Petersen, J. Jensen, T.B.S. Jensen, N.H. Andersen, N.B. Christensen, C. Niedermayer, M. Kenzelmann, M. Skoulatos, M.D. Le, K. Lefmann, S.R. Hansen, J. Li, J.L. Zarestky, and D. Vaknin, *Physical Review B* ***84***, 054408 (2011).
[4] E. Fogh, R. Toft-Petersen, E. Ressouche, C. Niedermayer, S.L. Holm, M. Bartkowiak, S. Sloth, O. Prokhnenko, F.W. Isaksen, D. Vaknin, and N.B. Christensen, *Physical Review B* ***96***, 104420 (2017).

SESSION 4. SPIN EXCITATIONS IN HELIMAGNETS.

Electron spin resonance of an interacting spinon liquid with uniform Dzyaloshinski-Moriya interaction

A.I. Smirnov[1], K. Yu. Povarov[2], T.A. Soldatov[1], Ren-Bo Wang[3], O.A. Starykh[3]

[1] *P. L. Kapitza Institute for Physical Problems RAS, Moscow, Russia*
[2] *Laboratory for Solid State Physics, ETH Zürich, Zürich, Switzerland*
[3] *Department of Physics and Astronomy, University of Utah, Salt Lake City, Utah, USA*

Corresponding Author's Email: smirnov@kapitza.ras.ru

The S=1/2 Heisenberg antiferromagnetic spin chain has quantum critical ground state with absence of the ordered spin components and power law decay of the correlation function. This ground state and its excitations are often described in terms of quantized fractionalized dynamic spin structures referred to as spinons. The concept of spinons is derived by a theory based on exact procedure of Bethe Ansatz [1,2], as well as via effective low-energy field theory formulated in terms of neutral spin-1/2 fermions [3]. The theory of free fermions in spin S=1/2 antiferromagnetic chains is supported by numerous experiments, e.g., by observation of the continuum of S=1 excitations (so called two-spinon continuum) in neutron scattering experiments [4] or by finding the field-dependent soft modes appearing within the continuum of longitudional fluctuations in a magnetic field [3].

A specific fine structure of the two-spinon continuum of transverse fluctuations was predicted for a spin S=1/2 chain with a uniform Dzyaloshinsky-Moriya (DM) interaction. This interaction causes a shift of the continuum in q-space by a characteristic wavevector $q_{DM}=D/(Ja)$. Here D is the Dzyaloshinsky-Moriya parameter and a - interspin distance. The shift results in an energy gap $\Delta=\pi D/2$ and a doublet of electron spin resonance (ESR) frequencies

$$\nu_{\pm} = (g\mu_B H \pm \Delta)/2\pi\hbar \tag{1}$$

The frequencies $\nu_{\pm}$ correspond to lower and upper boundaries of the continuum of a purely Heisenberg (i.e. D=0) chain at the wavevector q_{DM}. The ESR doublet $\nu_{\pm}$ was indeed experimentally observed in [5,6], confirming the fermion nature of the ground state and its excitations.

Now we report the measurements of ESR spinon doublet for an almost ideal 1D S=1/2 Heisenberg antiferromagnet $K_2CuSO_4Br_2$ in a strong magnetic field, where we observe a significant deviation of ESR modes $\nu_{\pm}$ from the simple relation (1).

According to a recent theoretical study [7], the continuum boundaries should be shifted from the positions corresponding to noninteracting spinons due to the interaction of the backscattering type. The parameter of this interaction u is defined by a Hamiltonian term

$$V= -\frac{u}{2}\int dx\,\left(\psi^\dagger_{R\uparrow}\psi_{R\downarrow}\psi^\dagger_{L\downarrow}\psi_{L\uparrow}+\psi^\dagger_{R\downarrow}\psi_{R\uparrow}\psi^\dagger_{L\uparrow}\psi_{L\downarrow}\right) -\frac{u}{4}\int dx\,(\psi^\dagger_{R\uparrow}\psi_{R\uparrow}-\psi^\dagger_{R\downarrow}\psi_{R\downarrow})(\psi^\dagger_{L\uparrow}\psi_{L\uparrow}-\psi^\dagger_{L\downarrow}\psi_{L\downarrow}) \tag{2}$$

which describes backscattering interaction between right/left moving spinons $\psi_{R/Ls}$ (here s is the spin index ↑,↓), living near the right/left Fermi points of the one-dimensional Fermi surface, correspondingly [7]. The additional interaction-induced gap between the lower and upper boundaries of the continuum is represented by $\Delta_{int}=uM/\mu_B$, where M is the magnetic moment per unit length. Using these relations of [7] we can explain the deviation of the experimentally observed frequencies of the spinon doublet from the above interaction-neglecting relation (1). Fig.1 demonstrates the difference between the observed ESR frequencies and Larmor frequency $\nu_{Lar} = g\mu_B H/2\hbar$ measured in different magnetic fields. This difference should be constant when the interaction between spinons is neglected (this behavior is illustrated by horizontal dashed lines at ±8.7 GHz). The fit according to the predictions of [7] with the parameter u=3.5·10^5 cm/s demonstrates a good quantitative correspondence of the experimental doublet frequencies to the theory with a reasonable value of the parameter u which is about 50% larger than spinon velocity. The fit is presented by solid lines. Fig. 2 shows the frequency dependence of the intensity ratio of the components of the ESR doublet along with the theoretical prediction [7] for this ratio. At u=0, i.e. without spinon interaction, this ratio should be equal to one in this frequency range. A good correspondence of the data and theory on this graph explains the dramatic vanishing of the upper component of the doublet, which was a puzzling result of the experiment [6].

These observations confirm the fundamental concept of interacting fractionalized fermions-spinons as a basic feature of the ground state of S=1/2 Heisenberg antiferromagnetic chains in a dielectric crystal. The value of the spinon backscattering parameter is found experimentally. These experimental consequences of the spinon-spinon interaction reveal a Fermi-liquid (not a Fermi-gas) behavior of quasiparticles in a 1D antiferromagnet. Thus the collective excitations of 1D Heisenberg S=1/2 antiferromagnetic chain demonstrate amazing analogy with the ensemble of electrons in a normal metal and specific Silin spin waves [8] in a normal metal.

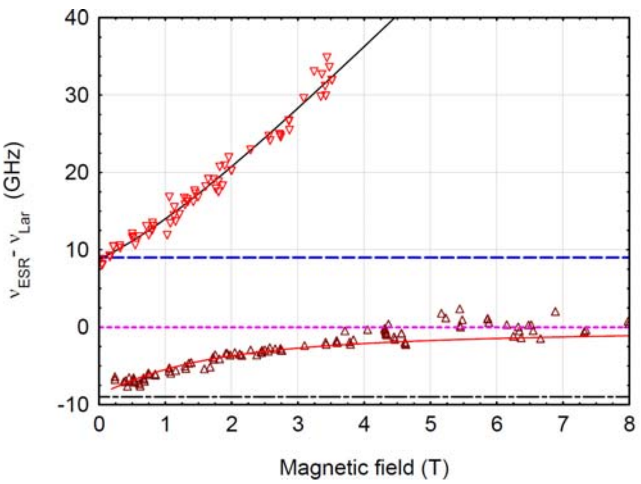

Fig.1 $_{ESR}$-ν_{Lar} vs magnetic field at T=0.5 K
Solid lines-theory, dashed – see text

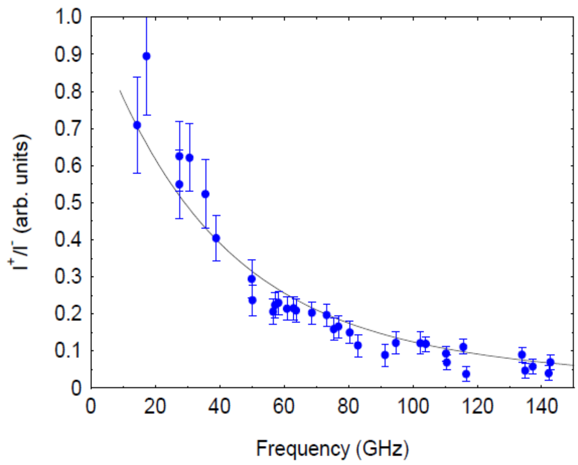

Fig.2 Ratio of intensities within spinon doublet vs frequency. T=0.5 K

Support of RSCF Grant 17-02-01505 is acknowledged.

References

[1] L. Faddeev and L. Takhtajan, Physics Letters A 85, 375 (1981).
[2] G. Müller, H. Thomas, H. Beck, and J.C. Bonner, Phys. Rev. B 24, 1429 (1981).
[3] D.C. Dender, P.R. Hammar, D.H. Reich, C. Broholm, G. Aeppli, Phys. Rev. Lett. 79, 1750 (1997).
[4] D.A. Tennant, R.A. Cowley, S.E. Nagler, A.M. Tsvelik, Phys. Rev. B 52, 13368 (1995).
[5] K.Yu. Povarov, A.I. Smirnov, O.A. Starykh, S.V. Petrov, A.Ya. Shapiro, Phys. Rev. Lett. 107, 037204 (2011).
[6] A.I. Smirnov, T.A. Soldatov, K.Y. Povarov, M. Hälg, W. E. A. Lorenz, A. Zheludev, Phys. Rev. B 92, 134417 (2015).
[7] A. Keselman, L. Balents, and O.A. Starykh, Physical Review Letters 125 (2020).
[8] V.P. Silin, Sov. Phys. JETP 6, 945 (1958); V.P. Silin, Sov. Phys. JETP 8, 870 (1959).

Spin waves of the conical helix in cubic chiral magnets

M. Garst

Institute of Theoretical Solid State Physics, Dresden, Germany
Karlsruhe Institute of Technology , Karlsruhe, Germany

Corresponding Author's Email: markus.garst@kit.edu

Non-reciprocity of spin waves arises if the magnetic response function $\chi''(\mathbf{q},E)$ is not invariant under a reversal of the wavevector **q**. This can be attributed to either an asymmetric spin wave dispersion $\varepsilon(\mathbf{q}) \neq \varepsilon(-\mathbf{q})$ or an asymmetry of the spectral weight distribution. In cubic chiral magnets like MnSi, FeGe, and Cu_2OSeO_3 non-reciprocity of spin waves arises due to the Dzyaloshinskii-Moriya interaction. In the field-polarized phase their nonreciprocal dispersion at low energies is given by a shifted parabola with a minimum at a finite wavevector. The spin wave gap decreases as a function of decreasing field and vanishes at the transition to the conical helix state. In this talk, I will discuss the non-reciprocity of spin waves for the emerging conical helix. Due to the periodicity of the helimagnetic order, the spin wave dispersion is backfolded giving rise to a magnetic Brillouin zone. As a consequence, the magnon dispersion for wavevector q_z along the helix axis becomes symmetric in the conical helix phase, $\varepsilon(q_z)= \varepsilon(-q_z)$. However, we theoretically demonstrate that the spectral weight distribution remains asymmetric even down to zero magnetic field, which is experimentally confirmed by polarized inelastic neutron scattering. In the presence of a wavevector with a finite perpendicular component, $\mathbf{q}_\perp$, we show that the spectrum recovers non-reciprocity due to an interplay of Dzyaloshinskii-Moriya and dipolar interaction, see Fig. 1. This non-reciprocity emerges for wavevectors that are small compared to the helix wavevector Q. This regime can be probed by inelastic Brillouin light scattering (BLS) experiments, which confirmed quantitatively the theoretical predictions [3].

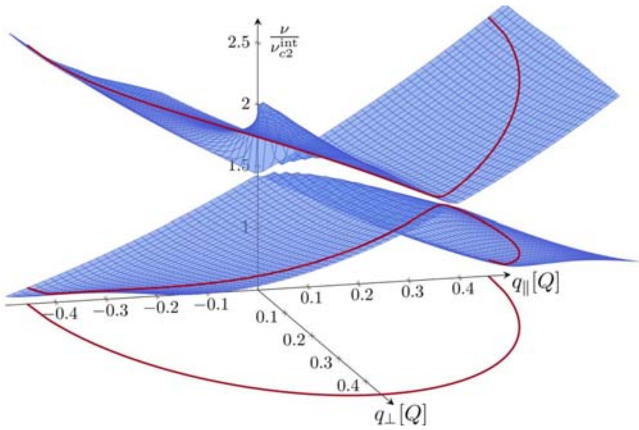

Fig. 1: Non-analytic and non-reciprocal spin wave dispersion of the conical helix. The red line indicates the excitations that are accessible in the BLS experiment.

References

[1] T. Weber et al., *Field dependence of nonreciprocal magnons in chiral MnSi*, Phys. Rev. B 97, 223304 (2018).
[2] T. Weber et al., Polarized inelastic neutron scattering of nonreciprocal spin waves in MnSi, Phys. Rev. B 100, 060404(R) (2019).
[3] N. Ogawa et al., Nonreciprocity of spin waves in the conical helix state, PNAS 118, e20229227118 (2021).

Dynamics of chiral solitons driven by polarized currents

V. Laliena[1], S. Bustingorry[2], J. Campo[3]

[1] *Department of Applied Mathematics, University of Zaragoza, Zaragoza, Spain*
[2] *Instituto de Nanociencia y Nanotecnología, CNEA-CONICET, Centro Atómico Bariloche, Río Negro, Argentina*
[3] *Aragon Nanoscience and Materials Institute (CSIC-University of Zaragoza) and Condensed Matter Physics Department, University of Zaragoza, Zaragoza, Spain*

Corresponding Author's Email: sbusting@cab.cnea.gov.ar

Chiral solitons are localized metastable topological magnetic structures whose metastability is greatly enhanced in monoaxial helimagnets by the Dzyaloshinskii-Moriya interaction (DMI) and the uniaxial magnetic anisotropy. Though topological textures in general provide a very interesting playground for new spintronics phenomena, how to properly create and control single chiral solitons is still unclear. We show here that chiral solitons in monoaxial helimagnets, characterized by a uniaxial DMI, can be stabilized with external magnetic fields. The dynamics of the soliton is governed by the Landau-Lifshitz-Gilbert (LLG) equation. It is shown that a solution of the LLG exists in which the soliton moves steady, i.e. with constant velocity, in response to a polarized electric current, provided the induced spin-transfer torque has a dissipative (nonadiabatic) component, in analogy to what happens with domain walls. The stationary solutions exist only if the applied current density is lower than a critical value, which depends on the applied field and on the DMI strength. We show that the structure of the soliton depends on the applied current density in such a way that steady motion exists only if the applied current density is lower than a critical value, beyond which the soliton is no longer stable [1]. These results are contrasted against micromagnetic simulations. The destruction of the soliton by supercritical currents can be a very useful tool to manipulate information in potential spintronic devices that use the presence or absence of solitons as bits.

References

[1] V. Laliena, S. Bustingorry and J. Campo, Sci. Rep. *10*, 2043 (2020).

SESSION 5. EXOTIC SPIN STRUCTURES (SKYRMIONS, ETC.).

Mean-field approach for square skyrmion lattice in centrosymmetric tetragonal magnets

O.I. Utesov

Konstantinov Petersburg Nuclear Physics Institute of National Research Centre «Kurchatov Institute», Gatchina, Russia
Saint-Petersburg School of Physics, Mathematics, and Computer Science, HSE University, Saint-Petersburg, Russia
Saint-Petersburg State University, Saint Petersburg, Russia

Corresponding Author's Email: utiosov@gmail.com

Individual skyrmions, their ordered arrays – skyrmion lattices (SkL), and various other topologically non-trivial structures are among the most extensively studied objects of contemporary physics. In magnetism, they are mostly investigated experimentally and theoretically in chiral non-centrosymmetric systems, for example, MnSi. However, it was shown recently that in centrosymmetric frustrated helimagnets skyrmion lattices can be also observed, which results in, e.g., the giant topological Hall Effect [1].

From the theoretical point of view, it is generally believed that topological phases with SkL can be stabilized by a subtle interplay between various interactions in the system, such as exchange interaction, Dzyaloshinskii-Moriya interaction, Zeeman energy, magnetic anisotropy, biquadratic exchange, etc. Usually, the importance of thermodynamical spin fluctuations is also highlighted.

The present study was motivated by the recent experimental research [2], where square SkL has been observed in the tetragonal centrosymmetric $GdRu_2Si_2$ compound. Incommensurate structures modulation vectors were shown to lie in the tetragonal plane with absolute values being equal to 0.22 in the reciprocal lattice units.

We propose a mean-field theoretical approach for the description of the high-temperature part of the phase diagram of tetragonal frustrated centrosymmetric helimagnets [3]. The main ingredients are the following: exchange interaction, magneto-dipolar interaction, and Zeeman energy in the magnetic field along the c-axis. Importantly, in $GdRu_2Si_2$ magnetic Gd ions are in 3+ state, with L=0 and S=7/2. Then, the dipolar forces should play a significant role in the magnetic properties of this compound. Moreover, both compass anisotropy terms (which were shown to stabilize topologically-nontrivial structures at low temperatures in tetragonal magnets [4,5]) and single-ion anisotropy can be easily included in the analysis.

We show that in the considered model dipolar forces play a role of momentum-dependent biaxial anisotropy, and due to them, various phases emerge in the temperature-magnetic field phase diagram: (i) single-modulated sinusoidal spin-density wave (1S), (ii) vortex-like combination of two 1S structures with perpendicular modulation vectors (2S), (iii) single-modulated spiral (1Q), (iv) conical helix (XY), and (v) double-modulated superposition of spirals (2Q). The last one can become topologically non-trivial (square SkL) in the external magnetic field. Using the Landau-like expansion of the free energy in powers of order parameters up to the quartic terms, we analytically calculate the boundaries between various phases.

The phase diagram properties are essentially dependent on the axis hierarchy. Without additional anisotropy terms, for $GdRu_2Si_2$ lattice and modulation vectors, magneto-dipolar interaction provides the easy axes perpendicular to the modulation vectors and the middle c-axis for both of them. In this case, the phase diagram shown in figure (1) was obtained (here we use parameters values estimated for $GdRu_2Si_2$ using the results of Ref. [2]). The conical XY phase emerges in the region of the phase diagram, where our small order parameters expansion fails. So, the question “whether the SkL phase stability domain is terminated at low temperatures or not” remains an open one.

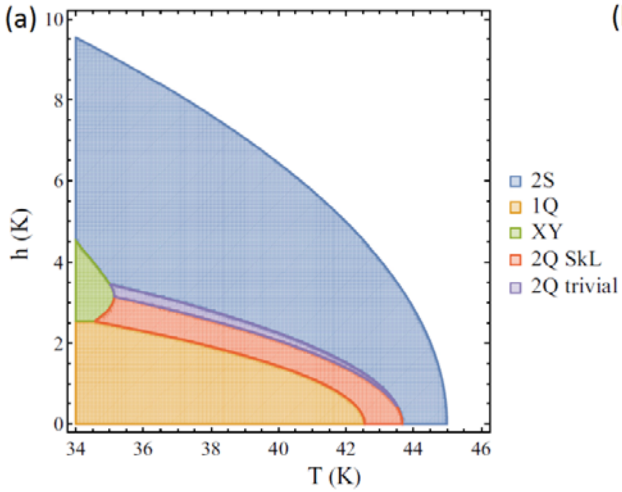

Fig.1

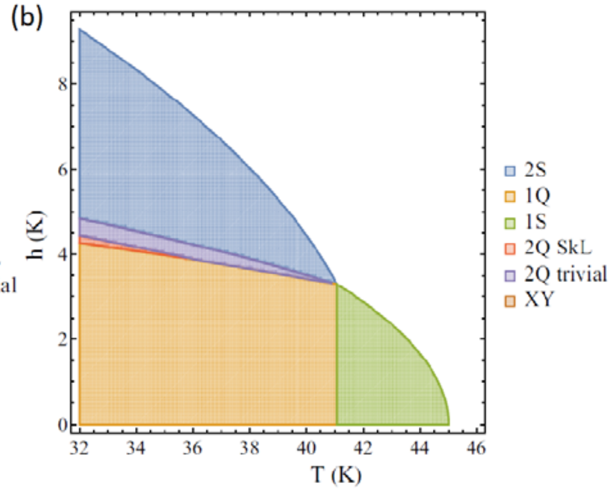

Fig.2

If the easy-axis single-ion anisotropy is taken into account, the easy and the middle axes can be swapped. In this case, we observe the phase diagram shown in figure (2). There is a polycritical point, where five phases (including paramagnetic one) are in equilibrium. The topologically non-trivial part of the 2Q phase has a shape of a small wedge, which appears only at lower, than polycritical, temperatures. The conical XY phase can be possibly stable at even lower temperatures, which are not drawn in the plot. Importantly, this type of phase diagram describes the main features of the experimentally observed one in $GdRu_2Si_2$ [2].

To conclude, in the present study it was shown that the magneto-dipolar interaction can be a key element in the stabilization of nanometer-sized skyrmions in frustrated helimagnets on centrosymmetric tetragonal lattices. Moreover, we observe the similar stabilization of usual hexagonal SkL in triangular frustrated antiferromagnets due to dipolar forces, which can be relevant to, e.g., experimental findings of Ref. [1].

I am grateful to V.A. Ukleev and A.V. Syromyatnikov for valuable discussions. The reported study was supported by the Foundation for the Advancement of Theoretical Physics and Mathematics “BASIS”.

References

[1] T. Kurumaji, et al., Science 365, 914 (2019).
[2] N.D. Khanh, et al., Nat. Nanotechnol. 15, 444 (2020).
[3] O.I. Utesov, Phys. Rev. B 103, 064414 (2021).
[4] S. Hayami and Y. Motome, Phys. Rev. B 103, 024439 (2021).
[5] Z. Wang, Y. Su, S.-L. Lin, and C.D. Batista, Phys. Rev. B 103, 104408 (2021).

Spirals and skyrmions in magnets and their emergent electromagnetism

M. Hirschberger

The University of Tokyo, Tokyo, Japan

Corresponding Author's Email: hirschberger@ap.t.u-tokyo.ac.jp

Spirals and skyrmion textures are complex magnetic states in solids which, through coupling to the Fermi sea, may generate fascinating non-dissipative electromagnetic responses. A unified description is currently being developed through the concept of quantum-mechanical Berry curvature, in this case corresponding to an emergent magnetic field $\boldsymbol{\Omega}_\mathbf{k}$ living in reciprocal space ($\boldsymbol{k}$-space).

We used extensive material search, as well as transport and resonant x-ray scattering experiments, to identify a new, centrosymmetric family of rare earth intermetallics with spirals and skyrmion spin-vortices of very short characteristic length scale (<5 nanometers) [1,2].

In the model compound Gd_2PdSi_3, $\boldsymbol{\Omega}_\mathbf{k}$ is shown to arise from a combination of canted spin texture and degeneracies in $\boldsymbol{k}$-space [3]. Moreover, spin-dynamics induced by an applied AC current in the related $Gd_3Ru_4Al_{12}$ generate a phase-shifted voltage. This emergent inductance grows as the lateral dimensions of the sample become smaller and smaller – contrary to the case of, e.g., a classical coil-based inductor [4].

References

[1] T. Kurumaji *et al.*, Science 365, 914-918 (2019).
[2] M.H. *et al.*, Nat. Commun. 10, 5831 (2019).
[3] M.H. *et al.*, Phys. Rev. Lett. 125, 076602 (2020).
[4] T. Yokouchi *et al.*, Nature 586, 232–236 (2020).

Helitronics and (anti-)skyrmions in magnets with DMI

J. Masell

RIKEN Center for Emergent Matter Science (CEMS), Wako, Japan

Corresponding Author's Email: an.masell@riken.jp

Magnetic textures can establish various orders beyond trivial ferromagnetism, including non-collinear order as in the helical phase, where the magnetization rotates in space in a plane that is defined by some q-vector, see panel (a). Such lamellar phases are interesting from a fundamental perspective but usually considered useless for applications. In turn, non-coplanar textures like skyrmions, panel (b), attracted a lot of attention as they might potentially be useful for storage devices or unconventional computing. Moreover, their quantized real-space winding number gives rise to a topological Hall.

In my talk, I will present our recent theoretical and experimental studies of these magnetic objects. We opened the field of "*helitronics*", showing that helical phases can be combed by electric currents [1] and suggest a new mechanism for detecting defects in the helical order [2]. We then smoothly switch to skyrmions by first discussing properties of skyrmions in the helical phase [3], followed by a presentation of our recent real-space observations of moving skyrmions in thermal gradients [4], static defects in skyrmion-strings [5], and our discovery of a new class of materials that hosts antiskyrmions [6], see panel (c).

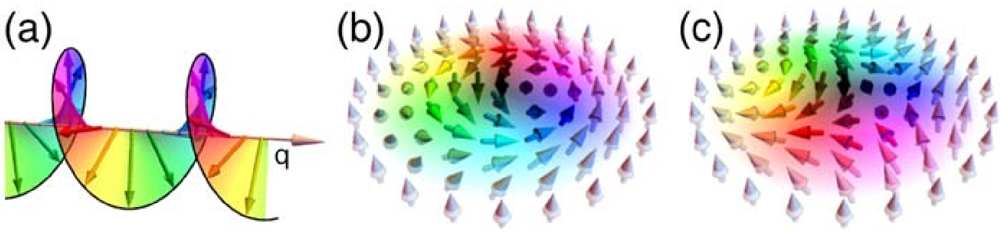

Fig.1 Helix (a), skyrmion (b), and anti-skyrmion (c). Taken from Refs. [1] and [7].

References

[1] J. Masell, X.Z. Yu, N. Kanazawa, Y. Tokura, and N. Nagaosa. Phys. Rev. B 102, 180402(R) (2020).
[2] M. Stepanova*, J. Masell*, E. Lysne*, *et al.*, arXiv preprint 2103. 14449.
[3] R. Knapman, D.R. Rodrigues, J. Masell, K. Everschor-Sitte. arXiv preprint 2105. 06859.
[4] X.Z. Yu, F. Kagawa, J. Masell, *et al.*, preprint DOI: 10.21203/rs.3.rs-156692/v1.
[5] X.Z. Yu*, J. Masell*, F.S. Yasin, *et al.*, Nano Lett. 20, 10, 7313-7320 (2020).
[6] K. Karube, L.C. Peng, J. Masell, *et al.*, Nature Materials 20, 335-340 (2021).
[7] J. Masell, K. Everschor-Sitte. Chapter 7 in: Topics in Applied Physics, vol. 138, Springer, Cham (2021).

Magnonic goos-hänchen effect induced by one dimensional solitons

V. Laliena[1], J. Campo[2]

[1] *Department of Applied Mathematics, University of Zaragoza, Zaragoza, Spain*
[2] *Aragon Nanoscience and Materials Institute (CSIC-University of Zaragoza) and Condensed Matter Physics Department, University of Zaragoza, Zaragoza, Spain*

Corresponding Author's Email: laliena@unizar.es

The magnon spectral problem is solved in terms of the spectrum of a diagonalizable operator for a generic class of magnetic states that includes several types of domain walls and the chiral solitons of monoaxial helimagnets. Focusing on the isolated solitons of monoaxial helimagnets, it is shown that the spin waves scattered (reflected and transmitted) by the soliton suffer a lateral displacement analogous to the Goos-Hänchen effect of optics. The displacement is a fraction of the wavelength, but can be greatly enhanced by using an array of well separated solitons. Contrarily to the Goos-Hänchen effect recently studied in some magnetic systems, which takes place at interfaces between different magnetic systems, the effect predicted here takes place at the soliton position, what it is interesting from the point of view of applications since solitons can be created at different places and moved across the material. This kind of Goos-Hänchen displacement is a consequence of the dependence of the phase shift on the transverse component of the wave vector, which does not appear in other known one dimensional systems, as quantum mechanical particles moving in a one dimensional potential. However, it is not particular of the solitons of monoaxial helimagnets, but it is generic for a class of magnetic states, including domain walls in systems with interfacial Dzyaloshinskii-Moriya interaction. The conditions under which the soliton induced Goos-Hänchen effect takes place are discussed [1].

Grants No PGC-2018-099024-B-I00-ChiMag from the Ministry of Science and Innovation (MCIN) of Spain, SpINS-OTR2223 from CSIC/MCIN and DGA-M4 from the Diputación General de Aragón, are acknowledged.

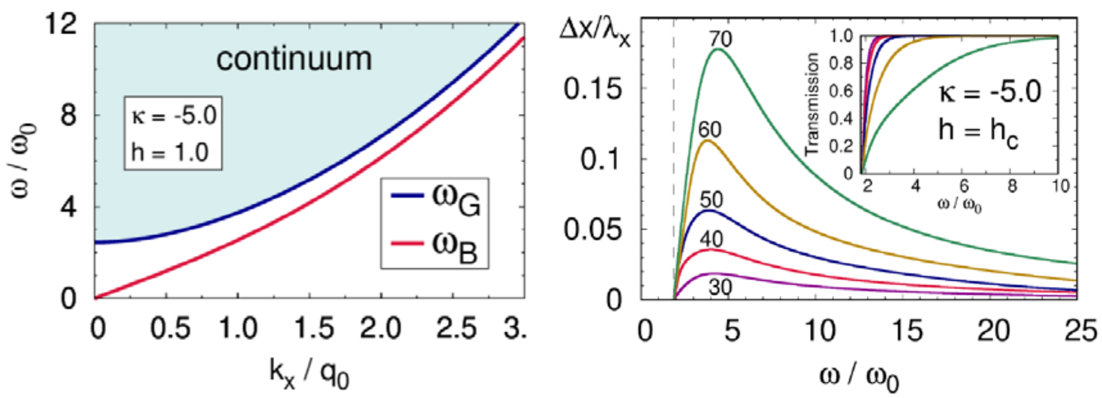

Fig.1 Magnon spectrum as a function of the transverse wave vector (left) and lateral shift as a function of frequency for several values of the incidence angle (right).

References

[1] V. Laliena and J. Campo, arXiv:2011.07886 (2020).

Evolution of the skyrmion lattice in MnGe-based compounds under high pressure

E.V. Altynbaev[1,2,3,4], D.O. Skanchenko[1,3,4], A. Heinemann[5], N. Martin[6], A. Tsvyashenko[4], S. Grigoriev[1,2,3,4]

[1] *Konstantinov Petersburg Nuclear Physics Institute of National Research Centre «Kurchatov Institute», Gatchina, Russia*
[2] *Saint-Petersburg State University, Saint Petersburg, Russia*
[3] *National Research Centre «Kurchatov Institute», Moscow, Russia*
[4] *Institute for High Pressure Physics, Troitsk, Moscow, Russia*
[5] *Helmholtz Zentrum Geesthacht, Geesthacht, Germany*
[6] *Laboratoire Leon Brillouin, CEA Saclay, Cedex, France*

Corresponding Author's Email: altynbaev_ev@pnpi.nrcki.ru

We have grown $Mn_{1-x}Fe_xGe$ compounds with $x = 0.1$ and 0.3 using high pressure synthesis [1]. The appearance of the skyrmion lattice (SkX) in MnGe-based compounds with Fe-replacement of Mn atoms was observed under external magnetic field within the wide field range at temperatures far below T_C [2]. The increase of the field range of its presence is accompanied by the linear increase of the DMI in $Mn_{1-x}Fe_xGe$ with increase of Fe concentration [3-5]. The temperature range of the presence of the SkX is most likely connected to the intrinsic instability of the magnetic structure found for MnGe and Fe-doped compounds [6].

Here we report on the evolution of the magnetic system of the $Mn_{1-x}Fe_xGe$ compounds with x = 0.1 and 0.3 under external magnetic field and qasi-hydrostatic pressure up to 1.0 GPa. As the result the (H-T) phase diagram has been plotted for each compound. The phase diagrams for $Mn_{0.7}Fe_{0.3}Ge$ at ambient pressure and under pressure P = 1.0 GPa are presented in Fig.1a and Fig.1b, respectively.

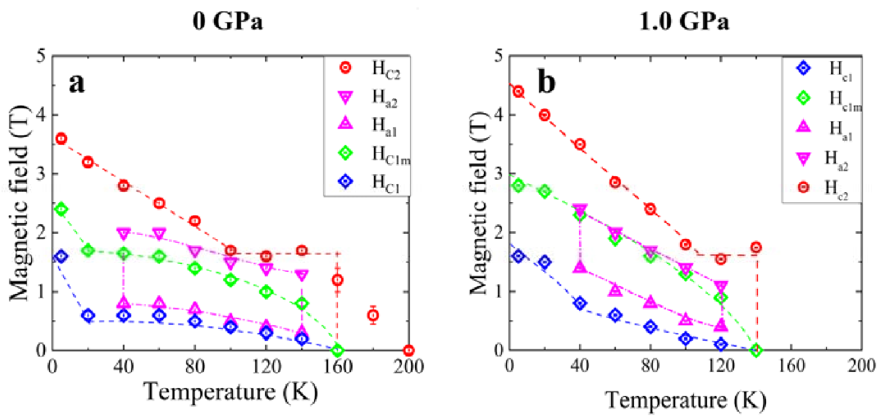

Fig.1 (H-T) phase diagrams of $Mn_{1-x}Fe_xGe$, with x = 0.3 at ambient pressure (a), under pressure P = 1.0 GPa (b).

With pressure increase all of the critical fields increases at low temperatures for both compounds, while the ordering temperature decreases. The temperature and field ranges of the existence of the SkX decreases with pressure increase. We believe that these facts are connected to the stabilization of the magnetic structure of MnGe-based compounds under pressure. This process is opposite to the Fe-replacement of Mn atoms despite the fact that the lattice constant continues to decrease. We hope that these findings will serve for further development of the theoretical description of the influence of DMI for the appearance of the A-phase in $Mn_{1-x}Fe_xGe$ solid solutions with *x* increase.

Authors thank for support the Russian Scientific Foundation (Grant No 17-12-01050).

References

[1] A.V. Tsvyashchenko, J. Less-Common Met. 99, L9 (1984).
[2] E. Altynbaev, et al., Physical Review B vol. 101 N. 100404(R) (2020).
[3] T. Koretsune, et al., Sci. Rep. 5, 13302 (2015).
[4] J. Gayles, et al., Phys. Rev. Lett. 115, 036602 (2015).
[5] T. Kikuchi, et al., Phys. Rev. Lett. 116, 247201 (2016).
[6] E. Altynbaev, et al., Physical Review B vol. 94 N. 17 (2016).
[7] D. Skanchenko, et al., J. of All. and Comp. vol. 865 N. 158606 (2021).

Frustration-driven magnetic fluctuations as the origin of the low-temperature skyrmion phase in $Co_7Zn_7Mn_6$

V. Ukleev[1], K. Karube[2], P.M. Derlet[3], C.N. Wang[4], H. Luetkens[4], D. Morikawa[2], A. Kikkawa[2], L. Mangin-Thro[5], A.R. Wildes[5], Y. Yamasaki[6], Y. Yokoyama[6], L. Yu[1,8,9], C. Piamonteze[10], N. Jaouen[11], Y. Tokunaga[12], H.M. Ronnow[13], T.-h. Arima[2,12], Y. Tokura[2,14,15], Y. Taguchi[2], and J.S. White[1]

[1] Laboratory for Neutron Scattering and Imaging, Paul Scherrer Institute, Villigen, Switzerland
[2] RIKEN Center for Emergent Matter Science, Wako, Japan
[3] Condensed Matter Theory Group, Paul Scherrer Institute, Villigen, Switzerland
[4] Laboratory for Muon Spin Spectroscopy, Paul Scherrer Institute, Villigen, Switzerland
[5] Institut Laue-Langevin, Grenoble, France
[6] Research and Services Division of Materials Data and Integrated System, National Institute for Materials Science, Tsukuba, Japan
[7] PRESTO, Japan Science and Technology Agency, Kawaguchi, Japan
[8] Laboratory for Ultrafast Microscopy and Electron Scattering, Institute of Physics, Ecole Polytechnique Federale de Lausanne, Lausanne, Switzerland
[9] Laboratory of Nanoscale Magnetic Materials and Magnonics, Institute of Materials, Ecole Polytechnique Federale de Lausanne, Lausanne, Switzerland
[10] Swiss Light Source, Paul Scherrer Institute, Villigen, Switzerland
[11] Synchrotron SOLEIL, Saint-Aubin, Gif-sur-Yvette Cedex, France
[12] Department of Advanced Materials Science, University of Tokyo, Kashiwa, Japan
[13] Laboratory for Quantum Magnetism, Institute of Physics, Ecole Polytechnique Federale de Lausanne, Lausanne, Switzerland
[14] Department of Applied Physics, University of Tokyo, Tokyo, Japan
[15] Tokyo College, University of Tokyo, Tokyo, Japan

Corresponding Author's Email: victor.ukleev@psi.ch

The competition between the magnetic interactions in non-centrosymmetric compounds results in complex phase diagrams. Thus, the interplay between exchange interaction, antisymmetric Dzyaloshinskii-Moriya interaction (DMI) and anisotropy can stabilize long range modulated magnetic phases hosting helical, conical and skyrmion lattice (SkL) orders. Skyrmions are of particular interest since they can be manipulated easily by external current pulses with ultra-low current densities, microwave fields and temperature gradient. Moreover, the typical size of a skyrmion varies in range from a few to a few hundred nm making them promising candidates for spintronics applications [1]. In chiral cubic helimagnets, SkL phases are usually stabilized by thermal fluctuations over a narrow region directly below the magnetic ordering temperature T_c [2]. Due to often being touted for use in applications, there is a high demand to identify new ways to stabilize equilibrium skyrmion phases far below Tc where they may display an enhanced robustness against external perturbation due to a larger magnetic order parameter. Recently a class of chiral magnets with *β*-Mn structure was found to be skyrmion-hosting where, moreover, SkL formation in CoZnMn compounds occurs close to the room temperature or even above [3]. Frustration of the Mn site in Co-Zn-Mn alloys results into the spin-glass transition observed at T_g~10 K in $Co_8Zn_8Mn_4$ and at T_g~30 K in $Co_7Zn_7Mn_6$ [3–6]. Moreover, an additional low-temperature frustration-induced equilibrium skyrmion phase (LTSk) has been recently found in the latter [5]. Here we report on complementary study of dynamical frustration effects in $Co_7Zn_7Mn_6$ by the quantum beam probes: muon spin relaxation spectroscopy (μSR), magnetic diffuse wide-angle neutron scattering (MDNS), x-ray magnetic circular dichroism (XMCD), resonant elastic small-angle x-ray scattering (REXS) and Lorentz transmission electron microscopy (TEM). The μSR experiment revealed the increment of the relaxation rate just above the temperature of the spin-glass transition caused by frustration-induced dynamics. This additional slow fluctuation regime is reminiscent of the thermal fluctuations near T_c and triggers stabilisation of the disordered equilibrium skyrmion phase. Analysis of neutron MDNS on powdered sample suggests that a quasi-static magnetic disorder persist in $Co_7Zn_7Mn_6$ up to the room temperature. Element-specific XMCD and REXS data points to the unambiguous conclusion that the frustration is driven by Mn sublattice, while Co atoms keep long-range helimagnetic order even below the spin-glass transition temperature. Finally, bulk magnetization and Lorentz TEM probes show unimportance of the cubic anisotropy at low temperatures, thus excluding anisotropy-driven LTSk stabilization mechanism that was previously suggested for Cu_2OSeO_3 [6].

In summary, we unveil a direct correlation between the stability of its second skyrmion phase – stable far from T_c, and a concomitant enhancement of an underlying magnetic fluctuation rate that is driven by geometric magnetic frustration. The influences of other leading skyrmion stability mechanisms, such as those derived from thermal fluctuations and low T cubic anisotropies, are shown to be weak in this system. We therefore advance the existence of a fundamental mechanism for stabilizing topological skyrmions in $Co_7Zn_7Mn_6$ chiral magnet that draws upon magnetic frustration as the key ingredient [7].

V.U., P.M.D., L.Y., H.M.R. and J.S.W. acknowledge funding from the SNSF Sinergia CRSII5_171003 NanoSkyrmionics. This research was supported in part by JSPS Grant- in-Aids for Scientific Research (Grant No. 20K15164) and JST CREST (Grant No. JPMJCR1874 and JPMJCR20T1). The research leading to this result has been supported by the project CALIPSOplus under the Grant Agreement 730872 from the EU Framework Programme for Research and Innovation HORIZON 2020.

References

[1] Nagaosa, N., Tokura, Y., Nature Nanotechnology, 8(12), 899 (2013).
[2] Mühlbauer, S. et al., Science 323, 915–919 (2009).
[3] Tokunaga, Y., et al., Nature Communications, 6, 7638 (2015).
[4] Karube, K., et al., Nature Materials, 15, 1237 (2016).
[5] Karube, K., et al., Science Advances, 4(9), eaar7043 (2018).
[6] Bocarsly, J., et al., Physical Review Materials, 3(1), 014402 (2019).
[7] Chacon, A. et al., Nature Physics 14, 936 (2018).
[8] Ukleev, V., et al., npj Quantum Materials 6.1, 1-8 (2021).

Triple and double helix vs. skyrmion lattice in two-dimensional non-centrosymmetric magnets.

V. Timofeev[1,2], D. Aristov[1,3]

[1] Konstantinov Petersburg Nuclear Physics Institute of National Research Centre «Kurchatov Institute», Gatchina, Russia
[2] Saint-Petersburg Electrotechnical University LETI, Saint-Petersburg, Russia
[3] Saint-Petersburg State University, Saint Petersburg, Russia

Corresponding Author's Email: timofeeviktor@gmail.com

It is commonly assumed that a lattice of skyrmions, emerging in two-dimensional noncentrosymmetric magnets in external magnetic fields, can be represented as a sum of three magnetic helices. In order to test this assumption, we compare two approaches to a description of regular skyrmion structure. We construct (i) a triangular lattice of Belavin-Polyakov-like skyrmions within the stereographic projection method, and (ii) a deformed triple helix defined with the use of elliptic functions [1]. In comparison with triple helix consideration, stereographic projection approach effectively takes into account interaction between individual skyrmions.

The estimates for the energy density and magnetic profiles show that these two methods are nearly identical at zero temperature for intermediate magnetic fields. However, at higher magnetic fields, near the transition to topologically trivial uniform phase, the stereographic projection method is preferable, particularly, for the description of disordered skyrmion liquid phase [2]. To testify our conclusions about preference of the stereographic projection approach, we also consider a situation of square skyrmion lattice [3] and compare it with the model of double helix.

We suggest to explore the intensities of the secondary Bragg peaks to obtain the additional information about the magnetic profile of individual skyrmions. We estimate these intensities to be several percents of the main Bragg peak at high magnetic fields [4].

References

[1] V.E. Timofeev, A.O. Sorokin, and D.N. Aristov, Phys. Rev. B **103**, 094402 (2021).
[2] P. Huang, T. Schönenberger, M. Cantoni, et al. Nature Nanotechnology **15**, 761 (2020).
[3] K. Karube, J.S. White, N. Reynolds, et al. Nature materials 15.12 (2016).
[4] T. Adams, S. Mühlbauer, C. Pfleiderer, et al. Phys. Rev. Lett. **107**, 217206 (2011).

Majorana bound states induced by antiferromagnetic skyrmion textures

S.A. Díaz[1,2], J. Klinovaja[2], D. Loss[2], S. Hoffman[2,3]

[1] *Faculty of Physics, University of Duisburg-Essen, Duisburg, Germany*
[2] *Department of Physics, University of Basel, Basel, Switzerland*
[3] *Department of Physics, University of Florida, Gainesville, Florida, USA*

Corresponding Author's Email: sebastian.diaz@uni-due.de

Majorana bound states are zero-energy states predicted to emerge in topological superconductors and intense efforts seeking a definitive proof of their observation are still ongoing. A standard route to realize them involves antagonistic orders: a superconductor in proximity to a ferromagnet. Here, we show that this issue can be resolved using antiferromagnetic rather than ferromagnetic order. We propose to use a chain of antiferromagnetic skyrmions, in an otherwise collinear antiferromagnet, coupled to a bulk conventional superconductor as a novel platform capable of supporting Majorana bound states that are robust against disorder. Crucially, the collinear antiferromagnetic region neither suppresses superconductivity nor induces topological superconductivity, thus allowing for Majorana bound states localized at the ends of the chain. Our model introduces a new class of systems where topological superconductivity can be induced by editing antiferromagnetic textures rather than locally tuning material parameters, opening avenues for the conclusive observation of Majorana bound states.

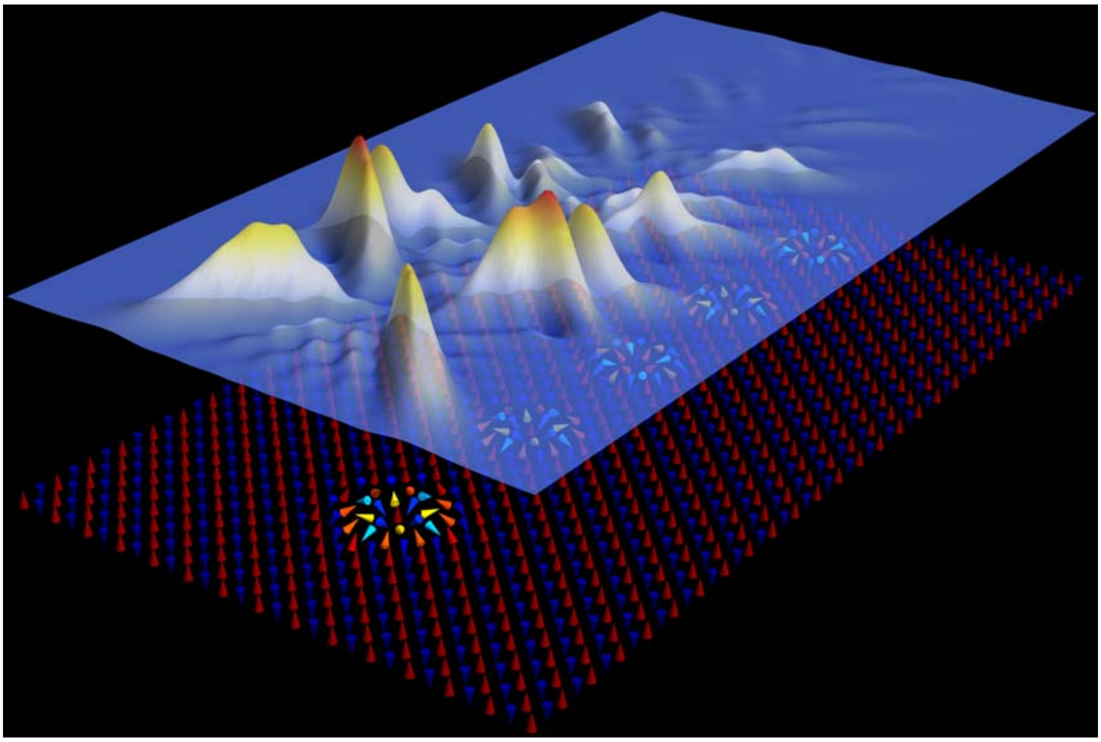

Fig.1 Probability density of a Majorana bound state (top) localized at one end of a chain of antiferromagnetic skyrmions embedded in a collinear antiferromagnet (bottom).

References

[1] S.A. Díaz, J. Klinovaja, D. Loss, and S. Hoffman, arXiv:2102.03423.

Metastability and creation of single chiral soliton states in monoaxial helimagnets

S.A. Osorio[1], V. Laliena[2], J. Campo[3], S. Bustingorry[1]

[1] *Instituto de Nanociencia y Nanotecnología, CNEA-CONICET, Centro Atómico Bariloche, Río Negro, Argentina*
[2] *Department of Applied Mathematics, University of Zaragoza, Zaragoza, Spain*
[3] *Aragon Nanoscience and Materials Institute (CSIC-University of Zaragoza) and Condensed Matter Physics Department, University of Zaragoza, Zaragoza, Spain*

Corresponding Author's Email: santiago.osorio@cab.cnea.gov.ar

Topology and chirality are the principal avenues along which the field of spintronics currently transits. While topology is usually related to the presence of robust states against continuous or weak fluctuations, chirality refers to the handedness of a state that are commonly encountered in systems whose inversion symmetry is broken. In magnetic systems, both, topological and chiral features, meet together in systems where the antisymmetric Dzyaloshinskii-Moriya interaction plays a key role.

In monoaxial chiral helimagnets the Dzyaloshinskii-Moriya interaction favors inhomogeneous distributions of the magnetization with chiral modulations termed chiral solitons. These localized magnetization textures have the structure of a 360° domain wall and crystallize at low magnetic field leading to the emergence of a chiral soliton lattice [1]. In a magnetic field perpendicular to the chiral axis the system undergoes a phase transition to the uniform state at a critical field [2]. Above this critical field value, a single chiral soliton comprises the lowest level excitation over the stable uniform state, surviving as a metastable configuration [3]. The single chiral soliton states have interesting properties for potential applications in spintronic devices and are thus important to study their creation and stability.

We study the metastability of individual chiral solitons through micromagnetic simulations based on the Landau-Lifshitz-Gilbert equation. The characteristic field for metastability limit and the instability mechanism are determined. Finally, we study a feasible protocol to obtain a state with a single chiral soliton from the chiral soliton lattice. We show that using spin-polarized currents chiral solitons in the chiral soliton lattice can be pushed against each other and it is possible to annihilate the solitons one-by-one in a controlled way. A state with one chiral soliton can be obtained by these means for a suitable choice of the external field and the current density. Remarkably, our proposal exhibits a strong robustness against the magnetization distribution in the initial state, even if the initial state is metastable. Our proposal could be relevant in the study of metastable solitons from both the experimental and technological applications.

References

[1] Y. Togawa, Y. Kousaka, K. Inoue and J. Kishine, J. Phys. Soc. Jpn. 85, 112001 (2016).
[2] V. Laliena, J. Campo, J. Kishine, A.S. Ovchinnikov, Y. Togawa, Y. Kousaka, and K. Inoue, Phys. Rev. B 93, 134424 (2016).
[3] V. Laliena, S. Bustingorry and J. Campo, Sci. Rep. 10, 2043 (2020).

Exotic spin structure in the pseudogap phase of high-T_c superconductor $HgBa_2CuO_4$

V.E. Dmitrienko, V.A. Chizhikov

A.V. Shubnikov Institute of Crystallography,
FSRC "Crystallography and Photonics" RAS, Moscow, Russia

Corresponding Author's Email: dmitrien@crys.ras.ru

A possible intra-unit-cell magnetic ordering in the so-called pseudogap state of different high-Tc superconductors is discussed for many years (see recent survey [1] and references therein). Very exotic theoretical models were suggested but they are still controversial. For example, it was supposed that the magnetic order could be related with Oxygen ions [2]. Experimentally, the problem is that it is difficult to detect any details of weak antiferromagnetic-type order when the magnetic unit cell coincides with the atomic one.

In this report we suggest a reasonable magnetic symmetry of intra-unit-cell spin arrangement and perform *ab initio* simulations with QUANTUM ESPRESSO DFT package for typical high-T_c superconductor $HgBa_2CuO_4$. Our main idea is that the atoms in highly symmetrical positions should have zero dipole magnetic moments but could have non-zero higher moments (toroidal, *etc*.). Similar idea was used in [3] for the hidden order in URu_2Si_2. It was found that the considered magnetic phase is energetically more favorable then the non-magnetic state. We have also calculated the magnetic structure factors for many reflections and have found the best conditions for neutron diffraction.

This work was supported by the Ministry of Science and Higher Education of the Russian Federation within the State assignment FSRC "Crystallography and Photonics" RAS.

References

[1] P. Bourges, D. Bounoua, J. Jeong, L. Mangin-Thro, Y. Sidis, "Evidence for Intra-Unit Cell Magnetism in Superconducting Cuprates: a Technical Assessment", Journal of Physics: Conference Series 1316, 012003 (2019).
[2] A.S. Moskvin, "Pseudogap phase in cuprates: Oxygen orbital moments instead of circulating currents", JETP Letters 96, 385 (2012).
[3] V.E. Dmitrienko, V.A. Chizhikov, "Hidden order in URu_2Si_2: Symmetry-induced antitoroidal vortices", Phys. Rev. B. 98, 165118 (2018).

Spiral texture of the helical ground state of a frustrated chiral magnet

A. Cano

Institut NEEL, CNRS, Grenoble, France

Corresponding Author's Email: andres.cano@neel.cnrs.fr

The langasites with chemical formula Ba3MFe3Si2O14 (M = Sb, Nb, Ta) are multichiral magnets. They crystallize in a non-centrosymmetric P321 space-group symmetry where the Fe atoms form a triangular latticeof triangles in the ab plane. The antiferromagnetic interactions between the spins within these Fe triangles lead to a non-collinear 120° order that is helically modulated along c due to competing out-of-plane exchange couplings. The chirality of the 120° order is determined by additional magnetocrystalline single-ion anisotropy and Dzyaloshinskii–Moriya interactions, which links the chirality of the helical modulation to the chirality of the crystal lattice. I will discuss the emergence of an unprecedented texture of such a peculiar 120° helical order in Ba3TaFe3Si2O14 due to the application of a magnetic field [1].

References

[1] M. Ramakrishnan et al., npj Quantum Mater. 4, 60 (2019).

SESSION 6. THIN FILMS AND SURFACE EFFECTS.

Spin waves non reciprocity in magnetic ultrathin films, magnonic crystals and nanostructures as a tool to quantify interfacial Dzyaloshinskii-Moriya interaction

G. Carlotti

Dipartimento di Fisica e Geologia, Università di PerugiaPerugia, Italy

Corresponding Author's Email: giovanni.carlotti@unipg.it

It is well known that the breaking of translational symmetry in thin films, together with the axial character of the magnetic field, may induce a marked non-reciprocal character of both the frequency and the amplitude distribution of spin waves propagating in opposite directions in the so-called Damon-Eshbach configuration [1].

After a short review of the different causes of spin-waves non-reciprocity, in this talk I will focus on the non-reciprocity induced by interfacial Dzyaloshinskii-Moriya interaction (DMI). It relies on the fact that the chirality of waves propagating along ±x, as shown in Fig. 1, is opposite so that their frequencies are different and such a difference can be easily measured by Brillouin light scattering (BLS) so this technique has affirmed in the last decade as the most versatile tool to quantify interfacial DMI [2]. Starting from the results of both virtual experiments, based on micromagnetic simulations, and real BLS experiments, it will be shown that the effect of DMI can be quantified not only in the case of plane films, but also for artificially nanostructured systems consisting, for example, of isolated magnetic nanostructures where the presence of DMI induces a substantial red-shift of the eigenmodes frequencies and the appearance of new peaks in BLS spectra, corresponding to odd modes that would remain invisible in the absence of DMI [3]. In addition, it will be shown how DMI strongly affects the band structure of 1D magnonic crystals consisting of either arrays of interacting Permalloy nanowires [4] or a chain of Nèel skyrmions [5].

Financial support from the EMPIR programme 17FUN08-TOPS, co-financed by the Participating States and from the European Union's Horizon 2020 research and innovation program, is kindly acknowledged.

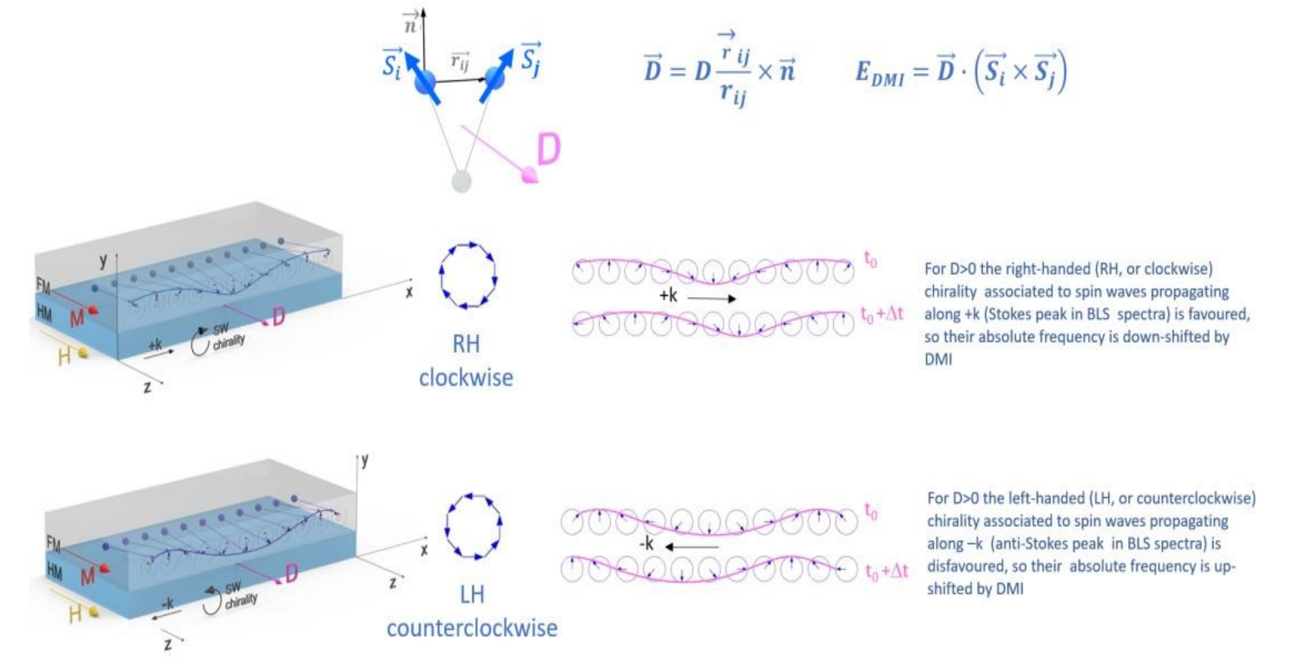

Fig. 1 Sketch of a spin wave, in the Damon-Eshbach configuration, propagating towards the positive x direction, with a wavevector + k, in the ferromagnetic (FM) film. All the individual magnetic moments (blue arrows) are precessing anticlockwise around the z-axis, i.e. around the direction of the static magnetization and of the external field H. Due to the phase delay from one spin to the next, moving from left to right, the chirality associated with the SW is clockwise, that is favoured by a positive DMI (magenta D vector). In thin bilayer films of FM / HM, the latter couples two neighbouring spins via a three-site exchange mechanism with the underlying atom of the heavy-metal (HM, white atoms). As a consequence, the absolute frequency of spin waves with + k is down-shifted in frequency. (b): SW propagating along the negative x-direction. i.e. with wavevector -k, are characterized by an anticlockwise chirality, the is disfavoured by a positive D, resulting in an up-shift of their absolute frequency. Note that the sign of D depends on the convention chosen in relation with the Hamiltonian which can be either positive or negative. Here we use the plus sign in the Hamiltonian, so that, in terms of domain walls (DWs), positive D corresponds to Nèel DWs with the right-handed (RH or clockwise) chirality (↑→↓ or ↓←↑), while negative D corresponds to left-handed (LH or counterclockwise) chirality (↑←↓ or ↓→↑).

References

[1] P. Landeros, R.A. Gallardo, and G. Carlotti, "Spin-wave Nonreciprocity", in The 2021 Magnonics Roadmap, Journal of Physics: Condensed Matter, in press.

[2] M. Kuepferling, A. Casiraghi, G. Soares, G. Durin, F. Garcia-Sanchez, L. Chen, C.H. Back, C.H. Marrows, S. Tacchi, G. Carlotti, "Measuring interfacial Dzyaloshinskii-Moriya interaction in ultra thin films", review article, arXiv.org cond-mat > arXiv:2009.11830

[3] R. Silvani, M. Alunni, S. Tacchi, G. Carlotti, "Effect of the interfacial Dzyaloshinskii-Moriya interaction on the spin waves eigenmodes of isolated stripes and dots magnetized in-plane: a micromagnetic study", Appl. Sci. 11, 2929 (2021).

[4] R. Silvani, M. Kuepferling, S. Tacchi and G. Carlotti, "Impact of the interfacial DMI on the band structure of one-dimensional artificial magnonic crystals: a micromagnetic study", JMMM submitted.

[5] Mattia Bassotti, Master thesis in Physics, University of Perugia (2021).

Effect of interfacial Dzyaloshinskii-Moriya interaction on polarized neutrons reflection

D.A. Tatarskiy

Institute for Physics of Microstructures RAS, Nizhny Novgorod, Russia
Lobachevsky State University of Nizhny Novgorod, Nizhny Novgorod, Russia

Corresponding Author's Email: tatarsky@ipmras.ru

It was pointed out [1] that even in a high-symmetry lattice, where the antisymmetric Dzyaloshinskii–Moriya interaction (DMI) would normally vanish, this interaction is present in the vicinity of any lattice defect. Hence, based on these considerations, one may expect that the DMI substantially influences the magnetic microstructure of polycrystalline materials with a large defect density. In a sense, microstructural defects act as a source of additional local chiral interactions, similar to the above mentioned (intrinsic) DMI in noncentrosymmetric crystals. The impact of such defect-induced DMI has been studied both theoretically [2] and experimentally [3] in small angle neutron scattering (SANS). It leads to small chiral variations of magnetization fluctuations. These variations have a helix–like type, so the effect on SANS observed when the magnetic field is applied perpendicular to the scattering plane.

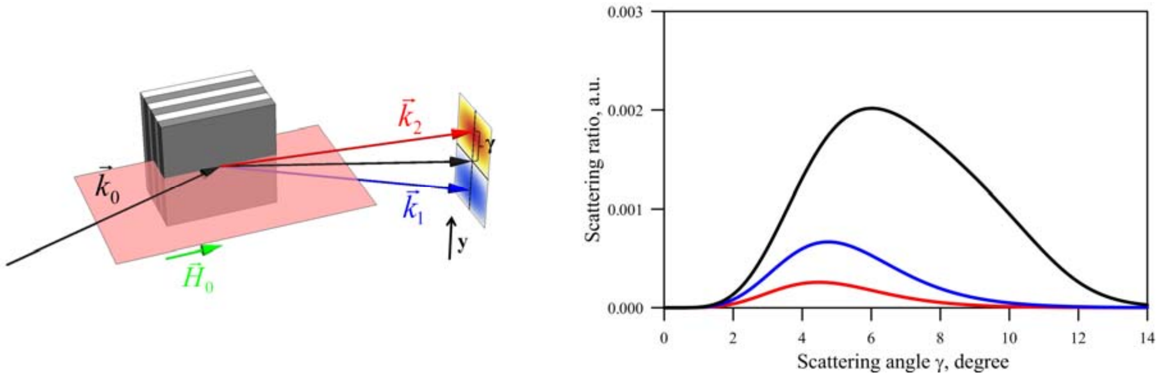

(a) *(b)*

Fig.1 (a) – experimental scheme proposal; (b) – chiral/Specular differential cross-section ratio vs. transversal scattering angle γ. Red, blue and black curves for D = 0.5, 1.0 and 1.5 erg/cm^2 consequently.

On the other hand thin polycrystalline films with heavy metal–ferromagnet interfaces shows a strong interfacial–induced DMI [4]. Homochiral magnetic textures are studied in them by Brillouin light scattering [5] or Lorentz transmission electron microscopy [6]. In case of small enough interfacial DMI constant the fluctuations of magnetization near saturation in a high homogeneous external field can also be calculated.

Let the external magnetic field is applied along x axis in plane of the film with interfacial DMI (Fig. 1a). The magnetization is determined by balance of torque equation

$$\left[\vec{M}(\vec{r})\times\vec{H}_{eff}(\vec{r})\right]=0 \qquad (1)$$

where $\vec{M}(\vec{r})$ is magnetization distribution and $\vec{H}_{eff}(\vec{r})$ is an effective field. It is defined as the functional derivative of the magnetostatic energy-density functional. We consider the case when the external field is applied in plane of the film along x axis. The z axis is oriented along the normal to the film. The Eq.(1) can be linearized near saturation. We suppose every crystalline in the film is characterized by its own uniaxial anisotropy direction. Such random magnetocrystalline anisotropy is the source for small fluctuations of the magnetization near saturation. The solution for small variations $M_{y,z}$ can be given in Fourier form [7]

$$\begin{cases} \widetilde{M}_y = \dfrac{\widetilde{H}_{Ay}\left(A + 4\pi \dfrac{q_z^2}{q^2}\right) - \widetilde{H}_{Az} B}{A^2 + 4\pi \dfrac{q_y^2 + q_z^2}{q^2} - q_y^2 L_{DMI}^2}, \\ \widetilde{M}_z = \dfrac{\widetilde{H}_{Az}\left(A + 4\pi \dfrac{q_y^2}{q^2}\right) - \widetilde{H}_{Ay} B^*}{A^2 + 4\pi \dfrac{q_y^2 + q_z^2}{q^2} - q_y^2 L_{DMI}^2}, \end{cases} \tag{2}$$

where $A = \dfrac{H_0}{4\pi M_0} + L_{ex}^2 q^2$ and $B = 4\pi \dfrac{q_y q_z}{q^2} + i q_y L_{DMI}$ and $\widetilde{H}_{Ay,z}$ are the Fourier components of the random magnetocrystalline anisotropy field. The chiral-dependent part of neutron cross-section in case of neutron polarization along x axis is

$$\frac{\partial \sigma(\vec{q})^{(\chi)}}{\partial \Omega} \sim \operatorname{Im}\left(\vec{q} \cdot \left[\tilde{\tilde{\vec{M}}}^* \times \tilde{\tilde{\vec{M}}}\right]\right). \tag{3}$$

The resulting ratios of chiral to specular part of the differential scattering cross-section for different typical interfacial DMI values are shown on Fig.1b.

Comparing [2,3] we see the difference in chiral fluctuation for small transversal magnetization deviations in case of the bulk DMI and the interfacial DMI. In bulk materials the chiral part of deviations is a long range helix-like textures. Thus the asymmetry in polarized neutron scattering exists when the external field applied along this helix axis and perpendicular to the scattering wavevector. The iDMI give rise to the long range cycloidal-like fluctuations. That is why the asymmetry effect appears when the external field applied in the specular reflection plane.

Thus we show that the random magnetocrystalline anisotropy with interfacial DMI in polycrystalline films give rise to chiral part of magnetic ripple. This ripple can be detected by GISANS experiment.

This research was supported by the Russian Science Foundation (Grant #21-12-00271).

References

[1] A. Arrott, J. Appl. Phys. 34, 1108 (1963).
[2] A. Michels, D. Mettus, D. Honecker, K.L. Metlov, *Phys.Rev.B* 94, 054424 (2016).
[3] A. Michels, D. Mettus, I. Titov et al., *Phys. Rev.B* 99, 014416 (2019).
[4] H. Yang, A. Thiaville, S. Rohart, A. Fert, M. Chshiev, Phys. Rev. Lett. 115, 267210 (2015).
[5] M. Belmeguenai, J.-P. Adam, Y. Roussigne et al., Phys. Rev. B 91, 180405(R) (2015).
[6] L.-C. Peng, Y. Zhang, S.-L. Zuo et al., Chin. Phys.B 27 066802 (2018).
[7] D.A. Tatarskiy, J.Magn. Magn.Mater. 509, 166899 (2020).

Direct observation of topological Hall effect in Co/Pt nanostructured films

M.V. Sapozhnikov[1,2], N.S. Gusev[1], S.A. Gusev[1], D.A. Tatarskiy[1,2], Yu.V. Petrov[3], A.G. Temiryazev[4], A.A. Fraerman[1]

[1] *Institute for Physics of Microstructures RAS, Nizhny Novgorod, Russia*
[2] *Lobachevsky State University of Nizhny Novgorod, Nizhny Novgorod, Russia*
[3] *Saint Petersburg State University, Saint Petersburg, Russia*
[4] *Kotelnikov Institute of Radioengineering and Electronics RAS, Fryazino Branch, Fryazino, Russia*

Corresponding Author's Email: msap@ipmras.ru

We investigate the topological Hall effect (THE) in dense artificial lattices of magnetic skyrmions. Skyrmion lattices are formed in the process of magnetization reversal of nanostructured multilayer Co/Pt films with perpendicular magnetic anisotropy. The method has been developed for the simultaneous measurement of the Hall effect and the magneto-optical Kerr effect (MOKE) in samples for direct observation of THE. The method is based on the idea that topological effects at zero and optical frequencies have different values.

Although to date the observation of the topological Hall effect has been reported in a large number of experimental works, there is still the problem to experimentally distinguish the anomalous and THE. Usually one assumes a-proiri some form of anomalous effect, which is then subtracted from the total signal. In our work, we analytically estimate the value of the topological contribution to magneto-optical effects and found that it is small. This allowed us to reasonably use the method of simultaneous measurement of MOKE and the Hall effect to extract THE values during the experiment.

The analytical estimation of the topological contribution to MOKE is done in the classical approximation used previously to calculate DC THE [1]. The additional approximation is that the frequency of the electric field exciting the electrons (ω) is much higher than the frequency of exchange splitting of electrons (ω_R), which is quite consistent with the optical frequencies. The value of the effective topological magnetic field in this case is $B = \Phi_0\psi(\omega_R/\omega)^2$, where Φ_0 is the quantum of the magnetic flux, and ψ is the local density of the topological charge of the magnetization distribution. Thus, an additional factor $(\omega_R/\omega)^2 \sim 10^{-2} \div 10^{-4}$ appears in the expression for B, which is absent in the expression for the effective DC THE field.

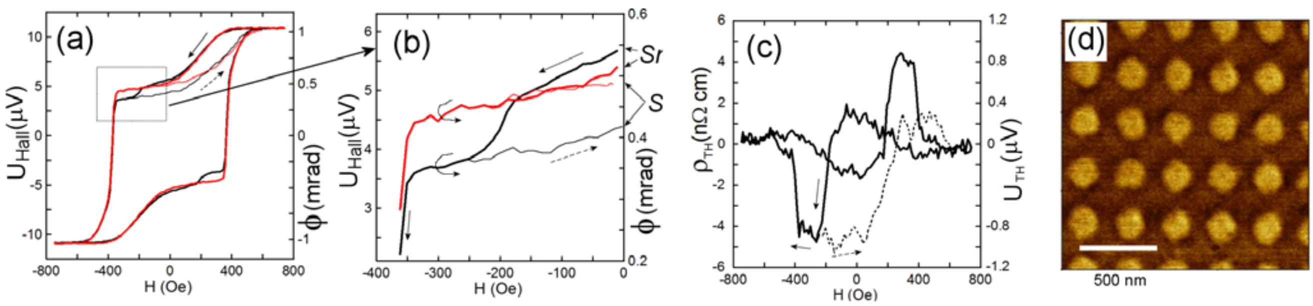

Fig. 1. Experimental data for sample 1 (grating period 300 nm, irradiated spot diameter 200 nm) (a) MOKE hysteresis loops (red line) and Hall effect (black line) plotted on the same scale. Minor loops are drawn with thinner lines. (b) Detail view of a step on the Hall curve. (c) Hysteresis curve of the topological Hall effect. The dashed line is the minor hysteresis loop. (d) Magnetic force microscope image of the MB (skyrmion) lattice.

Nanostructured samples of multilayer films (Co 0.5 nm/Pt 1 nm)$_5$ were prepared to measure the THE. By the method of local irradiation with He^+ ions, the value of this anisotropy was locally reduced (the diameter of the irradiated spots is 200÷300 nm, the He^+ fluence is $2 \div 4 \times 10^{15}$ cm^{-2}). Such structures demonstrate the formation of dense lattices of magnetic bubbles (MB) in the process of magnetization reversal (Fig. 1d). Preliminary micromagnetic calculations showed that the topology of arising MB depends on the distribution of the He + ion fluence over the area of the illumination spot. If the fluence of He^+ is concentrically distributed (leading to concentrically modulated value of the anisotropy) the forming MB have the topology of a magnetic skyrmion. This fact is experimentally confirmed by Lorentz transmission electron microscopy (LTEM) methods (Fig.2a).

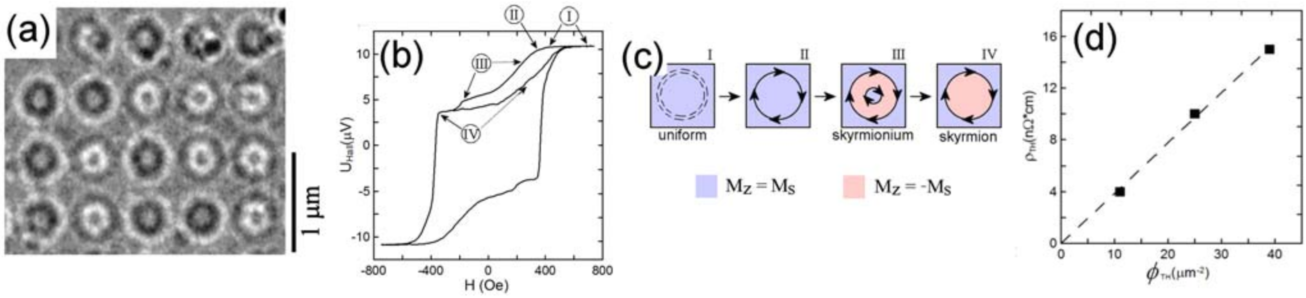

Fig. 2 (a) LTEM image of the lattice of Bloch skyrmions in the demagnetized state. (b) Hysteresis loop of the Hall effect of sample 1. The numbers indicate the parts of the loop corresponding to different magnetic states of the system. (c) Schematic presentation of the of the sequence of magnetic states in the samples during magnetization reversal (the result of micromagnetic simulation). Arrows indicate the direction of magnetization in the plane. (e) The THE value dependence on the density of irradiated spots in the system.

Magnetic skyrmion lattices are formed at the Hall bridge (150 × 150 μm^2). The He-Ne laser beam is focused onto the sample, which make it possible to measure polar MOKE and Hall effect simultaneously in the same run. The characteristic hysteresis loops for MOKE and Hall voltage are shown in Fig. 1 at the same scale. It can be seen that the value of the Hall voltage demonstrates a sharp step in the place where no specific features of MOKE are observed. Since there is no topological contribution to the MOKE at the optical frequency, the difference between the Hall voltage and the magnitude-scaled MOKE is directly the THE value (Fig.1).

The observed THE is associated with the formation of a skyrmion lattice. As it is shown by micromagnetic simulation, the formation of a skyrmions occurs as a result of the collapse of the central core of the initially formed ring domain, which has recently been named "skyrmionium". In its turn, the formation of skyrmionium is provoked by the concentric distribution of the anisotropy value over the irradiated spot. Since at the moment of collapse the core of the skyrmionium has a small magnetic volume, there is practically no change in MOKE. At the same time, a topological charge arising at the same time in the system leads to the appearance of THE and a step on the Hall curve. The observed step size in the Hall effect for different samples is directly proportional to the density of the skyrmion lattices formed in them (Fig. 2).

This research was supported by the Russian Science Foundation (Grant No. 21-12-00271).

References

[1] Aharonov Y., and Stern A., *Phys. Rev. Lett. 69*, 3593 (1992).

Control of DMI with strain in artificial multilayer structures

N.S. Gusev[1], R.V. Gorev[1], E.V. Skorohodov[1], A.V. Sadovnikov[2], M.V. Sapozhnikov[1], I.S. Beloborodov[3], O.G. Udalov[1,3]

[1] Institute for Physics of Microstructures RAS, Nizhny Novogorod, Russia
[2] Saratov State University, Saratov, Russia
[3] Department of Physics and Astronomy, California State University Northridge, Northridge, California, USA

Corresponding Author's Email: oleg.udalov@csun.edu

Skyrmions in magnetic thin films with perpendicular anisotropy are nontrivial magnetic textures promising various applications such as memory and logics. Therefore, manipulating (creating, annihilating, and moving) the skyrmions is an urgent but still challenging quest of modern spintronics. So far, several approaches have been used. Electrical-current-based techniques utilizing spin torque and spin-orbit torque allow one to control the skyrmions but require a high current density and, therefore, have low energy efficiency. A lot of groups work on electric-field-based approaches where the heat losses are minimized. One of the most actively studied approaches is based on voltage controlled magnetic anisotropy. Since a skyrmion stability is defined by the competition of the magnetic anisotropy and the Dzyaloshinskii–Moriya interaction (DMI), tuning of one of these contributions opens the way to control the skyrmions. So far, the field was focused on the variation of the magnetic anisotropy via a strain-mediated magnetoelectric coupling or a chargemediated magnetoelectric effect.

In the present work, we investigated (theoretically and experimentally) a different approach where the DMI in artificial films is controlled by strain. At first, we experimentally demonstrate that the DMI can be also controlled with a strain. We performed Brillouin light scattering (BLS) and magneto-optic Kerr effect (MOKE) studies of strained Pt/Co/Pt films. We demonstrated that the strain strongly influences the DMI in the system. Moreover, strong DMI anisotropy appears under compressive strain. The DMI constant perpendicular to the strain direction changes sign, while the constant along the strain direction does not. Fig. 1 describes the experiment performed and presents the dependence of DMI in Co/Pt film on applied strain.

To explain the observation a toy model of Co/Pt bilayer was considered theoretically. We showed that DMI is sensitive to the strain perpendicular to the film plane. It can vary 40% under the strain of 0.3%. Such a strong variation is in agreement with experiment. The DMI coefficient variation is mostly related to the change of the distance between heavy-metal atomic planes under the strain.

Since the DMI favors formation of domain walls, it should essentially influence the domain structure of the Co/Pt films. We investigated this question both theoretically and experimentally. Micromagnetic simulations and analytical modelling show that the domain structure is modified essentially upon application of anisotropic strain to the sample. The anisotropic strain induces anisotropic DMI and the domain structure also acquires anisotropy. In particular, zig-zag domains appear. We observed domain structure transformation in bent Co/Pt film experimentally. Fig. 2 shows the results.

Finally, we theoretically consider the influence of DMI anisotropy on the topological structures such as skyrmions and bimerons. Skyrmion and antiskyrmion become elliptic and orient along the main axes of the iDMI tensor even for small anisotropy. In contrast, bimeron (antibimeron) orientation changes fluently with varying the iDMI anisotropy. Depending on the iDMI anisotropy the bimeron may consist of a vortex and antivortex pair or of "hedgehog" state and antivortex.

We acknowledge Dr. D.A. Tatarskiy for helping in introducing anisotropic iDMI into the OOMMF package. This research is supported by the Russian Science Foundation (Grant 18-72-10026). Numerical simulations were performed under the support of the Russian Foundation for Basic Research (Grant 18-42-520013). I.S.B. was supported by NSF under Cooperative Agreement Award EEC-1160504. A.V.S. is supported by the Russian Science Foundation (Grant 20-79-10191). The facilities of the center "Physics and Technology of Micro- and Nanostructures" at IPM RAS were used for the analysis of the samples.

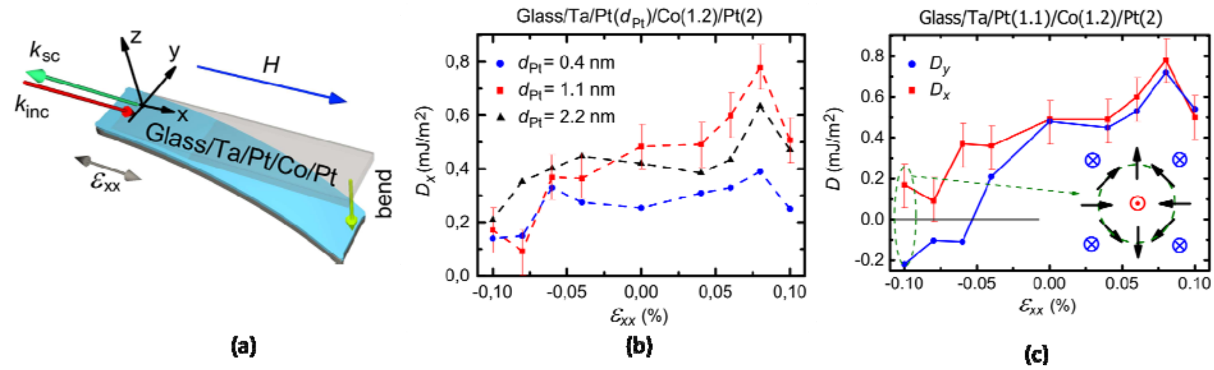

Fig.1 (a) experimental geometry. The sample is the Co/Pt multilayer film deposited on a glass substrate. The sample is bent and the strain in the Co/Pt film appears. The BLS measurements were performed for different orientation of the sample. (b) Dependence of the DMI constant along the sample long side as a function of applied strain for the samples with different thickness of the Pt layer. (c) DMI constants along the long (Dx) and short (Dy) sides of the sample as a function of strain. The inset shows an antiskyrmion which can appear when DMI has opposite sing along different direction.

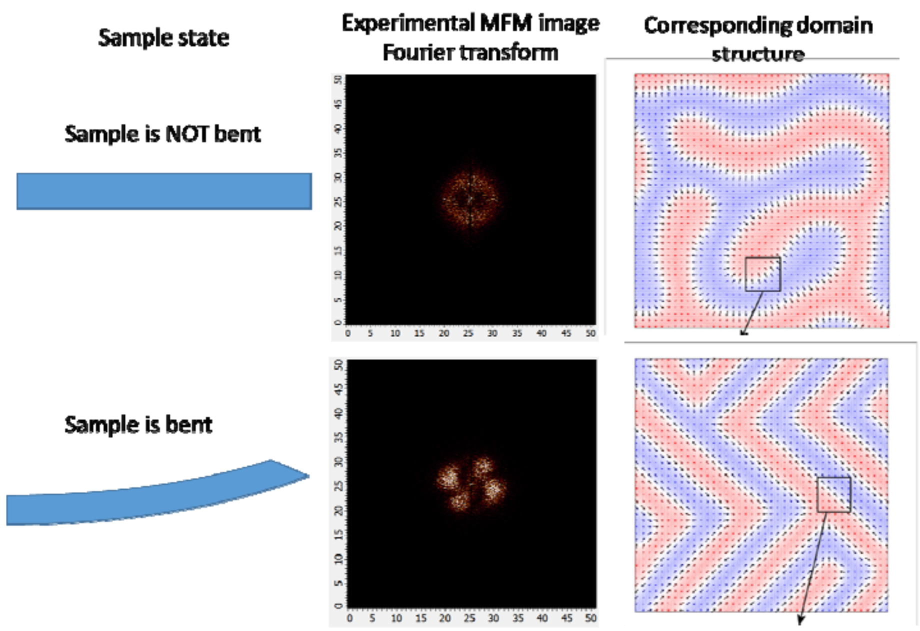

Fig.2 Dependence of the Co/Pt domain structure on the strain. Upper row – NOT bent sample. Bottom row – bent sample. In the state with no strain the Co/Pt domain structure is isotropic giving the circularly symmetric Fourier transform. When the sample is bent the anisotropic DMI appears leading to formation zig-zag domain structure (with 4 spots in the Fourier transform).

Dzyaloshinskii-Moria interaction in multiferroic and magnetoelectric materials: the cases of $BiFeO_3$, magnetic films and interfaces

A.P. Pyatakov[1]., A.K. Zvezdin[2,3]

[1] *Physics Department, M.V. Lomonosov Moscow State University, MSU, Moscow, Russia*
[2] *M. Prokhorov General Physics Insitute of the Russian Academy of Science, Moscow, Russia*
[3] *Moscow Institute of Physics and Technology State University, Dolgoprudny, Russia*

Corresponding Author's Email: pyatakov@physics.msu.ru

Since the beginning of the century the multiferroics, i.e. the media with coexisting magnetic and ferroelectric orders have been remaining on the agenda of condensed matter physics [1-4].

Due to the violation of the spatial inversion symmetry in magnetoelectric media and interfaces the electron and atoms participate in Dzyaloshinskii-Moria interaction (DMI) proportional to the vector product of the localized spins [$\mathbf{S_1}$x$\mathbf{S_2}$] that gives rise to non-uniform magnetic structures [5-7]. It should be noted, however, that the existence of the DMI does not always mean the formation of the spatially modulated structures. The immediate result of the DM-type exchange coupling is the microscopic canting of the spins of neighboring atoms. The relation between this *microscopic Dzyaloshinskii-Moriya interaction* (μ-DMI) and spatially modulated structure corresponding to the *macroscopic* free energy contribution of Lifshitz-type [8] (m-DMI) is not so straightforward.

In this report the relation between microscopic canting and spatially modulated structure will be discussed including the phenomenon of coexistence of weak ferromagnetism and spin cycloid in prototypical multiferroics $BiFeO_3$ [7], on magnetic interfaces [9-11] as well as recent reports on DMI in iron garnet films [12] and magnetoelectric properties of domain structures in them [13].

The support from RFBR grant #19-02-00828 is acknowledged. AKZ acknoledges the support from grant #19-52-80024.

References

[1] N.A. Hill, J. Phys. Chem. B 104, 6694 (2000).
[2] A.P. Pyatakov and A. K. Zvezdin, Physics-Uspekhi 55, 557 (2012).
[3] M. Fiebig, T. Lottermoser, D. Meier, and M. Trassin, Nat. Rev. Mater. 1, 16046 (2016).
[4] N.A. Spaldin, Proc. R. Soc. A Math. Phys. Eng. Sci. 476, 20190542 (2020).
[5] A. Sparavigna, A. Strigazzi, and A. Zvezdin, Phys. Rev. B 50, 2953 (1994).
[6] M. Mostovoy, Phys. Rev. Lett. 96, 67601 (2006).
[7] A.K. Zvezdin and A. P. Pyatakov, EPL (Europhysics Lett. 99, 57003 (2012).
[8] I.E. Dzyaloshinskii, J. Exp. Theor. Phys. 19, 960 (1964).
[9] A.K. Zvezdin, Bull. Lebedev, Phys. Inst. 29, 5 (2002).
[10] M. Bode, M. Heide, K. von Bergmann, P. Ferriani, S. Heinze, G. Bihlmayer, a Kubetzka, O. Pietzsch, S. Blügel, and R. Wiesendanger, Nature 447, 190 (2007).
[11] A. Fert, V. Cros, and J. Sampaio, Nat. Nanotechnol. 8, 152 (2013).
[12] R. Schlitz, S. Vélez, A. Kamra, C.-H. Lambert, M. Lammel, S. T.B. Goennenwein, and P. Gambardella, Phys. Rev. Lett. 126, 257201 (2021).
[13] A.P. Pyatakov, Phys. B Condens. Matter 542, 59 (2018).

SESSION 7. DMI IN MOLECULAR MAGNETS.

Multiferroics - polymer composites based on organometallic dimers with the Dzyaloshinsky-Moria effect

V.G. Shevchenko, A.I. Aleksandrov

Enikolopov Institute of Synthetic Polymeric Materials RAS, Russia, Moscow

Corresponding Author's Email: alivaleksandr@mail.ru

Polymer composites based on polystyrene (PS) and organometallic dimers of manganese and cobalt, exhibiting multiferroic properties, have been synthesized [1, 2]. The experimental setup is shown in Fig. 1a. It was found by the EPR method that the chemical transformation of the mixture ($M(acac)_3$ + Q + QH_2) в $M(QH)_2$ (M=Mn, Co) yields 100% at 190^{0}C during 30 min. The determination was carried out from the EPR spectra at 77 K using a Bruker EMX EPR spectrometer (black lines in Fig. 1b, c). Computer simulation of the EPR spectra (Fig.1b, c red lines) shows that these spectra can only be attributed to organometallic binuclear complexes (BA) of manganese or cobalt (BA - Mn, BA - Co), which have a total spin S = 1 and exhibit interaction Dzyaloshinsky - Moriah. The Hamiltonian describing the EPR spectra of such paramagnetic centers can be represented in the following general form:

$$\mathbf{H} = \mu_B\ \mathbf{B}\cdot\mathbf{g}_a\cdot\mathbf{S}_a + \mu_B\ \mathbf{B}\cdot\mathbf{g}_b\cdot\mathbf{S}_b + D\mathbf{S}_a\cdot\mathbf{S}_b - 3DS_{az}S_{bz} + E(S_{ax}S_{bx} - S_{ay}S_{by}) + J\mathbf{S}_a\cdot\mathbf{S}_b + \mathbf{G}\cdot[\mathbf{S}_a \times \mathbf{S}_b] + \mathbf{I}_a\cdot\mathbf{A}_a\cdot\mathbf{S}_a + \mathbf{I}_b\cdot\mathbf{A}_b\cdot\mathbf{S}_b,$$

where μ_B is Bohr magneton, **B** is external magnetic field vector, **g** is g-factor tensor, **S** is electron spin operator, D and E are electron dipole-dipole interaction constants, J is scala exchange interaction constant. The vector **G** (directed along the z axis if the spins $\mathbf{S}_a$ and $\mathbf{S}_b$ lie in the xy plane) corresponds to a scalar quantity G, the magnitude of the anisotropic exchange interaction, **I** is the nuclear spin operator, **A** is the electron - nuclear hyperfine interaction tensor. The geometric structure of the $(HQ)_2M(II)\cdot\cdot O\cdot\cdot M(II)(QH)_2$ complex was determined by the DFT method using the GAUSSIAN98 program, which is shown in Fig. 1d. The direct dynamic magnetoelectric effect (MEE) is investigated, when at different values of H0, an alternating magnetic field H = H(ω) was applied to the sample with a frequency change from 0 to 50 MHz. In this case, we measured the alternating electric field arising on the sample E(ω) = V(ω)/δ where V(ω) is the alternating voltage across the aluminum electrodes, and δ is the thickness of the sample. It was found that the value of the direct MEE μE = E(ω)/H(ω) varies depending on ω and H_0, as shown in Fig. 1e, k. The reverse MEE was also investigated, when a sinusoidal electric field E = E(ω) with an amplitude of 10V was applied to the sample (ω varied from 0 to 50 MHz), and the arising alternating magnetic field was recorded using Helmholtz coils. It was found that the value of the inverse MEE μH = H(ω)/E(ω) changes depending on ω, as shown in Fig.1.

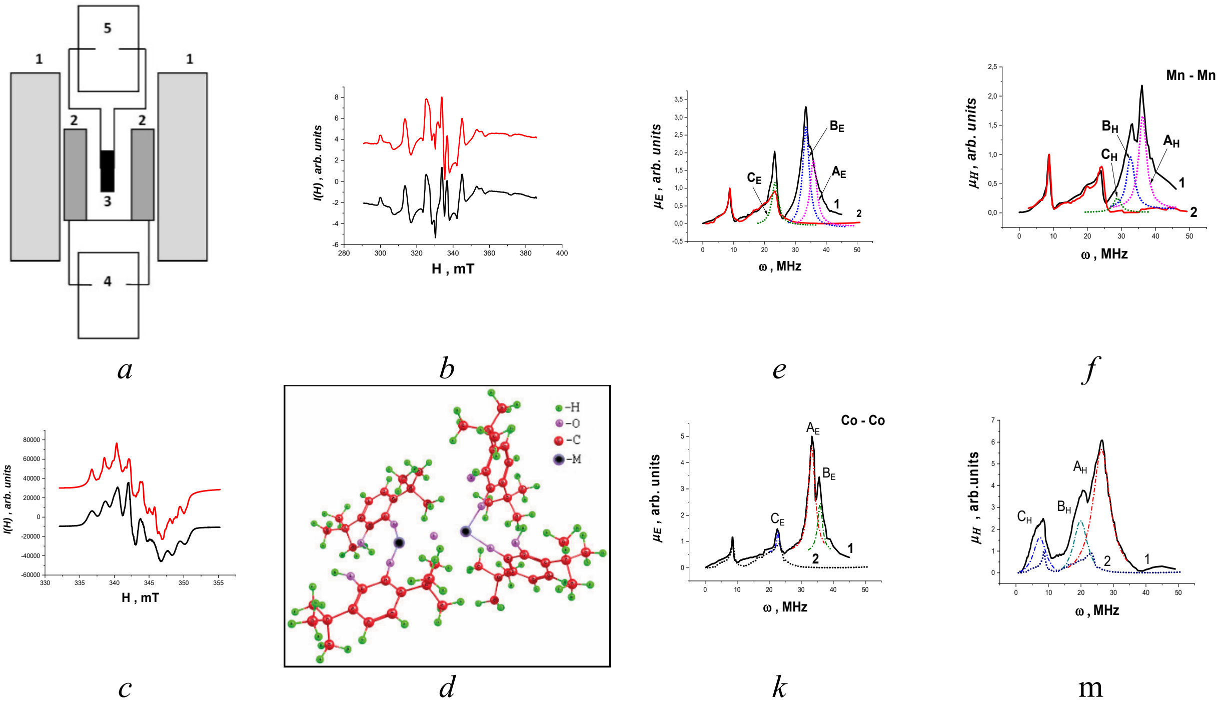

Fig.1 a) Block diagram of the measuring setup. 1 - magnet, 2 - Helmholtz coils, 3 - sample, 4 - signal generator, 5 – oscilloscope. b, c) EPR spectra of BA – Mn (b) and BA – Co (c) complexes in the PS matrix at 77 K (blak) and their theoretical anamorphoses (red). d) the geometric structure of the dimer $(HQ)_2M(II)\cdot\cdot O\cdot\cdot M(II)(QH)_2$ (M = Co, Mn) after optimization by the DFT method. e, f) the change in the values of the magneto-electric coefficients μE (e), μH (f) as a function of ω, the frequency of the alternating magnetic or electric field applied to the composite sample (PS - $(HQ)_2Mn(II)\cdot\cdot O\cdot\cdot Mn(II)(QH)_2$)) at constant magnetic field H_0 on the sample equal to 0 mT (spectra 1) and polymer matrix (spectrum 2). k, m) the change in the values of the magneto-electric coefficients μE (k), μH (m) depending on ω, the frequency of the alternating magnetic or electric field applied to the composite sample (PS - $(HQ)_2Co(II)\cdot\cdot O\cdot\cdot Co(II)(QH)_2$) spectrum 1) and polymer matrix (spectrum 2) at a constant magnetic field H_0 = 0.

References

[1] A.I. Aleksandrov, I.A. Aleksandrov, V.G. Shevchenko. Multiferroic based on metal – organic dimers with the Dzyaloshinskii – Moriya effect. JETP Letters, 2016, v. 104, No 8, pp. 568 – 572. DOI: 10.1134/S0021364016200066.

[2] A.I. Aleksandrov, V.G. Shevchenko, I.A. Aleksandrov. Multiferroic: A Polymer Composite Based on Organometallic Cobalt Dimers with Dzyaloshinskii–Moriya Effect. Polymer Science, Series A, 2018, Vol. 60, No. 1, pp. 74–80.DOI: 10.7868/S2308112018010017.

Time resolved FORC analysis and magnetic anisotropy in molecular based magnets

O.V Koplak, R.B. Morgunov

[1] *Institute of Problems of Chemical Physics, Chernogolovka, Russia*
[2] *I.M. Sechenov First Moscow State Medical University, Moscow, Russia*

Corresponding Author's Email: o.koplak@gmail.com

Magnetic structure of soliton spin sublattice and the existence of new types of domain walls are very promising for development of novel magnetic materials and their application, because magnetic and microwave responses of these structures manifest narrow band frequency selectivity and extremely low switching microwave power. The K0.4[Cr(CN)6][Mn(S)-pn](S)-pnH0.6 chiral crystal is bulk ferrimagnet manifesting long-range magnetic order. In contrast to single molecule magnets and molecular chains, the existence of spin solitons and domain walls of unknown types can be expected in the crystals studied in this work. A fruitful and powerful method to distinguish different types of spin configurations is the first order reversal curves (FORC) method (Fig. 1).

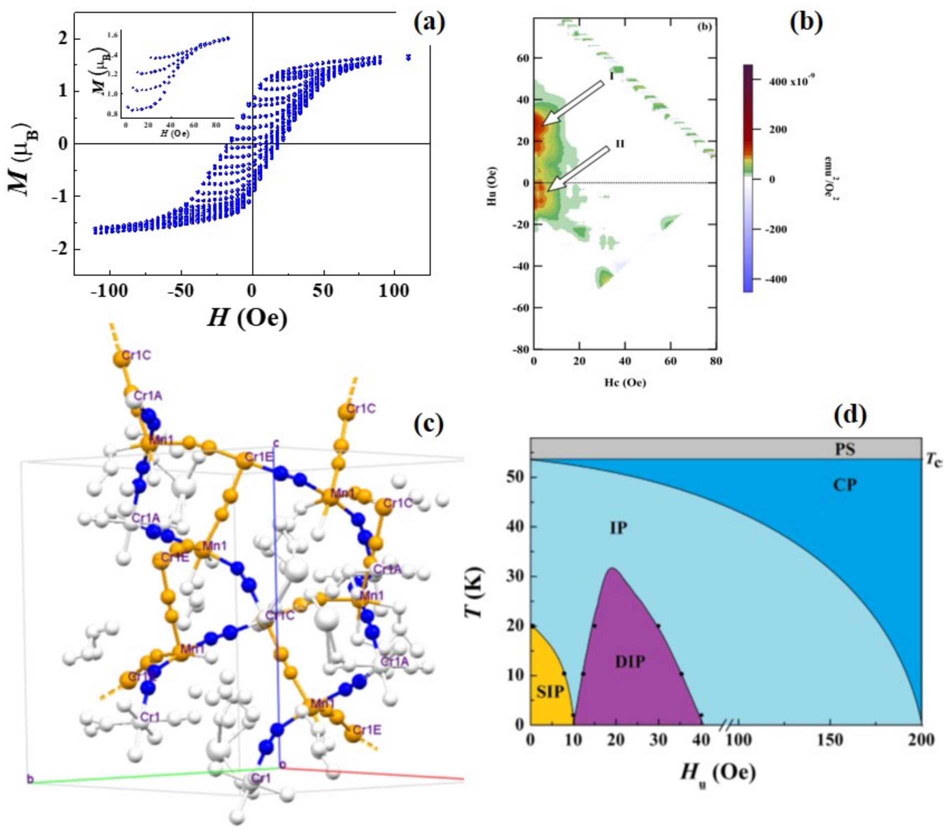

Fig.1 Series of field dependences of magnetization M(H) (a) and FORC diagram (b) at T = 2 K, ΔHa = 4 Oe, ΔHr = 4 Oe; Fragment of crystal structure with –CN– groups marked by orange in the case of short distance 5.372 A between C and N atoms, and marked by blue color in the case of long distance 5.457 A (c). Phase diagram in H-T coordinates plotted by experimental data extracted from AC measurements and FORC diagram. Designation PS is paramagnetic state, CP is commensurate phase, IP is incommensurate phase containing SIP (soliton incommensurate phases) and DIP (domain incommensurate phases) (d).

The two distinguished maxima distributed along Hu axis at 20 K directly confirm the existence of two different spin configurations well isolated from each other and contributing to reversal magnetization (Fig 2b). Increase of the length of the – CN – group obviously causes decrease of the wave function overlapping resulting in exchange interaction decrease. Thus, structural data allow one to distinguish spin spirals linked by extended CN bridges manifesting week exchange interaction. The FORC analysis allowed one to judge about the existence of domain walls (DIP) and soliton (SIP) states in the incommensurate phase (IP). Plot of the integrated phase map in Fig.1d was done by contour borders of FORC maxima I and II corresponding to the DIP and SIP in H-T space. The approximate magnetic phase diagram in H-T coordinates is presented in Fig.1d.

The FORC map as well as reversal magnetization is governed by magnetic anisotropy analyzed in our work. Application of the Callen – Callen formalism for the treatment of the temperature dependence of magnetic anisotropy results in power deviation from theoretical predictions for single sublattice ferromagnet. The importance of the second term of magnetic anisotropy decomposition can be explained by the contribution of the Dzyaloshinskii – Moria interaction to the spin-orbital interaction additionally to the Heisenberg exchange. The temperature dependence of magnetic anisotropy indicates contributions of two different sources of magnetic anisotropy balancing amounts of the dynamic and static solitons with different magnetic relaxation time.

Authors acknowledge support from the Ministry of Science and Higher Education of the Russian Federation (Agreement No. 14.W03.31.0001-Institute of Problems of Chemical Physics, Chernogolovka).

References

[1] R.B. Morgunov, O.V. Koplak, M.V. Kirman, Journal of Physics: Condensed Matter 31(8), 085801 (2019).

Effect of deformation on topological properties of cobalt monosilicide

S. Nikolaev, D. Pshenay-Severin, Y. Ivanov, A. Burkov

Ioffe Physico-Technical Institute of the RAS, Saint Petersburg, Russia

Corresponding Author's Email: d.pshenay@mail.ru

Recently, it was shown that materials with certain crystal structures can exhibit multifold band crossings with large topological charges [1,2]. CoSi is one this type of materials that belongs to non-centrosymmetric space group $P2_13$ (#198) and possesses multifold band crossings at the time reversal invariant (TRIM) points with a topological charge of 4 [3–5]. The change of crystal symmetry, e.g., by means of external stress, can lift the degeneracy, and change its topological properties.

In the present work the influence of deformation on the band structure and topological properties of CoSi was studied theoretically. The symmetry prescribed $\boldsymbol{k}\cdot\boldsymbol{p}$ Hamiltonians at the Γ and R points taking into account deformation were written down for the cases with and without spin-orbit coupling (SOC). The parameters of $\boldsymbol{k}\cdot\boldsymbol{p}$ Hamiltonians were fitted to the results of *ab initio* calculations that allowed to obtain the absolute deformation potentials, and the work function of CoSi (4.55eV), which correlates with available experimental data (4.47–4.54eV [6]). The transformation of multifold band crossings into nodes of other types with different topological charges, their shift both in energy and in reciprocal space, the tilt of dispersion around nodes and the evolution of surface Fermi arcs shape were studied in detail depending on the direction of uniaxial deformation.

It was shown that in almost all considered cases, the degeneracy is partially lifted at the TRIM points. The only exception is the fourfold degenerate level at the R point (without SOC) under [100] strain. A lowering in symmetry leads to the appearance of a significant number of different band crossings with topological charges from ±1 to ±3 around the TRIM points. The nodes often have a tilted dispersion.

The unusual results were obtained upon deformation of CoSi along the [111] direction. Without spin-orbit coupling, the doubly degenerate nodes with quadratic dispersion in the plane orthogonal to the [111] direction appear at the Γ and T points of the deformed Brillouin zone. These band crossings have Chern numbers of ±2 and resemble the well-known double-Weyl nodes, but they are spin degenerate. Calculation with account of SOC revealed doubly degenerate nodes with the topological charges of ±3 at the TRIM points. These band crossings are located on the threefold rotation axis and are analogous to triple-Weyl nodes.

The band structure with SOC around the R point under [100] strain exhibits another example of the change of node type. The double spin-1 node with topological charge of 4 splits into pairs of double spin-1/2 nodes with topological charges of 2 per node. Thus, using mechanical deformation, the transition between different types of topological nodes can be realized in the same material.

A lowering of the crystal symmetry under strain also leads to a modification of the surface Fermi arcs shape. A change in the sign of the deformation and the Fermi level position switches the ends of the Fermi arcs from one group of nodes to another. However, the number of Fermi arcs always remains equal to two without taking into account SOC and four with SOC.

The study was supported by the Russian Foundation for basic Research, project 18-52-80005 (BRICS).

References

[1] J.L. Mañes, Physical Review B 85, 155118 (2012).

[2] B. Bradlyn, J. Cano, Z. Wang et al., Science 353, aaf5037 (2016).
[3] G. Chang, S.-Y. Xu, B.J. Wieder et al., Physical Review Letters 119, 206401 (2017).
[4] P. Tang, Q. Zhou, and S.-C. Zhang, Physical Review Letters 119, 206402 (2017).
[5] D.A. Pshenay-Severin, Y.V. Ivanov, A.A. Burkov, and A. T. Burkov, Journal of Physics: Condensed Matter 30, 135501 (2018).
[6] J. Kedzierski, E. Nowak, T. Kanarsky et al., *Metal-Gate FinFET and Fully-Depleted SOI Devices Using Total Gate Silicidation*, in *Digest. International Electron Devices Meeting,* (8-11 Dec. 2002, San Francisco, CA, USA, IEEE).

POSTER SESSION

Radio-frequency superradiance upon mechanical activation of polymer composites based on organometallic dimers with the Dzyaloshinsky – Moria effect

A.I. Aleksandrov, V.G. Shevchenko

Enikolopov Institute of Synthetic Polymeric Materials RAS, Moscow, Russia

Corresponding Author's Email: alivaleksandr@mail.ru

A parametric mode of radio-frequency superradiance has been established under the external action of elastic wave pulses and high pressure on a polymer paramagnetic composite [1, 2]. Composite based on polystyrene, containing a system of crossed spins of a system of binuclear clusters $Co(QH)_2$–O–$Co(QH)_2$ или $Mn(QH)_2$–O–$Mn(QH)_2$ (QH is a ligand, based on QH_2 – 3,6-di-tert-butylpyrocatechol), which exhibit the Dzyaloshinsky – Moria effect, which was confirmed by analyzing the EPR spectra of these composites. DFT showed that one of the metal atoms of the binuclear cluster in polymer matrix is captured by benzene rings of polystyrene in the same manner as ferrocene. Binuclear clusters form 2D nanoobjects 50–100 nm in diameter and ~ 1–2 nm thick. To study the processes of superradiance pulses under mechanical action on film sample by pulses of elastic waves (EWP) from a rheological explosion, we used a special high-pressure cell (Fig. 1a). An external rheological explosion from an EWP, initiating mechanochemical processes in the sample (Fig. 1a - 5), occurs upon rapid uniaxial compression of a pure polystyrene film (Fig.1a - 1) 10 mm in diameter and 2 mm thick at the same pressure ~ 2 GPa and compression speed of 0.5 GPa / s. Under the action of elastic wave pulse on the sample, an alternating current $J(t)$ (Fig. 1c) generated by the electric component E(t) of electromagnetic radiation was recorded. Since $J(t) \sim E(t)$, and the power (intensity) of electromagnetic radiation $I(t) \sim [E(t)]^2$, then $I(t) \sim [J(t)]^2$ (Fig. 1d). It was found that the intensity of the peaks $I(t_0)$ (at $t = t_0$) is proportional to the square of the numbed of binuclear complexes N^2 (N = from 0.1×10^{20} to 0.7×10^{20} binuclear complexes per cm^3), which is typical for superradiance processes. This is clearly seen in Fig. 1e, which shows the dependence of the normalized amplitude $I(t0)$ on N^2 for binuclear cobalt and manganese clusters (N_{max} is the maximum value for a binuclear manganese cluster). It was found that the line shape of the emission bands (dashed line in Fig. 1d) also corresponds to a law, characteristic of superradiance processes - an exponential symmetric rise and fall. A probable scheme for the emergence of the superradiance process is proposed - under the external influence of elastic wave pulses, the inverse population of the electron-spin Zeeman reservoir, formed by Dzyaloshinsky - Moria dimers, occurs, i.e. a system of non-collinear spins. Such a Zeeman spin reservoir is the source of the observed electromagnetic superradiance arising from the annihilation of triplet excitations (Fig.1).

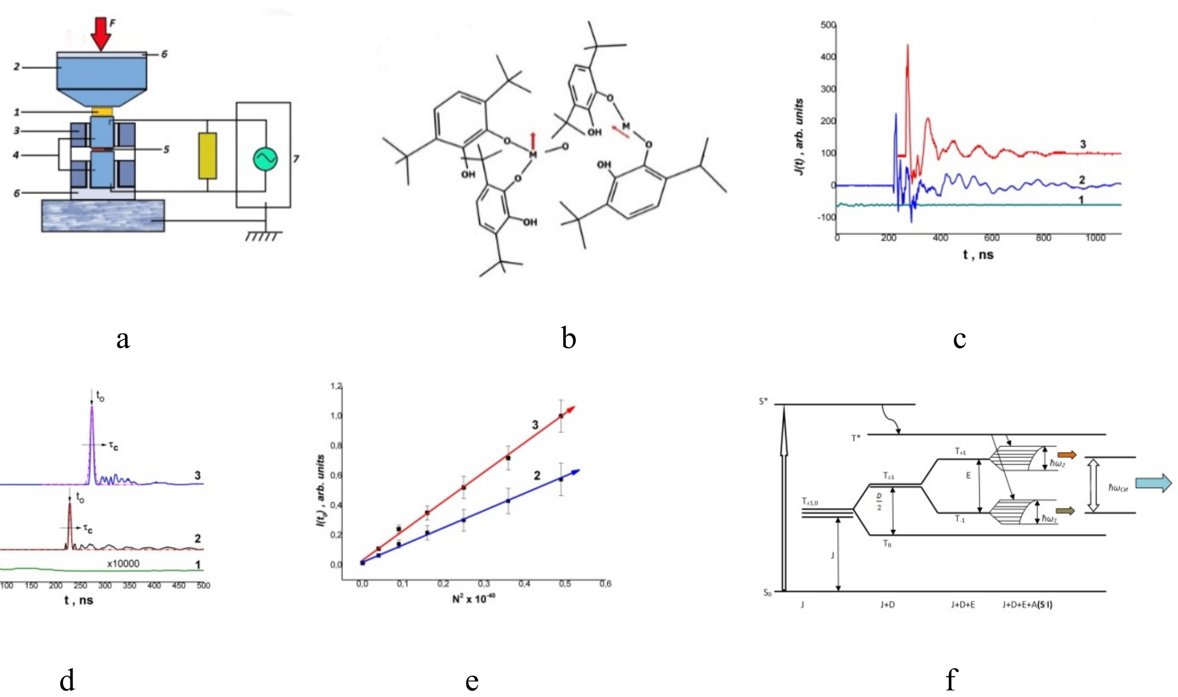

Fig.1 a - schematic of a high-pressure cell. b - geometric structure of the complex $(HQ)_2M\cdot\cdot O{=}M(QH)_2$with full optimization by the DFT method (M = Co, Mn). c, d - the time base of the electrical signal J(t) ~ E(t) and the time base of the normalized signals I(t) ~ $[E(t)]^2$ for the PS matrix (1) and samples containing BC – Co (2) and BK – Mn (3). e - the normalized dependence of $I(t_0)$ on the square of the number of complexes in 1 cm^3 of the composite. f - energy diagram of the population inversion of T_{+1} and T_{-1} levels (the length of the horizontal segments is proportional to the population of the levels in the splitting of T_{+1} and T_{-1} by the mechanism of spin-spin interaction).

References

[1] Aleksandrov, V.G. Shevchenko, I.A. Aleksandrov. Generation of Superradiance by Pulsed Mechanical Action. *Technical Physics Letters, 2020, Vol. 46, No. 4, pp. 346–349.* DOI: 10.1134/S1063785020040021.

[2] A.I. Aleksandrov, V.G. Shevchenko, I.A. Aleksandrov, E.N. Degtyarev, and S.S. Abramchuk. Radiofrequency Superradiance on Exposure of Paramagnetic Polymer Composites to Elastic Wave Pulses. Polymer Science, Series A, 2020, Vol. 62, No. 5, pp. 550–561. DOI: 10.1134/S0965545X2004001X.

Brillouin spectroscopy of the interfacial Dzyaloshinskii–Moriya interactions in alloy embedded Pt-Co nanostructures

V.D. Bessonov[1], A.V. Telegin[1], M.V. Makarova[1], I.D. Lobov[1], A.S. Samardak[2]

[1] M.N. Miheev Institute of Metal Physics UB of RAS, Ekaterinburg, Russia
[2] Far Eastern Federal University, Vladivostok, Russia

Corresponding Author's Email: bessonov@imp.uran.ru

The interfacial Dzyaloshinskii–Moriya interaction (iDMI) has recently drawn considerable attention as a physical background in next-generation information storage devices [1,2]. iDMI is an antisymmetric exchange interaction occurring in heterostructures comprising non-magnetic metal (NM) and ferromagnetic (FM) layers with broken inversion symmetry which can lead to the generation of skyrmions [3]. Under active debate is the clarifying the effect of interfaces on the iDMI behavior in nanostructures NM/FM [4].

Herein we report the iDMI behaviors of Pt/Co nanostructures wherein an $Pt_{1-x}Co_x$ alloy was placed at the interface between Pt and Co layers. Inserting an artificially deposited alloy was supposed to enhance the damping-like torque and iDMI energy in a nanostructure.

Samples $Ta(2)/(Pt_{1-x}Co_x)_n(1.2)/Ta(2)$ were fabricated on thermally oxidized Si substrates using DC magnetron sputtering at room temperature. All the samples were characterized by X-ray diffraction and reflectometry, vibration sample magnetometry and magneto-optical Kerr effect, and transmission electron microscopy. Brillouin light scattering (BLS) spectroscopy [5] was applied to examine the iDMI energy density of each sample.

The BLS spectra showed an increase in the Stokes/anti-Stokes frequency difference (Fig.1) for the samples inserted with an alloy structure. Overall, the iDMI energy density was maintained despite the presence of Pt–Co alloys and reduced magnetization. The sample with an interface exhibiting a gradual composition change showed the iDMI value of −0.89 mJ/m^2, which was comparable to that of the sharp interface sample −0.88 mJ/m^2. As the insertion of the alloy layers deformed the interfacial characteristics of the structure studied, we could conclude that the iDMI energy density originates from the interfacial characteristics.

Finally, we experimentally investigated the iDMI behavior of Pt/Co heterostructures with an artificially created alloy layer. It was found that inserting the intralayer one could successfully engineer the iDMI behavior of the structure.

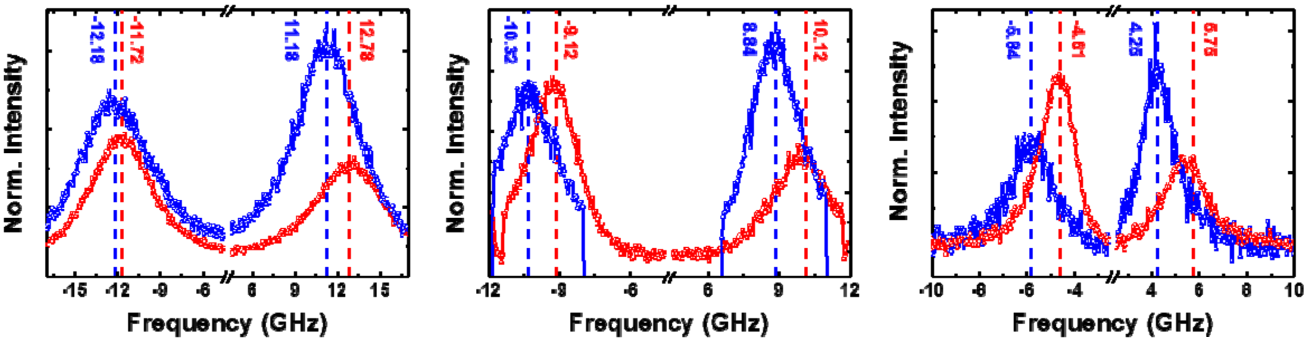

Fig.1 Raw BLS spectra of samples with different composition.

The research was supported by RSF (project No. 21-72-20160).

References

[1] A. Fert, N. Reyren, and V. Cros, *Nat. Rev. Mater.* **2,** (2017).
[2] F. Hellman et al., *Rev. Mod. Phys.* **89,** (2017).
[3] A. Fert, V. Cros, and J. Sampaio, *Nat. Nanotechnol.* **8**, 152 (2013).
[4] R. M. Rowan-Robinson, A.A. Stashkevich, Y. Roussigne et al., *Sci. Rep.* **7**, 16835 (2017).
[5] A. Samardak, A. Kolesnikov, M. Stebliy et al., *Appl. Phys. Lett.* **112**, (2018).

Study of positron annihilation lifetime in non-centrosymmetric monosilicides (B20) by ^{48}V source

D.A. Salamatin[1,2,3], A.V. Bokov[1,3,4], M.G. Kozin[4], I.L. Romashkina[4], A.V. Salamatin[2], M.V. Mikhin[2], D.V. Filosofov[2], P. Hordek[2], G.A. Kononenko[2], A.E. Petrova[3], V.A. Sidorov[1,3], A.V. Nikolaev[4], M. Budzynski[5], A.V. Tsvyashchenko[1,3]

[1] *Vereshchagin Institute of High Pressure Physics, RAS, Troitsk, Moscow, Russia*
[2] *Joint Institute for Nuclear Research, Dubna, Russia*
[3] *Lebedev Physical Institute, RAS, Moscow, Russia*
[4] *Skobeltsyn Institute of Nuclear Physics, Lomonosov MSU, Moscow, Russia*
[5] *Institute of Physics, M. Curie-Sklodowska University, Lublin, Poland*

Corresponding Author's Email: av.bokov@yandex.ru

When studying single crystals of monosilicides of *3d* transition metals, in which such properties as chiral magnetic ordering, skyrmion texture, Kondo states and Weyl fermions are observed, the defectiveness of crystals can be of significant importance. A positron annihilation lifetime spectroscopy (PALS) is a non-destructive technique that allows to study material defects / free volume at the sub-nm scale. The general working principle is based on correlating the lifetime of the injected positrons and the emission of annihilation radiation.

In the work we have studied single crystals of MnSi (helical magnet), FeSi (Kondo insulator), CoSi (Weyl semimetal) and Si by the means of PALS. The isotope of ^{48}V was used as a positron source. The isotope was produced in the $^{48}Ti(p,n)^{48}V$ reaction with 7 MeV protons at the Nuclear Physics Institute cyclotron (Moscow State University). The thin foil (50 μm) of natural titan was used as a target. The advantages of ^{48}V source are the possibility to use it in the experiments at high pressures and high temperatures, with non-aggressive liquids. The source has small positron self-absorption and in the PALS time spectra the long-lifetime component is absent [1]. The short half-life ($T_{1/2} \approx 16$ d) makes this source suitable for environmentally friendly nuclear experiments. It should be noted that the isotope of ^{48}V can be also produced via natTi(^{3}He,nx)^{48}Cr nuclear reaction.

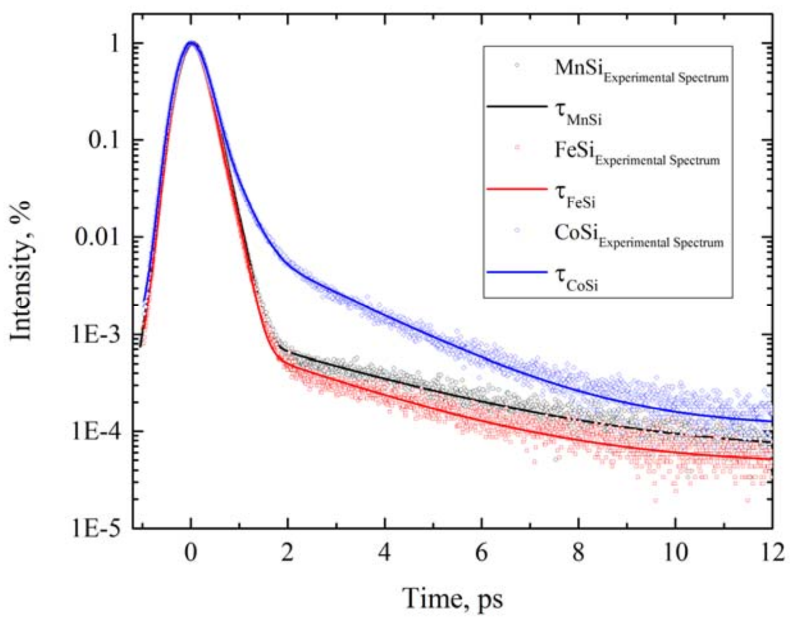

Fig.1 PALS spectrum of B20 monosilicides (B20) by ^{48}V source

The PALS measurements have been performed with compact spectrometer "VUKAP" equipped with four $LaBr_3$ detectors [2] (see Figure 1 and Table 1). The spectrometer is based on the digital electronics and digital signal processing techniques. The time resolution (FWHM) is equal to 380 ps at ^{60}Co. It should be note that this spectrometer can perform the measurements even with low activity radioactive sources. The contribution from the source was less than 4 %. The 1332 keV gamma quantum was used for a start.

The results of PALS measurements

Table 1

Material	τ_{exp}, ps	Data from literature, ps
MnSi	111(1)	τ_b = 111-119(3), $\tau_{V\text{-}Mn}$ = 185(4) [3]
FeSi	114(1)	τ_b = 108 [4], 130 [5]
CoSi	168(1)	τ_b = 115(2), $\tau_{V\text{-}Co}$ = 168, $\tau_{V\text{-}Si}$ = 173 [6]
Si	218(1)	τ_b = 218 [7]

τ_{exp} – experimental values of positron lifetimes measured in this work, τ_b – positron lifetime in the bulk, τ_V – positron lifetime in the monovacancy.

We are grateful for the support in development of digital TDPAC spectrometer to the Polish representative at the Joint Institute for Nuclear Research. The work was supported by Russian Science Foundation (Grant RSF 17-12-01050).

References

[1] K. Hinode, S. Tanigawa, M. Doyama and N. Shiotani. *Applied Physics 20*, pp. 185–188 (1979).

[2] D.A. Salamatin, A.V. Tsvyashchenko, A.V. Salamatin, A. Velichkov, M.V. Magnitskaya, N.M. Chtchelkatchev, V.A. Sidorov, L.N. Fomicheva, M.V. Mikhin, M.G. Kozin, A.V. Nikolaev, I.L. Romashkina and M. Budzynski. *Journal of Alloys and Compounds 850*, 156601 (2021).

[3] M. Reiner, A. Bauer, M. Leitner, T. Gigl, W. Anwand, M. Butterling, A. Wagner, P. Kudejova, C. Pfleiderer and C. Hugenschmidt. *Scientific Reports 6*, 29109 (2016).

[4] K.M. Mostafa, J. De Baerdemaeker, P.R. Calvillo, N.Van Caenegem, Y. Houbaert and D. Segers. *Acta Physica Polonica A 113*, 5 (2008).

[5] A. Bharathi, Y. Hariharan, A. Mani and C.S. Sundar. *Physical Review B 55*, R13385(R) (1997).

[6] S. Abhaya and G. Amarendra. *Physica Status Solidi C 6:11*, pp. 2519–2522 (2009).

[7] S. Dannefaer, W. Puff, and D. Kerr. *Physical Review B 55*, 2182 (1997).

On an ab initio theory of the temperature dependence of hyperfine quadrupole interaction in metals: application to hexagonal Zn and Cd

A.V. Nikolaev[1], N.M. Chtchelkatchev[2], D.A. Salamatin[2], A.V. Tsvyashchenko[2]

[1] *Skobeltsyn Institute of Nuclear Physics, MSU, Moscow, Russia*
[2] *Vereshchagin Institute of High Pressure Physics, RAS, Troitsk, Moscow, Russia*

Corresponding Author's Email: n.chtchelkatchev@gmail.com

Based on *ab initio* band-structure calculations, we formulate a general theoretical method for description of the temperature dependence of electric field gradients (EFG) in solids [1]. The method employs a procedure of averaging multipole electron density component ($l \neq 0$) inside a sphere vibrating with the nucleus at its center. As a result of averaging, each Fourier component ($K \neq 0$) on the sphere is effectively reduced by the square root of the Debye–Waller factor [exp($-W$)]. The EFG related to a sum of K components most frequently decreases with temperature (T), but under certain conditions, because of the interplay between terms of opposite signs, it can also increase with T. The method is applied to calculations of the temperature evolution of EFG in pristine zinc and cadmium crystallized in a hexagonal close packed structure. For calculations within our model, of crucial importance is the temperature dependence of rms displacements, which can be taken from experiment or obtained from the phonon modes in the harmonic approximation. In case of Zn, we used data obtained from single-crystal x-ray diffraction. In addition, for Zn and Cd, we calculated rms displacements with the density functional perturbation treatment of the QUANTUM ESPRESSO package [2]. With the experimental data for rms displacements in Zn, our calculations reproduce the temperature dependence of the EFG very accurately (Fig.1). Within the harmonic approximation [2], a decrease in the EFG of Zn and Cd with temperature is overestimated. Our calculations indicate that the anharmonic effects are of considerable importance in the temperature dependence of electric field gradients [1].

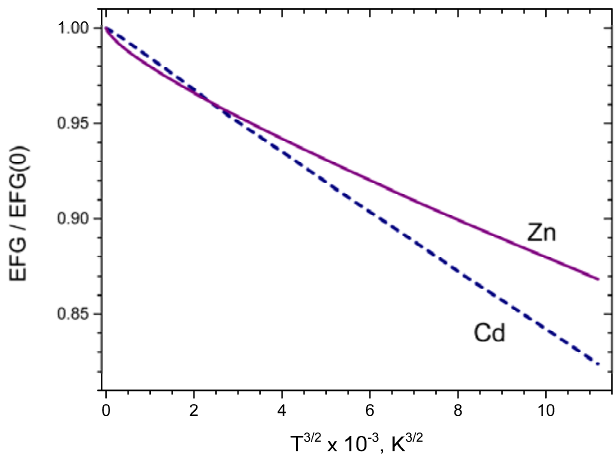

Fig. 1. Temperature dependence of electric field gradients in Zn and Cd.

The work was supported by the Russian Science Foundation (Grant No. 18-12-00438).

References

[1] A.V. Nikolaev, N.M. Chtchelkatchev, D.A. Salamatin and A.V. Tsvyashchenko, Phys. Rev. B 101 064310 (2020).
[2] P. Giannozzi, S. Baroni, N. Bonini et al., J. Phys.: Condens. Matter 21, 395502 (2009).

Position dependent stability and metastability of the skyrmion state in Ni substituted Cu_2OSeO_3

M. Crisanti[1,2], M.T. Birch[3], M.N. Wilson[3], S.H. Moody[3], A. Stefancic[1], B.M. Huddart[3], S. Cabeza[2], G. Balakrishnan[1], P.D. Hatton[3], R. Cubitt[2].

[1] *University of Warwick, Department of Physics, Coventry, CV4 7AL, United Kingdom*
[2] *Institut Laue-Langevin, , Grenoble, France*
[3] *Centre for Materials Physics, Durham University, Durham, United Kingdom*

Corresponding Author's Email: m.crisanti@warwick.ac.uk

Magnetic skyrmions are a new topological state of the magnetization currently at the center of great scientific interest given their potential application in spintronic devices. Skyrmions were first observed with Small Angle Neutron Scattering (SANS) in MnSi [1], since then, they have been observed in other materials with the same space group [2, 3], in non-centrosymmetric compounds [4, 5], in thin films [6, 7], and more recently also in frustrated magnets [8]. In bulk materials, skyrmions form only in a small region of temperature and applied magnetic field (skyrmion pocket), contrary to thin film materials, where the dimensions of the pocket are enhanced by the reduced dimensionality of the system [3].

In bulk non-centrosymmetric chiral magnets, the skyrmion state is stable over a small region (referred to as the skyrmion pocket) of the applied field vs. temperature phase diagram, just below the ordering temperature. For this set of materials, it is crucial to understand how to engineer the size and position of the skyrmion pocket in the phase diagram, and how these characteristics relate to the macroscopic characteristics of the material. In particular, in bulk samples it has already been shown how the skyrmion state nucleates at the edges of the sample and then propagates across it [9]. However, the relation between the macroscopic features of a bulk skyrmion host and the skyrmion state is yet to be fully characterized and understood.

In this talk, we present spatially resolved small angle neutron scattering measurements of the conical and skyrmion states of a bulk single crystal of nickel-substituted Cu_2OSeO_3 aimed to characterize the skyrmion state in different areas of the sample. We observed a spatially dependent structure of both the conical and skyrmion states, both showing an increased structural disorder at the edge of the sample compared to the center. Remarkably, we also observed an enlargement of the skyrmion pocket towards lower temperatures at the edge of the sample. In the same region, also the metastable skyrmion state did not show a clear Arrhenius-like time dependency, as reported for both pristine [10] and Zn substituted Cu_2OSeO_3 [11], as well as other bulk skyrmion hosts. We suggest that demagnetization effects present at the edge of the sample, inducing an increased local disorder and co-existence of conical and skyrmion state, are responsible for the increased stability of this skyrmion state, while affecting its metastable lifetime. The results presented in this talk have been published in [12].

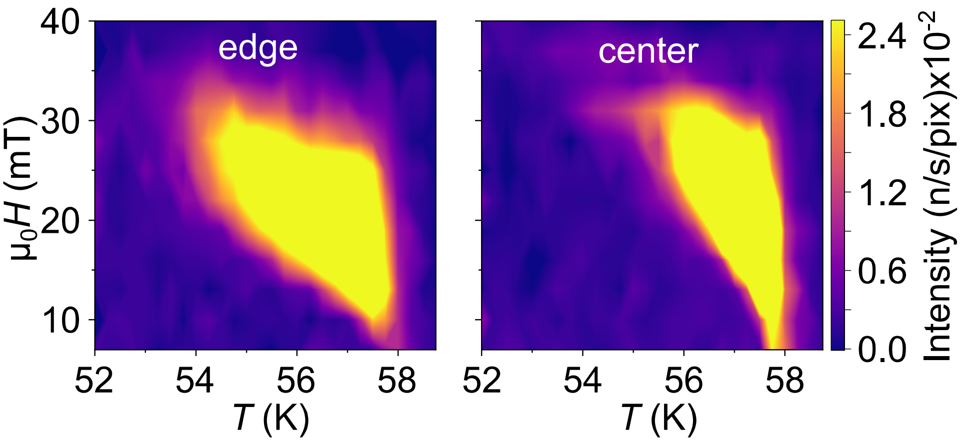

Fig. 1 Skyrmion pocket extent measured at the edge and in the center of the sample. The phase diagram has been obtained from neutron scattered intensity from the skyrmion state during a SANS experiment [12].

References

[1] S. Mühlbauer, B. Binz, F. Jonietz, C. Pfleiderer, A. Rosch, A. Neubauer, R. Georgii, P. Boni, *Science*, **323**, 5916 (2009).
[2] S. Seki, X.Z. Yu, S. Ishiwata, Y. Tokura, *Science*, **336** (2012).
[3] X.Z. Yu, N. Kanazawa, Y. Onose, K. Kimoto, W.Z. Zhang, S. Ishiwata, Y. Matsui, Y. Tokura, *Nature Materials*, **10** (2011).
[4] I. Kézsmárki, S. Bordács, P. Milde, E. Neuber, L.M. Eng, J.S. White, H.M. Rønnow, K. Yanai C.D. Dewhurst, M. Mochizuki, K. Yanai, H. Nakamura, D. Ehlers, V. Tsurkan, A. Loidl, *Nature Materials*, (2015).
[5] Y. Tokunaga, X.Z. Yu, J.S. White, H.M. Ronnow, D. Morikawa, Y. Taguchi & Y. Tokura, *Nature Communication*, **6** (2015).
[6] S. Henize, K. Von Bergmann, M. Menzel, J. Brede, A. Kubetzka, R. Wiesendanger, S. Blügel G. Bihlmayer, *Nature Physics*, **7** (2011).
[7] C. Moreau-Luchaire, C. Moutafis, N. Reyren, J. Sampaio, C.A.F. Vaz, N. Van Horne, K. Garcia K. Bouzehouane, C. Deranlot, P. Warnicke, P. Wohlhüter, J.M. George, M. Weigand, J. Raabe, V. Cros, A. Fert, *Nature Nanotechnology*, **11** (2016).
[8] T. Kurumaji, T. Nakajima1, M. Hirschberger, A. Kikkawa, Y. Yamasaki, H. Sagayama, H. Nakao, Y. Taguchi, T. Arima, Y. Tokura, *Science*, **365** (2019).
[9] T. Reimann, A. Bauer, C. Pfleiderer, P. Böni, P. Trtik, A. Tremsin, M. Schulz, and S. Mühlbauer, *Physical Review B,* **97**, 020406(R) (2018).
[10] J.S. White, A. Butykai, R. Cubitt, D. Honecker, C.D. Dewhurst, L.F. Kiss, V. Tsurkan, S. Bordács, *Physical Review B* **97**, 020401 (2018).
[11] M.T. Birch, R. Takagi, S. Seki, M.N. Wilson, F. Kagawa, A. Stefancic, G. Balakrishnan, R. Fan, P. Steadman, C.J. Ottley, M. Crisanti, R. Cubitt, T. Lancaster, Y. Tokura, P.D. Hatton, *Physical Review B,* **100**, 014425 (2019).
[12] M. Crisanti, M.T. Birch, M.N. Wilson, S.H. Moody, A. Stefancic, B.M. Huddart, S. Cabeza, G. Balakrishnan, P.D. Hatton, R. Cubitt, *Physical Review B,* **102**, 224407 (2020).

Anisotropy-induced soliton excitation in magnetized strong-rung spin ladders

Yu.V. Krasnikova[1,2], S.C. Furuya[3], V.N. Glazkov[1,2],
K.Yu. Povarov[4], D. Blosser[4], A. Zheludev[4]

[1] *P.L. Kapitza Institute for Physical Problems, RAS, Moscow, Russia*
[2] *Laboratory for Condensed Matter Physics, National Research University "HSE", Moscow, Russia*
[3] *Condensed Matter Theory Laboratory, RIKEN, Wako, Saitama, Japan*
[4] *Laboratory for Solid State Physics, ETH Zürich, Zürich, Switzerland*

Corresponding Author's Email: glazkov@kapitza.ras.ru

Spin-ladder magnets are one of the toy models of 1D magnetism. They feature a singlet ground state separated from the excited triplets by an energy gap Δ. The gap can be closed by an applied magnetic field $B_{c1} = \Delta/(g\mu_B)$, and up to the saturation field B_{c2} ideal 1D spin-ladder remains in a gapless Tomonaga-Luttinger spin liquid (TLL) state with the TLL interaction parameter determined by spin ladder exchange constants [1].

Metal-organic compound $(C_5H_{12}N)_2CuBr_4$ (called BPCB for short) is a well-established strong-rung spin ladder with the rung coupling J_{rung}=12.7 K and the couplings along the legs of the ladder J_{leg}=3.5 K [2,3]. Its critical field is about 6.6 T and saturation field is about 13.6 T [2].

We have performed low-temperature ESR study of this magnet at the temperatures down to 400 mK. We report observation of the low-energy excitation with anomalous energy-vs-field dependency in the fields around 10 T, i.e. in the midst of the TLL phase (Fig. 1).

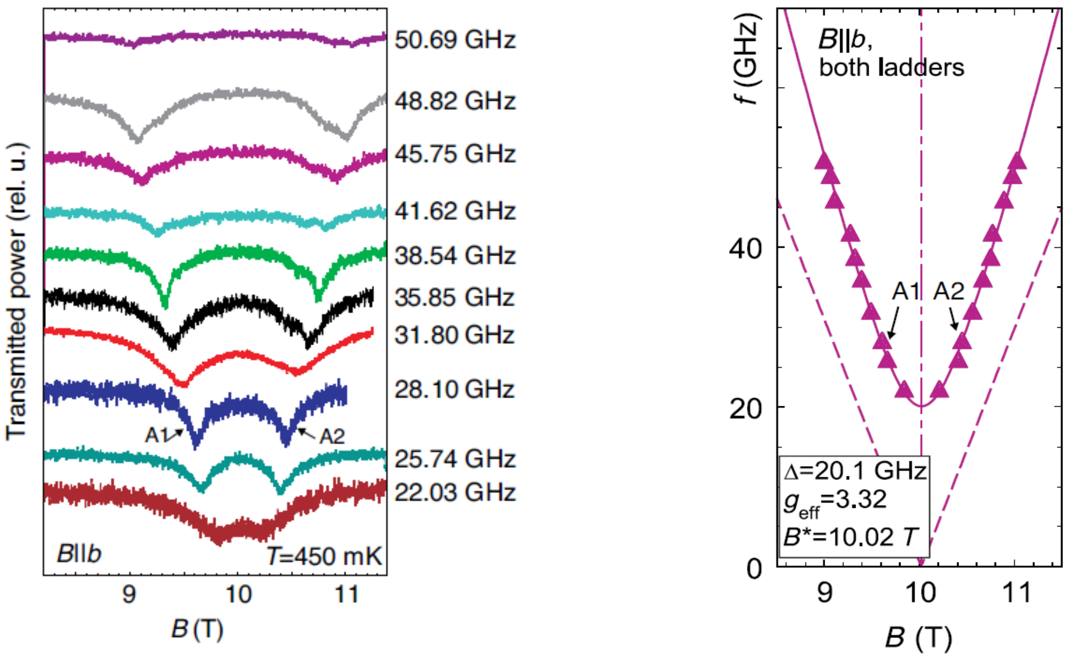

Fig.1 (left) Examples of low-temperature ESR absorption curves in BPCB at various microwave frequences. (right) ESR frequency-field diagram. Symbols - experimental data, dashed lines - excitations of isotropic model, solid curves - fit as described in the text. A1 and A2 marks indicate positions of the same absorption components on both panels.

Mapping of the "real spin" strong-rung spin ladder on an equivalent "pseudospin" XXZ-chain [3] predicts equivalence of the magnetized spin ladder at $B^* = (B_{c1} + B_{c2})/2$ to the XXZ chain at zero field, i.e. *zero excitation energy* at B^*. Field dependence of the excitations energy around B^* is still determined by the g-factor of the original spin ladder, which is slightly above 2 for Cu^{2+} ions. Instead, we observed anisotropic gap at B^* with the asymptotic slope of f(H) dependence corresponding to $g_{eff}\approx 3$:

$$2\pi\hbar\nu = \sqrt{\Delta^2 + [(g_{\text{eff}}\mu_B(B - B^*)]^2} \tag{1}$$

This behavior is explained by accounting for the Dzyaloshinskii-Moriya coupling which is symmetry-allowed in BPCB: it is uniform along the legs of the ladder and, due to the inversion centers on the rungs of the ladder, Dzyaloshinskii vectors on the ladder's legs are exactly opposite. The same ladder-to-chain mapping yields effective uniform DM interaction for the equivalent "pseudospin" model. Excitations of the spin chain with uniform DM interaction are known to be gapped at $q=0$ [4] in agreement with our observations.

However, the observed excitations turn out to be much more interesting. In the presence of DM interaction equivalent strongly anisotropic chain demonstrate transverse ordering of the "pseudospin" at B^* which allows for solitonic excitations of this anisotropic model. Our analysis proves that due to "real spins" to "pseudospin" transformation along the ladder-to-chain mapping only the solitonic "pseudospin" excitations remains ESR-active. Their frequency-field dependence is [5]

$$2\pi\hbar\nu = \sqrt{M^2 + [2Kg\mu_B(B - B^*)]^2}, \tag{2}$$

here the soliton "mass" M is proportional to the squared component of Dzyaloshinskii vector transverse to the applied field and the asymptotic slope depends on Luttinger parameter K, which is equal to 3/4 for the BPCP exchange couplings constants. The predicted effective g-factor value $g_{eff}=2Kg$ is in perfect agreement with the observed value (see Fig.1) without any additional fitting parameter [6].

Authors acknowledge support from Russian Science Foundation via Grant No. 17-12-01505. Work at ETHZ was supported by Swiss National Science Foundation, Division II.

References

[1] M. Jeong, D. Schmidiger, H. Mayaffre, M. Klanjšek, C. Berthier, W. Knafo, G. Ballon, B. Vignolle, S. Krämer, A. Zheludev, and M. Horvatic, Dichotomy between Attractive and Repulsive Tomonaga-Luttinger Liquids in Spin Ladders, Phys. Rev. Lett. 117, 106402 (2016).
[2] M. Klanjšek, H. Mayaffre, C. Berthier, M. Horvatic, B. Chiari, O. Piovesana, P. Bouillot, C. Kollath, E. Orignac, R. Citro, and T. Giamarchi, Luttinger liquid physics in the spin ladder material $(C_5H_{12}N)_2CuBr_4$, Phys. Status Solidi C 247, 656 (2010).
[3] P. Bouillot, C. Kollath, A.M. Läuchli, M. Zvonarev, B. Thielemann, C. Rüegg, E. Orignac, R. Citro, M. Klanjšek, C. Berthier, M. Horvatić, and T. Giamarchi, Statics and dynamics of weakly coupled antiferromagnetic spin-1/2 ladders in a magnetic field, Phys. Rev. B 83, 054407 (2011).
[4] K.Y. Povarov, A.I. Smirnov, O.A. Starykh, S.V. Petrov, and A.Y. Shapiro, Modes of Magnetic Resonance in the Spin-Liquid Phase of Cs_2CuCl_4, Phys. Rev. Lett. 107, 037204 (2011).
[5] S.C. Furuya and T. Momoi, Electron spin resonance for the detection of long-range spin nematic order, Phys. Rev. B 97, 104411 (2018).
[6] Yu.V. Krasnikova, S.C. Furuya, V.N. Glazkov, K.Yu. Povarov, D. Blosser, and A. Zheludev, "Anisotropy-induced soliton excitation in magnetized strong-rung spin ladders", Phys. Rev. Lett. 125**,** 027204 (2020).

Chiral phonons in helical single crystal Te by circularly polarized Raman spectroscopy

K. Ishito[1], H. Mao[1], K. Kobayashi[2], Jun-Ichiro Kishine[3], T. Satoh[1]

[1] *Department of Physics, Tokyo Institute of Technology, Tokyo, Japan*
[2] *Research Institute for Interdisciplinary Science, Okayama University, Okayama, Japan*
[3] *The Open University of Japan, Chiba, Japan*

Corresponding Author's Email: ishito.k.aa@m.titech.ac.jp

Recently, phonons with chirality (chiral phonons) have attracted much attention. Chiral phonons have angular momentum and pseudo-angular momentum [1]. In circularly polarized Raman scattering spectroscopy with backscattering along the helical axis of a helical crystal, the doubly-degenerated *E*-mode peaks split [2]. In addition, each of the two split peaks is observed under two different conditions where the angular momentum of the incident circular polarization is reversed [2]. However, the relationship between this circular polarization selection rule and the angular momentum and pseudo-angular momentum of the phonons was verified experimentally.

We therefore focused on single crystal Te, a material with a helical axis. We measured the phonon frequency and the Raman scattering selection rule by backward Raman scattering spectroscopy along the helical axis of this material. One of the split *E*-modes was observed in each of the two conditions where the angular momentum of the circular polarization of the incident light was reversed. The phonon at 1.4% of the wavenumber of A point was excited and we got *E*-mode splitting and the circular polarization selection rule.

We calculated the phonon dispersion by ABINIT, a first principle software. The calculation was consistent with the results of Raman scattering spectroscopy with a relative error of about 10%. We also calculated the angular momentum and pseudo-angular momentum of phonons from eigendisplacements and discussed the relation with the circular polarization selection rule of E-mode.

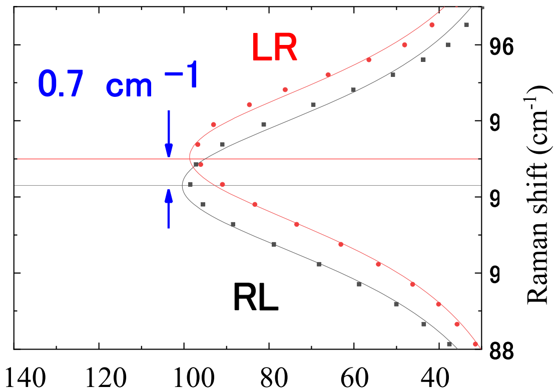

Fig.1 Circularly polarized Raman scattering spectroscopy in two different conditions: RL (right circularly polarized incident light, left circularly polarized scattered light) and LR

References

[1] L. Zhang and Q. Niu, Phys. Rev. Lett. 115, 115502 (2015).
[2] A.S. Pine and G. Dresselhaus, Phys. Rev. 188, 1489 (1969).

Revisit of Dzyaloshinskii-Moriya interaction with symmetry

H. Katsumoto, S. Blügel

Peter Grunberg Institut and Institute for Advanced Simulation, Forschungszentrum Jülich and JARA, Jülich, Germany

Corresponding Author's Email: h.katsumoto@fz-juelich.de

Complex magnetic structures and textures such as domain-walls, spin-spirals, skyrmions, bobbers and others are currently in the limelight of science. Descriptions of these textures hinges on atomistic spin-lattice and micromagnetic models with parameters determined from first-principles theory. Beyond the conventional Heisenberg interaction between pairs of spins, the one-site magnetic anisotropy and the Zeeman interaction with an external field, the chiral Dzyaloshinskii-Moriya interaction (DMI) [1,2,3], higher-order exchange interactions [4,5] and higher-order chiral interactions [6] have been discussed. This scenario puts the Dzyaloshinskii-Moriya interaction into a much broader context.

The first theoretical explanation of the DMI was given by Dzyaloshinskii using a phenomenological approach based on Landau theory to explain the weak ferromagnetism of α-hematite [1]. Later [3] he showed that globally non-zero DMI leads to globally modulated structures. Shortly after the publication of Ref [1], Moriya [2] provided a microscopic description of DMI in terms of an antisymmetric pair interaction by adding the on-site spin-orbit interaction to the Anderson model describing the superexchange interaction of magnetic ions in transition metal oxides and deriving the magnetic pair interaction in second-order perturbation theory. Ref. [2] includes also Moriya's rules which determine the symmetry conditions under which the prefactor of the DMI interaction, known as the DMI vector is nonzero. Many other microscopic models lead to the same functional form of antisymmetric pair interactions, e.g. Fert and Levy [7]. In addition to the classical and quantum mechanical description by Dzyaloshinskii and Moriya, respectively, both derivations differ in terms of symmetry: in the derivation by Dzyaloshinskii, the density distribution function is expanded in a basis of magnetic symmetry, whereas, the D vector that determines Moriya's microscopic DMI term is determined by the crystallographic space group without any reference to the magnetic symmetry. In this presentation, we would like to go back to the discovery of the DMI and discuss its detailed understanding.

References

[1] I.E. Dzialoshinskii, *Soviet Physics JETP* **5**, 1259 (1957).
[2] I.E. Dzialoshinskii, *Soviet Physics JETP* **19**, 964 (1964).
[3] T. Moriya, *Physical Review Letters* **4**, 228 (1960).
[4] M. Hoffmann and S. Blügel, *Physical Review B* **101**, 024418 (2020).
[5] S. Grytsiuk, J.-P. Hanke, M. Hoffmann, J. Bouaziz, O. Gomonay, G. Bihlmayer, S. Lounis, Y Mokrousov and S. Blügel, *Nature Communications* **11**, 511 (2020).
[6] S. Brinker, M. dos Santos Dias, and S. Lounis, *Physical Review Research* 2, 033240 (2020).
[7] A. Fert and P. M. Levy, *Physical Review Letters* 44, 1538 (1980).

Topological spin texture in centrosymmetric magnets

S. Lin

Los Alamos National Laboratory, T-4 and CNLS, Los Alamos, New Mexico USA

Corresponding Author's Email: szl@lanl.gov

We study magnetic orders stabilized by the Ruderman-Kittel-Kasuya-Yosida interaction between the moments in 2D electron gas. We find a robust skyrmion lattice in the presence of magnetic field and easy axis anisotropy. An attractive aspect of this mechanism for skyrmion stabilization is that the magnitude of the magnetic ordering wave vectors is dictated by the Fermi wave number. Consequently, the topological contribution to the Hall conductivity of the system becomes of the order of the quantized value e^2/h, when the local exchange coupling is comparable to the Fermi energy. When a compass anisotropy due to the spin-orbit coupling or by the dipolar interaction is present, other interesting topological spin textures including meron, skyrmion, and vortex crystals can be stabilized even in the absence of magnetic field. Our work demonstrates a promising route to stabilize topological spin textures by competing interactions in centrosymmetric magnets.

References

[1] Zhentao Wang, Ying Su, Shi-Zeng Lin, and Cristian D. Batista, Phys. Rev. Lett. 124, 207201(2020).
[2] Zhentao Wang, Ying Su, Shi-Zeng Lin, and Cristian D. Batista, Phys. Rev. B 103, 104408 (2021).

The magnetic and electronic properties of the $FeRhGe_2$ compound (B20)

D.A. Salamatin[1,2,3], A.V. Bokov[1,3], V.A. Sidorov[1,3], Z. Surowiec[2,4], M.V. Magnitskaya[1,3], N.M. Chtchelkachev[1], E.V. Altynbaev[1,3,5], D.O. Skanchenko[1,3,5], M. Wiertel[4], M. Budzynski[4], A.V. Tsvyashchenko[1,3]

[1] *Vereshchagin Institute of High Pressure Physics, RAS, Troitsk, Moscow, Russia*
[2] *Joint Institute for Nuclear Research, Dubna, Russia*
[3] *Lebedev Physical Institute, RAS, Moscow, Russia*
[4] *Institute of Physics, M. Curie-Sklodowska University, Lublin, Poland*
[5] *Konstantinov Petersburg Nuclear Physics Institute of National Research Centre «Kurchatov Institute», Gatchina, Russia*

Corresponding Author's Email: magnma@yandex.ru

FeGe in its B20 crystal phase (ϵ-FeGe) is a well-known chiral magnet with a rather high transition temperature T_N = 279 K [1]. The *H–T* (magnetic field–temperature) phase diagram of FeGe is rich and includes spiral, conical, skyrmion and field-polarized phases [2], which makes FeGe fruitful in terms of fundamental physics and practical usage.

RhGe compound can also crystallize in non-centrosymmetric B20 structure under high pressure. RhGe becomes superconductor below 4 K and weak itinerant magnetism was assumed in the compound [3]. Recent local microscopic study performed using the time-differential perturbed angular correlations (TDPAC) method was not able to clearly confirm the magnetism below 140 K down to helium temperature [4].

The high pressure–high temperature synthesis allows us to obtain $Fe_{1-x}Rh_xGe$ series in B20 crystal structure for a wide concentration range $0 \le x \le 1$. Here, we focus at the $FeRhGe_2$ (x = 0.5) compound. Rietveld refinement of X-ray powder diffraction (XRD) pattern of the compound revealed the occurrence of two B20 crystal phases with different lattice constants. For the sample studied here, the ratio of phase fractions of a denser (first) phase (a = 4.780 Å) to a less dense (second) one (a = 4.800 Å) is equal to 3:2. The additional investigations of the phase fraction ratio for another samples, with the same Rh concentration, showed that the phase fraction ratio depends on the synthesis procedure and particularly the rate of crystallization.

In the temperature dependence of magnetic susceptibility, we observe two transitions at 150 and 210 K. The temperatures of the transitions weakly increase with pressure up to 5 GPa. The Curie–Weiss temperature of $FeRhGe_2$ is about 225 K which is slightly smaller than 284 K in FeGe. The small angle neutron scattering (SANS) pattern at 5 K showed that the magnetic structure of $FeRhGe_2$ is ferromagnetic or spiral with a very large period (wave vector $k_s < 0.01$ nm^{-1}). No phase separation is detected on the SANS pattern.

To study magnetism of $FeRhGe_2$ in detail, we performed Mössbauer effect measurements at ^{57}Fe in the temperature range 4–300 K in Lublin, Poland. The radiation was obtained from $^{57}Co(Rh)$ source. Spectra (see Table 1) were analyzed with the SpectrRelax program [5]. All isomer shift (IS) values are referred to that of a 28-μm-thick α-Fe foil. At 300 K, the spectra could be well fitted with two quadrupole splittings (QS), with the amplitude ratio of 2:1, which is in good agreement with XRD results (Fig.1). The spectrum at 4 K is fitted with two hyperfine magnetic splittings (Fig.2).

We also made *ab initio* calculations of $FeRhGe_2$ in paramagnetic and ferromagnetic state using the Wien2k package. Both crystal phases were calculated at experimental lattice parameters and turned out stable, with a small energy preference of the first (denser) phase. The evaluated magnetic moments (1.37 and 1.58 μ_B) and hyperfine magnetic fields B_{hf} (–107.2 and –109.7 kOe) at the Fe atom are found to be larger for the second phase.

The fitted parameters of Mössbauer spectra of $FeRhGe_2$.

Table 1

T **(K)**	**Intensity (%)**	**IS (mm/s)**	**QS (mm/s)**	$\boldsymbol{B_{hf}}$ **(kOe)**
300	66.67 (5)	1.144 (3)	0.750 (4)	0
	33.33 (5)	1.254 (5)	1.106 (7)	0
4	66.67 (15)	0.669 (3)	0.000 (1)	98.3 (1)
	33.33 (15)	0.689 (3)	−0.062 (1)	113.6 (1)

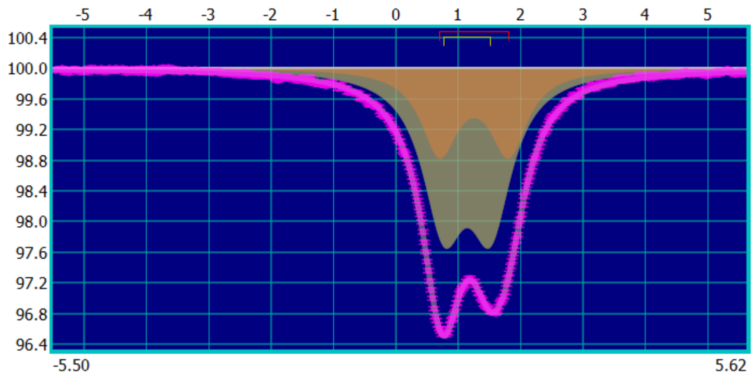

Fig.1 The experimental Mössbauer spectrum of $FeRhGe_2$ at 300 K (purple circles) with fit (grey line). The quadrupole splitting is shown as red and yellow shapes. The horizontal axis is velocity (mm/s) and vertical axis is relative intensity (%).

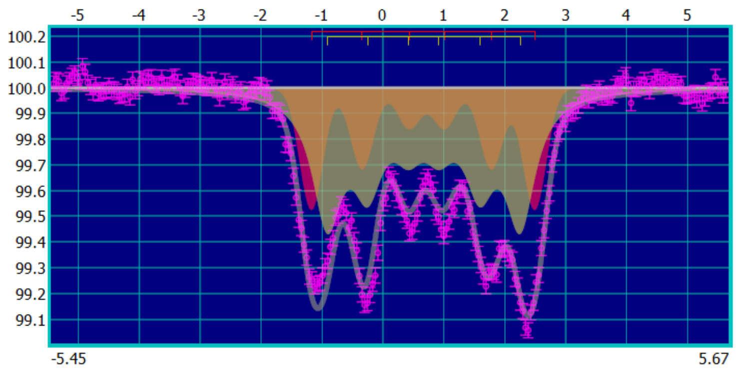

Fig.2 The Mössbauer spectrum of $FeRhGe_2$ at 4 K (purple circles) with fit (grey line).

This work was supported by Russian Science Foundation under Grants RSF No.17-12-01050 and No.18-12-00438. Support from Polish representative at the Joint Institute for Nuclear Research is also acknowledged.

References

[1] B. Lebech, J. Bernhard and T. Freltoft, J. Phys.: Condens. Matter 1, 35 (1989).
[2] H. Wilhelm, M. Baenitz, M. Schmidt, U.K. Rößler, A.A. Leonov and A.N. Bogdanov, Phys. Rev. Lett. 107, 127203 (2011).
[3] A. Tsvyashchenko, V. Sidorov, A. Petrova, L. Fomicheva, I. Zibrov and V. Dmitrienko, J. Alloys Compd. 686, 431 (2016).
[4] D.A. Salamatin, A.V. Tsvyashchenko, A.V. Salamatin, A. Velichkov, M.V. Magnitskaya, N.M. Chtchelkatchev, V.A. Sidorov, L.N. Fomicheva, M.V. Mikhin, M.G. Kozin, A.V. Nikolaev, I.L. Romashkina and M. Budzynski, J. Alloys Compd. 850, 156601 (2021).
[5] M.E. Matsnev and V.S. Rusakov, AIP Conf. Proc. 1489, 178 (2012); 1622, 40 (2014).

Magnetic properties of frustrated ytterbium and holmium rare earth titanates doped with yttrium and bismuth

O.V. Nemytova[1], A.B. Rinkevich[1], M.S. Koroleva[2]

[1] *M.N. Miheev Institute of Metal Physics, Ural Branch, RAS, Ekaterinburg, Russia*
[2] *Institute of Solid State Chemistry, Ural Branch, RAS, Ekaterinburg, Russia*

Corresponding Author's Email: mif--83@mail.ru

This work is devoted to an investigation of magnetic properties of ytterbium and holmium titanates doped with yttrium and bismuth. The magnetization curves and temperature dependences of the susceptibility have been measured in the fields up to 30 kOe at the temperatures from 2 K to 300 K. The comparative analysis of the magnetic properties of the doped and undoped titanates, as well as the titanates with various degree of doping, has been carried out. The task has been to estimate the effect of doping on the interaction features between rare earth ions.

Magnetic properties of pyrochlore titanates are of wide interest in connection with the problem of the specific magnetic state - «spin ice», which establishes in them at low temperatures. In a crystal lattice, rare-earth ions occupy positions at tetrahedron vertices, which allows frustrated magnetic moments to exist [1].

The measurement results obtained for the holmium and ytterbium titanates doped with yttrium and bismuth, as well as for the undoped ones, show that there is no hysteresis in all cases (Fig. 1). In the same time, for the holmium titanates at the temperature of T=2 K and in the fields of up to 30 kOe, the magnetization curves virtually achieve the saturation (Fig. 1a). Whereas, in the case of the doped and undoped ytterbium titanates, the magnetization curves (Fig. 1b) just show the signs of the saturation. However, in the fields of up to 30 kOe, total saturation is not achieved. In all cases, when increasing the doping degree, the saturation magnetization decreases. This is related to the fact that the Bi^{3+} and Y^{3+} ions do not have a magnetic moment. Preliminary results for the titanates doped with bismuth are published in [2].

Upon the doping, the bismuth and yttrium ions replace Ho^{3+} and Yb^{3+} ions in the crystal lattice. The choice of the bismuth and yttrium as the dopants is caused by the fact that upon the doping the titanates-pyrochlores with these elements, even in the case of the sufficiently large dopant fraction, the pyrochlore structure is retained. However, in the doped titanates, one can expect a change of interaction between the neighbor ions having the magnetic moment.

The results of the performed X-ray analysis show that the doping with yttrium and bismuth does not lead to any significant variation in the cell parameters. That is, we should not associate the reason of the change of the interaction nature with a change of a distance between the rare-earth ions. Further, Fig. 2 shows the dependences of the product of the susceptibility χ and temperature T on the reciprocal temperature 1/T, which are important for the determination of the dominating magnetic interaction in the titanates under study. The calculation of the temperature dependence of the susceptibility for the holmium titanate is performed in the Ising model [3].

$$\chi(T) = \frac{N(g\mu_B)^2}{k_B T}\frac{S^2}{3}\left[1 - \frac{3S^2}{2k_B T}\left(2.18J_D + 2.67J_S\right)\right], \tag{1}$$

where g=8/7 is the Lande factor of the $^2F_{7/2}$ multiplet, N is the number of magnetic ions per cm^3, k_B is the Boltzmann constant, μ_B is the Bohr magneton, S is the spin of an ion in the ground state. The J_D constant takes into account the dipole interaction of the nearest neighbors, the J_S constant - the superexchange interaction.

In the low-temperature region for the undoped and doped holmium titanates (Fig. 2a), there is the section with an approximately linear dependence. The deviation from linearity at the higher temperatures is associated in [3] with a violation of applicability of the Ising model. The negative slope of the low-temperature section for the undoped holmium titanate indicates the dominance of the magnetic dipole interaction. Doping with yttrium and bismuth leads to the significant decreasing the dependence slope, which is caused by the sharp weakening of the magnetic interactions between the rare-earth ions. For the undoped ytterbium titanate (Fig. 2b), there is also an approximately linear section of dependence at the low temperatures. The positive slope of the low-temperature section indicates the dominance of the exchange interaction. Doping with both yttrium and bismuth leads to the change of the slope sign. In the case of the ytterbium titanate, the change of the interaction between the neighbor ions upon the doping can be explained by the following way. The concentration of R^{3+}-O-R^{3+} ion pairs in this frustrated rare earth titanate, between which there is the superexchange, decreases because of the presence of a large number of the randomly distributed yttrium or bismuth ions, which occupy the positions of the ytterbium ions in the crystal lattice. In the doped compounds, the magnetic dipole interaction, which is capable to act at large distances than the exchange one, begins to dominate.

Acknowledgement: The work has been carried out within the grant from Russian Foundation for Basic Research No 20-02-00135.

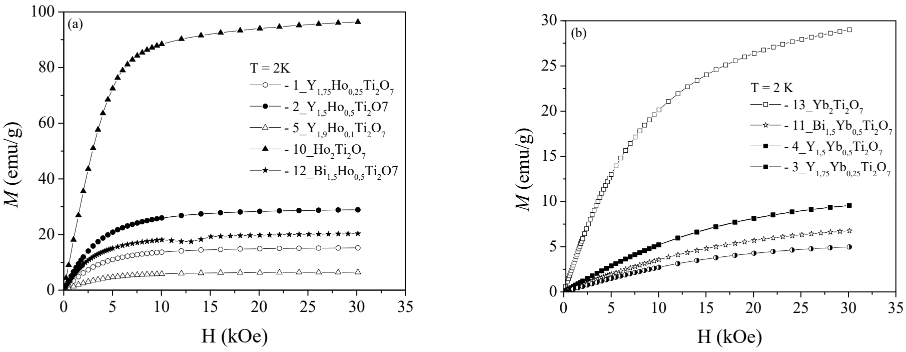

Fig.1. The magnetization curves of the samples under study.

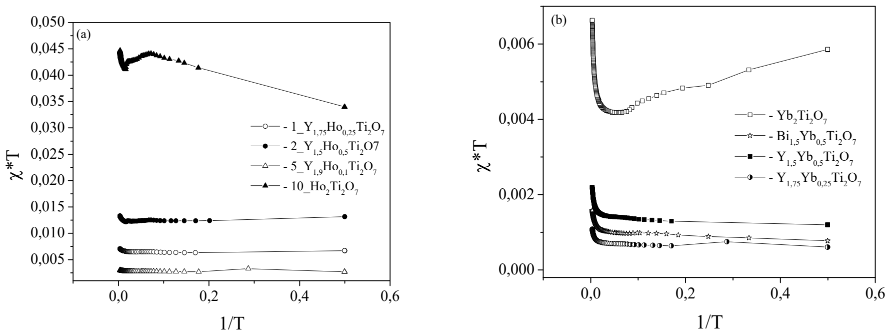

*Fig.2. The dependences of the product χ*T on the reciprocal temperature 1/T for the samples under study.*

References

[1] M.J.P Gingras, P.A. McClarty, Quantum spin ice: A search for gapless quantum spin liquids in pyrochlore magnets 77, 056501 (2014).

[2] A.B. Rinkevich, M.V. Koroleva, I.V. Piir, D.V. Perov, Magnetic Properties of Bismuth-Doped Ytterbium and Holmium Pyrochlore Titanates 61, 1401–1408 (2019).

[3] R. Siddharthan, B.S. Shastry, A.P. Ramirez, A. Hayashi, R.J Cava, S. Rosenkranz, Ising pyrochlore magnets: low-temperature properties, «ice rules»," and beyond 83, 1854 (1999).

Magnetic hedgehog lattice in a centrosymmetric cubic metal

S. Okumura[1], S. Hayami[2], Y. Kato[2], Y. Motome[2]

[1] The Institute for Solid State Physics, the University of Tokyo, Kashiwa, Japan
[2] Department of Applied Physics, the University of Tokyo, Tokyo, Japan

Corresponding Author's Email: okumura@issp.u-tokyo.ac.jp

Chiral magnets have attracted much attention due to their interesting properties associated with the peculiar spin structures originating from the Dzyaloshinskii-Moriya interaction. For instance, a series of the *B*20-type compounds, $MnSi_{1-x}Ge_x$ and $Mn_{1-y}Fe_yGe$, shows skyrmion lattices and hedgehog lattices (HLs), which induce interesting quantum transport phenomena, such as the topological Hall effect and the thermoelectric response [1].

Recently, a new generation of topological spin textures has been discovered in centrosymmetric metals where the Dzyaloshinskii-Moriya interaction is inactive. A typical example is a HL composed of four spin helices (4*Q*-HL) observed in the cubic perovskite $SrFeO_3$ [2]. While the HLs have been studied theoretically for noncentrosymmetic metals [3], their stability remains elusive in the centrosymmetric case.

In this study, we elucidate the ground state of a spin model with effective long-range interactions arising from itinerant nature of electrons on the cubic lattice, by performing simulated annealing. We show that a 4*Q*-HL is stabilized by the synergy of the bilinear and biquadratic interactions (Fig. 1). In the magnetic field, we find that the system shows the magnetic phase transitions from 4*Q* to 1*Q* and from 2*Q* to 1*Q* states, both of which are observed in $SrFeO_3$ [2]. We compare the results with those for the noncentrosymmetric case, focusing on the topological properties associated with the emergent magnetic monopoles and antimonopoles [4].

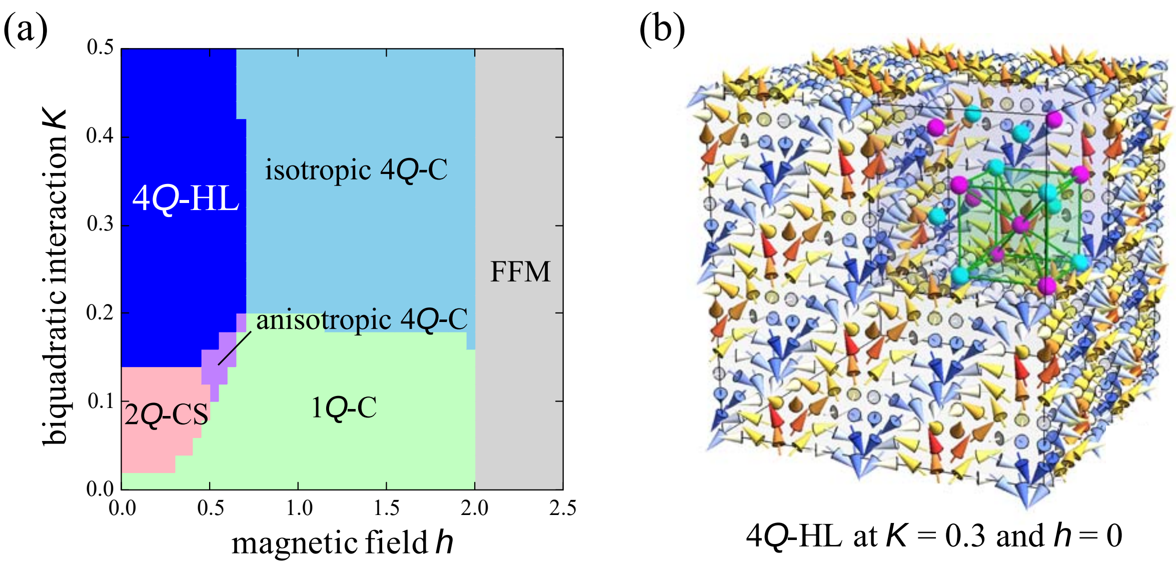

Fig.1 (a) Phase diagram for the magnetic field h and the biquadratic interaction K. (b) Spin texture of the 4Q-HL at zero field obtained by simulated annealing. The magenta (cyan) balls represent the magnetic (anti)monopoles in the magnetic unit cell shown by the black box.

This research was supported by JST CREST (No. JPMJCR18T2 and No. JPMJCR19T3), JST PREST (No. JPMJPR20L8), JSPS KAKENHI (No. JP18K13488 and No. JP19H05825), the Chirality Research Center in Hiroshima University, and JSPS Core-to-Core Program, Advanced Research Networks. This work was also supported by "Joint Usage/Research Center for Interdisciplinary Large-scale Information Infrastructures" and "High Performance Computing Infrastructure" in Japan (Project ID: EX20304). Parts of the numerical calculations were performed in the supercomputing systems in ISSP, the University of Tokyo. SO was supported by JSPS through the research fellowship for young scientists.

References

[1] Y. Fujishiro *et al*., Appl. Phys. Lett. 116, 090501 (2020).
[2] S. Ishiwata *et al*., Phys. Rev. B 101, 134406 (2020).
[3] S. Okumura, S. Hayami, Y. Kato, and Y. Motome, Phys. Rev. B 101, 144416 (2020).
[4] S. Okumura, S. Hayami, Y. Kato, and Y. Motome, in preparation.

Incommensurate magnetic phases of the multiferroic compound $MnCr_2O_4$ described with the superspace formalism

M. Pardo-Sainz[1,2], A. Toshima[3], G. Andre[4], J. Basbus[5], G. Cuello[6], T. Honda[7], T. Otomo[7], K. Inoue[3], Y. Kousaka[2], J. Campo[1]

[1] Instituto de Nanociencia y Materiales de Aragón, CSIC - Universidad de Zaragoza, Zaragoza, Spain
[2] Osaka Prefecture University, Osaka, Japan
[3] Graduate School of Science, Chirality Research Center and Institute for Advanced Materials Research, Hiroshima University, Japan
[4] Laboratoire Leon Brillouin, Saclay, France
[5] Centro Atomico Bariloche, INN - CNEA - CONICET, S. C. de Bariloche, Argentine
[6] Institut Laue-Langevin, Grenoble, France
[7] Institute of Materials Structure Science, High Energy Accelerator Research Organization (KEK), Tsukuba, Japan

Corresponding Author's Email: javier.campo@csic.es

Nowadays, chromium-based normal spinel oxides ACr_2O_4 are one of the most studied materials in the condensed matter community due to the interplay between its magnetic, electric and structural properties as well as to its potential application to different key industry sectors. In these compounds, several physical effects have been observed, which include magnetostriction, colossal magnetoresistance, multiferroic, spin frustration and more [1-4].

In particular, for $MnCr_2O_4$, the ground state magnetic structure is still controversial because the magnetic structures reported by different groups and investigated by independent techniques are inconsistent [1-7].

The magnetic structure of this compound was reinvestigated by magnetization, specific heat and neutron diffraction experiments at different temperatures. The results suggested that a new magnetic phase, not previously reported, is developed under 18 K when the sample is synthesized under a reductive atmosphere. The magnetic phases present in this sample were: long-range ferrimagnetic order below T_C = 45 K; incommensurate conical spin order with propagation vector $\vec{k}_{S1}$ = (0.62(1), 0.62(1), 0) below T_{S1} = 20 K; and incommensurate conical spin order with propagation vector $\vec{k}_{S2}$ = (0.660(3), 0.600(1), 0.200(1)) below T_{S2} = 18 K.

Using the superspace group formalism [8-10], the symmetry of the nuclear and magnetic structures is described. The presence of transverse conical magnetic structures in the lower-temperature phases implies the existence of multiferroicity. Using simple theoretical calculations, we derive the directions along which the electric polarization lies for each magnetic phase.

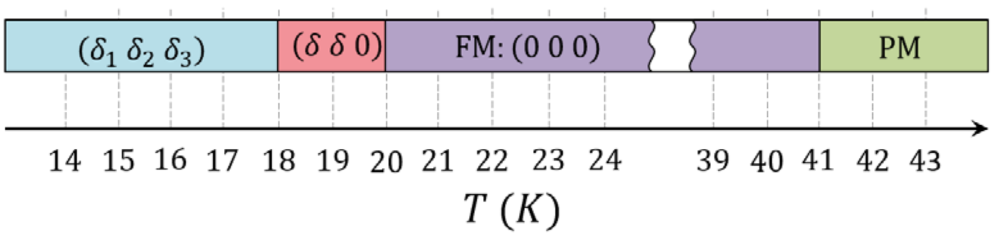

Fig.1 Phases present in $MnCr_2O_4$ together with their phase transition temperatures. Green: paramagnetic order, purple: ferrimagnetic order, pink: conical order with $\vec{k}_{S1}$ = (0.62(1), 0.62(1), 0), blue: conical order with $\vec{k}_{S2}$ = (0.660(3), 0.600(1), 0.200(1)).

References

[1] K. Dey, A. Indra, S. Majumdar, and S. Giri, Journal of Magnetism and Magnetic Materials 435, 15 (2017).
[2] K. Tomiyasu, J. Fukunaga, and H. Suzuki, Phys. Rev. B 70, 214434 (2004).
[3] E. Winkler, S. Blanco Canosa, F. Rivadulla, M.A. Lopez-Quintela, J. Rivas, A. Caneiro, M.T. Causa, and M. Tovar, Phys. Rev. B 80, 104418 (2009).
[4] N. Mufti, A.A. Nugroho, G.R. Blake, and T.T.M. Palstra, Journal of Physics: Condensed Matter 22, 075902 (2010).
[5] J.M. Hastings and L.M. Corliss, Phys. Rev. 126, 556 (1962).
[6] G.T. Lin, Y.Q. Wang, X. Luo, J. Ma, H.L. Zhuang, D. Qian, L.H. Yin, F.C. Chen, J. Yan, R.R. Zhang, S.L. Zhang, W. Tong, W.H. Song, P. Tong, X.B. Zhu, and Y.P. Sun, Phys. Rev. B 97, 064405 (2018).
[7] D. Tobia, J. Milano, M.T. Causa, and E.L. Winkler, Journal of Physics: Condensed Matter 27, 016003 (2015).
[8] A. Janner and T. Janssen, Acta Crystallographica Section A 36, 399 (1980).
[9] J.M. Perez-Mato, J.L. Ribeiro, V. Petricek, and M.I. Aroyo, Journal of Physics: Condensed Matter 24, 163201 (2012).
[10] J. Rodríguez-Carvajal and J. Villain, Comptes Rendus Physique 20, 770 (2019).

Fast magnetization reversal of a magnetic nanoparticle driven by a down-chirp microwave field pulse at finite temperature

M.A. J. Pikul[1], M.A. S. Akanda[1], M.T. Islam[1], X.S. Wang[2]

[1] *Physics Discipline, Khulna University, Khulna, Bangladesh*
[2] *School of Physics and Electronics, Hunan University, Changsha, China*

Corresponding Author's Email: torikul@phy.ku.ac.bd

First, we investigate the magnetization reversal of a single-domain magnetic nanoparticle driven by down-chirp microwave magnetic field pulse (DCMWP) [1]. Numerical simulations based on the schostacastic Landau-Lifshitz-Gilbert (sLLG) equation reveal that a down-chirp microwave pulse solely is able to induce fast magnetization reversal. Later, we study the DCMWP-driven magnetization reversal including finite temperature and found the fast reversal is valid even above room temperature [2]. Interestingly, any one of the three controlling parameters of a DCMWP, i.e. the amplitude, chirp rate, or initial frequency, decreases with increasing temperature while the other two are fixed. The maximal temperature at which the reversal, is valid, increases with enlarging the system size. These phenomena are related to the facts that the energy barrier induced by anisotropy increases with the system volume, and the effective magnetization decreases with temperature. We also provide a set of optimal parameters for practical realization of our proposal. These findings may provide a way to realize low-cost and fast magnetization reversal with a wide operating temperature.

References

[1] M.T. Islam, X.S. Wang, Y. Zhang, and X.R. Wang, "Subnanosecond magnetization reversal of a magnetic nanoparticle driven by a chirp microwave field pulse," Physical Review B97, 224412 (2018).
[2] M.T. Islam, M.A. J. Pikul, and X.S. Wang, "Thermally assisted magnetization reversal of a magnetic nanoparticle driven by a down-chirp microwave field pulse," Journal of Magnetism and Magnetic Materials 537, 168174 (2021).

Spin wave propagation in strain mediated magnonic waveguides

A.V. Sadovnikov, A.A. Grachev, E.N. Beginin, S.A. Nikitov

Saratov State University, Saratov, Russia

Corresponding Author's Email: SadovnikovAV@gmail.com

In recent years much research has been directed towards the use of spin waves for signal processing at microwave and subterahertz frequencies due to the possibility to carry the information signal without the transmission of a charge current[1]. In the framework of the 2021 magnonics roadmap the straintronic is separated as the versatile tool to control the spin wave propagation [2-3]. The strain-mediated spin-wave channels can be used to route the magnonic information signal. The magnon straintronics could provide to fabricating magnonic platforms for energy-efficient signal processing [3]. Recent theoretical and experimental studies suggest that strain can be used to engineer energy-efficient complicated 2D and 3D piezoelectric heterostructures such as ferromagnetic/piezoelectric bi- and multilayers [4]. The strain-mediated control of spin-wave propagation was demonstrated via the experimental observations of the spin-wave coupling phenomena in different magnonic structures based on the adjacent magnonic crystals and adjacent magnetic yttrium iron garnet stripes in the form of magnonic spin-wave couplers. The model describing the spin-wave transport was proposed based on the self-consistent equations[5] via the solution of the micromagnetic task in couple with the finite-element simulation of the static strain/stress in the ferromagnetic/piezoelectric structure. The obtained results open new perspectives for the future-generation electronics using integrated magnonic networks both in micro - and nanoscale [6].

In the framework of this presentation the strain mediated control of the spin-wave transport along the magnonic crystal with PZT layer was revealed by means of Brillouin light-scattering (BLS) spectroscopy and microwave spectroscopy techniques. We demonstrate the voltage-driven control of spin waves in the ferromagnetic-piezoelectric structure. The results of numerical model based on micromagnetic simulation are in good agreement with the BLS data. The proposed structure can be used for frequency selective spin-wave wave separation (demultiplexing) with the energy efficient tunability of microwave characteristics. It was shown, that the strain-mediated spin-wave channels can be used to route the magnonic information signal and thus the composite magnon-straintronic structure could provide to fabricating magnonic platforms for energy-efficient signal processing. The demonstrated voltage induced control of spin-wave propagation opens the promising alternative of the magnonic crystals in the way of energy efficient beyond-CMOS functional units.

This work was supported by the Russian Science Foundation (Project #20-79-10191).

References

[1] S.A. Nikitov, et al, *Phys. Usp.* **63,** 10 (2020).
[2] A.V. Sadovnikov, A.A. Grachev, E.N. Beginin, S.E. Sheshukova, Yu.P. Sharaevskii, and S.A. Nikitov, *Physical Review Applied*, **7**, 014013 (2017).
[3] A.V. Sadovnikov, A.A. Grachev, S.E. Sheshukova, Yu.P. Sharaevskii, A.A. Serdobintsev, D.M. Mitin, S.A. Nikitov, *Phys. Rev. Lett.* **120**, 257203 (2018).
[4] A.A. Bukharaev et al Phys. Usp. **61**, 1175–1212 (2018).
[5] A.V. Sadovnikov, A.A. Grachev, A.A. Serdobintsev, S.E. Sheshukova, S.S. Yankin, S.A. Nikitov, IEEE Magnetics Letters, **10**, 5506405 (2019).
[6] M. Collet, et al., Appl. Phys. Lett. **110**, 092408, (2017).

Observation of phonon modes in a chiral spin soliton lattice

Y. Shimamoto[1], Y. Matsushima[1], T. Hasegawa[1], Y. Kousaka[1], I. Proskurin[2], F.J. T. Goncalves[3], Y. Togawa[1]

[1] *Osaka Prefecture University, Sakai, Osaka, Japan*
[2] *Department of Physics and Astronomy, University of Manitoba, Winnipeg, Canada*
[3] *Helmholtz-Zentrum Dresden-Rossendorf, Dresden, Germany*

Corresponding Author's Email: y-shimamoto-spin@pe.osakafu-u.ac.jp

In chiral magnetic materials, the Dzalloshinskii-Moriya (DM) interaction is a key element for the formation of non-collinear spin textures such as a chiral spin soliton lattice (CSL) and magnetic skyrmions. In particular, the monoaxial chiral helimagnet hosts the CSL, which consists of nonlinear periodic arrays of chiral soliton kinks in the presence of magnetic fields, as shown in Fig. 1[1]. Note that the CSL exhibits controllability of its period by the field strength and a phase coherence over the macroscopic length scale. This situation is well reproduced by the effective one-dimensional chiral sine-Goldon model [2].

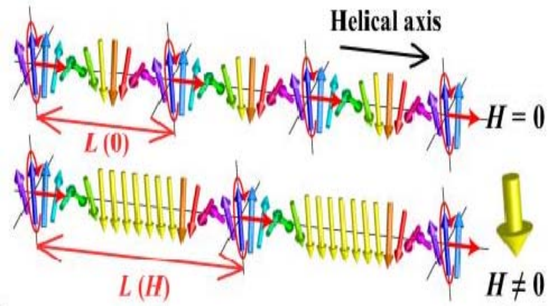

Fig.1 Chiral magnetic orders.

Due to the translational symmetry breaking of the CSL, the existence of the elementary excitation, which is described by 'phonon' mode of correlated chiral soliton kinks, is predicted theoretically [3, 4]. Interestingly, we can control the size of the first Brillouin zone which is formed in the band structure of the CSL phonon mode by changing the CSL period. In consequence, it is naturally expected that the frequency of higher order modes is modulated by the field strength. However, such an elementary excitation has not been observed experimentally yet. Experimental detection of the CSL phonon mode would be useful for further understanding fundamental physics on chiral magnetic materials because it would allow an evaluation of the interaction between two neighboring spins.

We present experimental results on the magnetic resonance of the $CrNb_3S_6$ bulk single crystals, which hosts the CSL. In the experiments, an inductive method was used for detecting signals of magnetic resonances vis the transmission parameter *S* as a function of the frequency and the magnetic field (See reference [5, 6] for details). We observed multiple resonance modes over a wide range of microwave frequencies at a temperature of 100 K, as shown in Fig. 2. The frequency of the lowest resonance mode ($n = 0$) varied between 15 and 21 GHz, while the frequency of the higher order modes ($n = 1, 2, 3$) increased from 15 GHz to 40 GHz with decreasing the field strength. We found that the theoretical equation of the CSL phonon mode can be well fitted to experimental data by taking the field dependence of CSL period into consideration. Furthermore, a DM interaction constant of 2.6 K was estimated based the energy gap at zero magnetic field.

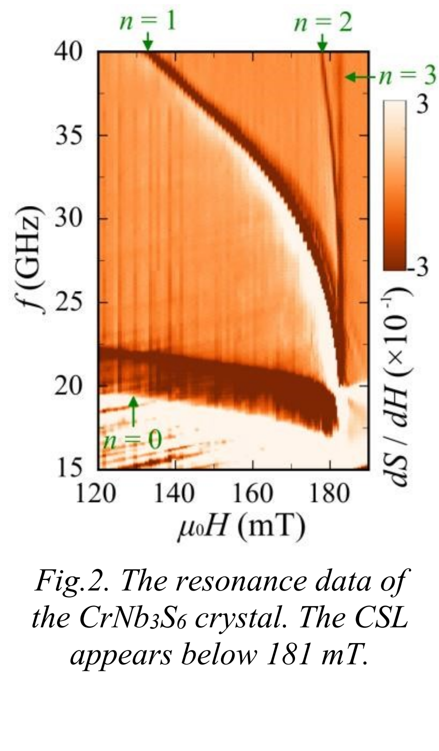

Fig.2. The resonance data of the $CrNb_3S_6$ crystal. The CSL appears below 181 mT.

References

[1] Y. Togawa *et al*., Phys. Rev. Lett. **108**, 107202 (2012).
[2] I. E. Dzyaloshinsky, Sov. Phys. JETP **19**, 960 (1964).
[3] J. Kishine and A.S. Ovchinnikov, Phys. Rev. B **79**, 220405(R) (2009).
[4] V.V. Kiselev and A.A. Raskovalov, J. Exp. Theor. Phys. **116**, 272 (2013).
[5] Y. Shimamoto *et al*., Appl. Phys. Lett. **115**, 242401 (2019).
[6] F.J. T. Goncalves *et al*., Appl. Phys. Lett. **116**, 012403 (2020).

Phase degree of freedom in multiple-Q topological spin textures

K. Shimizu[1], S. Okumura[2], Y. Kato[1], Y. Motome[1]

[1] *Department of Applied Physics, The University of Tokyo, Hongo, Bunkyo-ku, Tokyo, Japan*
[2] *The Institute for Solid State Physics, the University of Tokyo, Kashiwa, Japan*

Corresponding Author's Email: k.shimizu@aion.t.u-tokyo.ac.jp

Topological spin textures, such as skyrmion lattices (SkLs) and hedgehog lattices (HLs), have attracted a lot of interest due to the robustness protected by the topology and the intriguing transport and optical responses associated with the emergent electromagnetic field through the spin Berry phase mechanism [1,2]. Such spin textures are approximately represented by superpositions of multiple spin waves, and hence, called multiple-Q spin structures. Thus, not only the magnetic structures but also the topological properties are modulated by various parameters in the superpositions, e.g., the number, periods, amplitudes, and propagation directions of the constituent helices [3,4,5]. Among them, the phase degree of freedom of the superposed waves may play an important role in topological transitions between different multiple-Q spin structures (Fig. 1) [6,7], but the systematic investigation has not been performed thus far.

In this study, we theoretically investigate the evolution of the two-dimensional SkL composed of three spin waves (3Q-SkL) and the three-dimensional HL composed of four spin waves (4Q-HL) while changing the phases of the superposed waves [8]. For a systematic analysis of the phase degree of freedom, we construct a hyperspace representation of multiple-Q spin structures by introducing additional dimensions, where the phase degree of freedom in the original physical space can be regarded as a spatial translation in the hyperspace (Fig. 2). By using this framework, we elucidate the topological phase diagram for the 3Q-SkL while changing the sum of the phases of three waves, $\tilde{\varphi}$, and the uniform magnetization m (Fig. 3); the skyrmion number $N_{\rm sk}$ changes among -2, -1, 0, 1, and 2 in a different way depending on the type of the constituent waves. In the case of the 4Q-HL, we obtain richer phase diagrams where the density of topological objects called hedgehogs and antihedgehogs per magnetic unit cell changes in a wide range. Our results of the complete phase diagrams for the phase shift provide good references to discuss how the actual systems experience the magnetic and topological transitions in an applied magnetic field.

This research was supported by Grant-in-Aid for Scientific Research Grants (Nos. JP18K03447, JP19H05822, JP19H05825, and JP21J20812), JST CREST (No. JP-MJCR18T2), and the Chirality Research Center in Hiroshima University and JSPS Core-to-Core Program, Advanced Research Networks. K.S. was supported by the Program for Leading Graduate Schools (MERIT-WINGS). Parts of the numerical calculations were performed in the supercomputing systems in ISSP, the University of Tokyo.

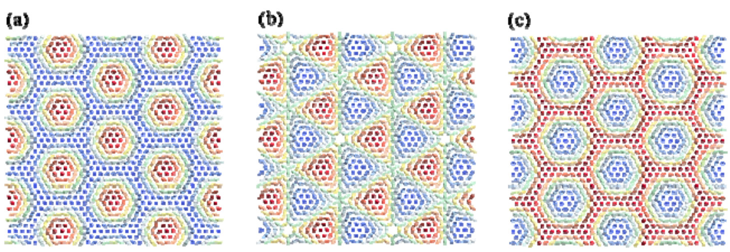

Fig.1 Variations of spin textures while changing the phase of the superpositions of three spin helices. (b) and (c) are obtained from (a) by the phase shift of $\pi/2$ and π, respectively. The skyrmion number changes from (a) N_{sk}=1 to (b) N_{sk}=0, and to (c) N_{sk}=-1.

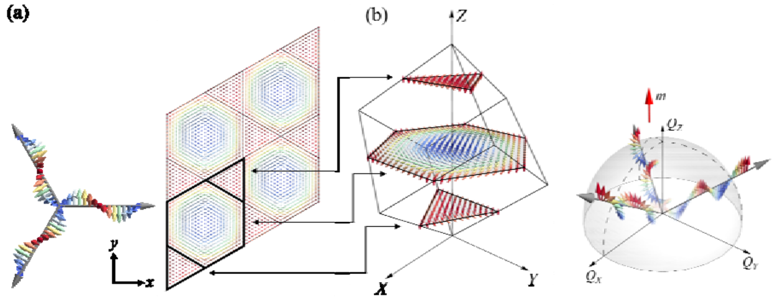

Fig.2 Hyperspace representation of the two-dimensional spin textures. (a) A 3Q-SkL composed of three spin helices. (b) The superposition of three helices in three-dimensional hyperspace. The SkL in (a) appears on a slice of the three-dimensional spin texture in (b).

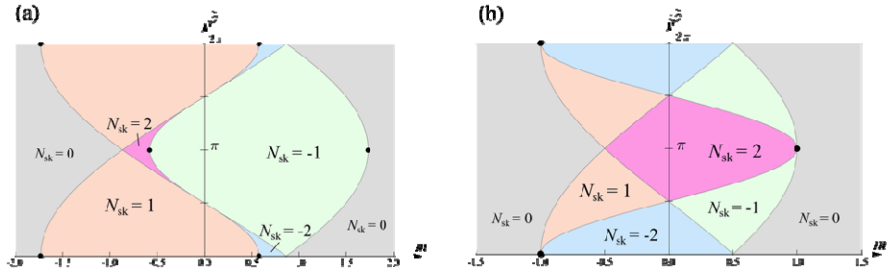

Fig.3 Topological phase diagrams determined by Nsk on the plane of m and $\tilde{\varphi}$ for the 3Q-SkLs represented by the superposition of (a) three spin helices and (b) three sinusoidal waves.

References

[1] G. E. Volovik, J. Phys. C 20, L87 (1987).
[2] N. Nagaosa and Y. Tokura, Nat. Nanotechnol. 8, 899 (2013).
[3] B. Binz, A. Vishwanath, and V. Aji, Phys. Rev. Lett. 96, 207202 (2006); B. Binz and A. Vishwanath, Phys. Rev. B 74, 214408 (2006).
[4] J. H. Park and J. H. Han, Phys. Rev. B 83, 184406 (2011).
[5] K. Shimizu, S. Okumura, Y. Kato, and Y. Motome, Phys. Rev. B 103, 054427 (2021); ibid, 103, 184421 (2021).
[6] T. Kurumaji et al., Science 365, 914 (2019).
[7] S. Hayami, T. Okubo, and Y. Motome, preprint (arXiv:2005.03168).
[8] K. Shimizu, S. Okumura, Y. Kato, and Y. Motome, in preparation.

Thin film growth of chiral magnet $YbNi_3Al_9$

H. Shishido[1,2,3], T. Ishiguri[1], T. Saimyoji[1], A. Okumura[1],
S. Nakamura[4], S. Ohara[4], and Y. Togawa[1]

[1] *Department of Physics and Electronics, Osaka Prefecture University, Sakai, Japan*
[2] *NanoSquare Research Institute, Osaka Prefecture University, Sakai, Japan*
[3] *The Center for Research & Innovation in Electronic Functional Materials, Osaka Prefecture University, Sakai, Japan*
[4] *Department of Physical Science and Engineering, Graduate School of Engineering, Nagoya Institute of Technology, Nagoya, Japan*

Corresponding Author's Email: shishido@pe.osakafu-u.ac.jp

$YbNi_3Al_9$ is a novel material in which the heavy-fermion state coexists with spin chirality, and becomes a chiral helimagnet below the transition temperature T_M=3.4 K [1-3]. It crystallizes in a trigonal structure with the space group of *R*32 (#155), which belongs to the Sohncke space group. Discrete magnetoresistance was reported in micrometer-sized samples, indicating a formation of the chiral spin soliton lattice (CSL) in $YbNi_3Al_9$ under magnetic fields perpendicular to the *c*-axis [4].

Establishing a method for thin film growth of chiral magnets is inevitable for utilizing chiral spin order for device applications. Moreover, carrier density control is feasible in thin films by applying a strong electric field. It may enable us to control material parameters such as T_m and the critical field H_c. Thus, thin film growth is an important first step toward the implementation of chiral magnetic device applications.

We grew $YbNi_3Al_9$ thin films on *c*-plane sapphire substrates by using molecular beam epitaxy [5]. They were grown under ultra-high vacuum while maintaining a deposition rate at a stoichiometric ratio among Yb, Ni, and Al. The resulting thin films contain epitaxial grains with the *c* axis parallel to the substrate surface. Figure 1 shows typical X-ray diffraction (XRD) pattern in the direction perpendicular to the film surface. The *hh*0 and 3*h*00 peaks, highlighted in color, appeared as the main peaks. Concomitantly, other small peaks corresponding to other orientation domains appeared. By combination with the grazing-incidence XRD results, we concluded that epitaxial grains oriented the [100] axis for the perpendicular to the film surface, while the [120] axis-oriented grain had no in-plane orientation. High orientation of the film was demonstrated by the rocking-curve measurements as shown by the inset of Fig. 1.

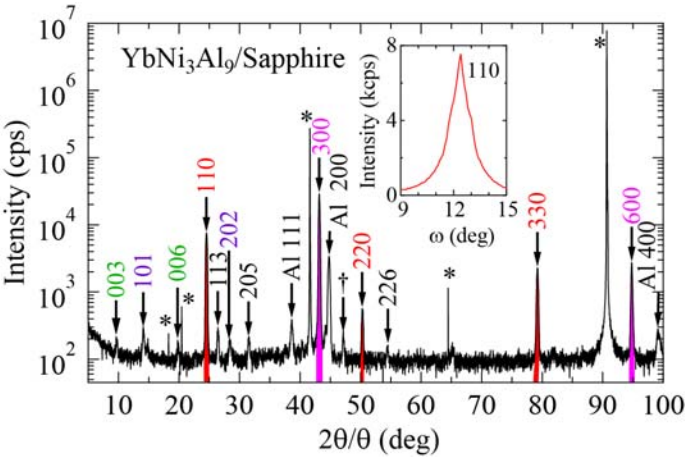

Fig.1 XRD pattern in the direction perpendicular to the film surface for $YbNi_3Al_9$ on the c-plane sapphire substrate. Substrate peaks are marked by asterisks. The unknown impurity peak is marked by a dagger. Rocking curves for 110 peaks are shown in the inset.

Figure 2(a) shows the temperature dependence of the electrical resistivity. (1) The temperature dependence of the resistivity has a maximum at ~40 K, and decreases with decreasing temperatures. It is a typical feature of a dense Kondo system. It also exhibits a kink as a signature of the chiral helimagnetic ordering at 3.6 K. These features are consistent with those previously observed in bulk samples. (2) We measured the temperature and field dependence of the resistivity for the field applied in the direction perpendicular to the c-axis to determine the magnetic phase diagram. A negative magnetoresistance was observed in thin films as same as in bulk samples, while it was largely suppressed. (3) We determined H_c from a finite change of the slope of the magnetoresistance. The magnetic phase diagram is shown in Fig.2(b). T_m exhibits no significant magnetic field dependence below 0.8 kOe. A crossover line between the paramagnetic (PM) phase and the forced ferromagnetic (FFM) state merges with the H_c line at ~0.8 kOe. The H_c line increases with decreasing the temperature, reaching 1.75 kOe at 2 K. The magnetic phase diagram well reproduces that for the bulk crystals, implying that the CSL phase arises under magnetic fields, even in thin films.

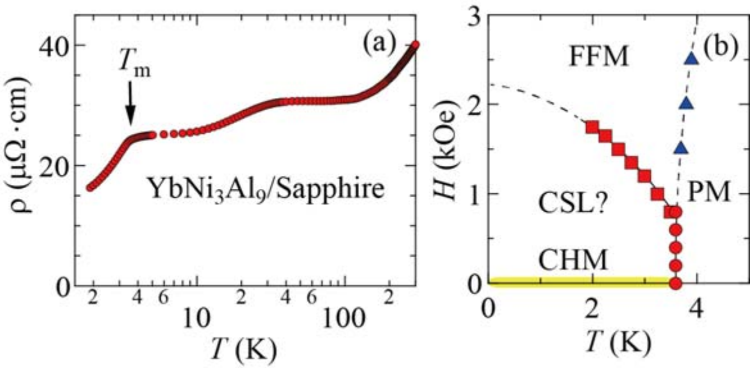

Fig.2 (a) Temperature dependence of the resistivity and (b) magnetic phase diagram for the field applied in the direction perpendicular to the c-axis.

This work was supported by Grants-in-Aid for Scientific Research (Nos. 19K03751, 17H02767, and 18K03539) and by an Innovative Areas "Quantum Liquid Crystals" Grant (KAKENHI Grant No. JP19H05826) from the Japan Society for the Promotion of Science.

References

[1] T. Yamashita, R. Miyazaki, Y. Aoki, and S. Ohara, *J. Phys. Soc. Jpn.* **81**, 034705 (2012).
[2] S. Ohara, S. Fukuta, K. Ohta, H. Kono, T. Yamashita, Y. Matsumoto, and J. Yamaura, *JPS Conf. Proc.* **3**, 017016 (2014).
[3] T. Matsumura, Y. Kita, K. Kubo, Y. Yoshikawa, S. Michimura, T. Inami, Y. Kousaka, K. Inoue, S. Ohara, J. Phys. Soc. Jpn, **86**, 124702 (2017).
[4] R. Aoki, Y. Togawa, and S. Ohara, *Phys. Rev. B* **97**, 214414 (2018).
[5] H. Shishido, A. Okumura, T. Saimyoji, S. Nakamura, S. Ohara, and Y. Togawa, *Appl. Phys. Lett.* **118**, 102402 (2021).

Sperimagnetic phase transitions in ferrimagnetic amorphous alloy GdFeCo

S.V. Solovyov[1], V.V. Yurlov[1], K.A. Zvezdin[1,2,3]

[1] *Moscow Institute of Physics and Technology, Moscow, Russia*
[2] *Prokhorov General Physics Institute, RAS, Moscow, Russia*
[3] *Russian Quantum Center, Moscow, Russia*

Corresponding Author's Email: solovyov.sv@mipt.ru

The progress in ultrafast magnetization reversal by femtosecond laser pulses has attracted attention to various types of magnetic materials which could be promising for magnetic recording applications. One of the first materials which has shown an ultrafast switching by laser pulses was "rare earth"-"transition metal" type (RE-TM) ferrimagnetic amorphous alloy GdFeCo [1], which magnetic properties can be widely tuned due to a variety of stoichiometric compositions. Like other amorphous compounds, these alloys are characterized by the absence of long-range order of atomic structure, which turns out into microscopic stochasticity of magnetic properties causing the sperimagnetic magnetic structure. Such ferrimagnetic alloys are perspective not only for ultrafast switching applications, but also for creating spintronic devices, which is caused by high resonant frequencies in comparison to resonant frequencies of transition metal films and high velocity of domain walls motion induced by spin-polarized current [2].

In our work we describe a body of amorphous RE-TM type ferrimagnet as a grid of N interacting particles of quite small volume V_0. We suggest that magnetic properties of particles inside their volume are uniform. Particles are composed from RE and TM ions with concentrations n_{RE} and n_{TM}, which depend on the stoichiometric coefficient z of the formula $Gd_z(FeCo)_{1-z}$. Exchange interactions in RE-TM type ferrimagnets obey the interaction hierarchy, which could be described as an inequality of exchange integrals of d- and f- sublattices: $J_{d\text{-}d} > J_{f\text{-}d} > J_{f\text{-}f}$. In our work we take into account only d-d and f-d exchange interactions, and the d-d exchange is ferrimagnetic, and the f-d exchange is antiferromagnetic, which in some circumstances leads to a presence of compensation point and some peculiarities of magnetic phase transitions [3]. One of the features of GdFeCo and other amorphous ferrimagnets of RE-TM type films is the presence of perpendicular magnetic anisotropy which can be described within the framework stochastic anisotropy model [4]. The system of interacting ferrimagnet particles can be described with the use of the Hamiltonian, which includes the d-d and f-d exchange Heisenberg-like interactions, stochastic uniaxial magnetic anisotropy for the f-sublattice, and the Zeeman interaction of f- and d-sublattices with the external magnetic field.

For the purpose of simplicity we consider a case, when the external magnetic field and the axes of magnetic anisotropy within the particles are align in parallel with the Oz axis, and the magnetic moments of f- and d-sublattices are oriented in same plane with the Oz axis. In this case we can describe magnetic states of every particle using only two polar angles θ_d and θ_f. Stochasticity of magnetic properties is described by random values of magnetic anisotropy constants for every particle. The description of thermal properties is done by the use of the Gibbs distribution function and the molecular field theory for d-sublattice. Because in this approach the magnetic moments of the d-sublattice are connected through the molecular field the Hamiltonian of the system can be presented as a sum of single-particle Hamiltonians, and the integral of distribution function becomes a product of integrals of only two variables θ_d and θ_f for every particle.

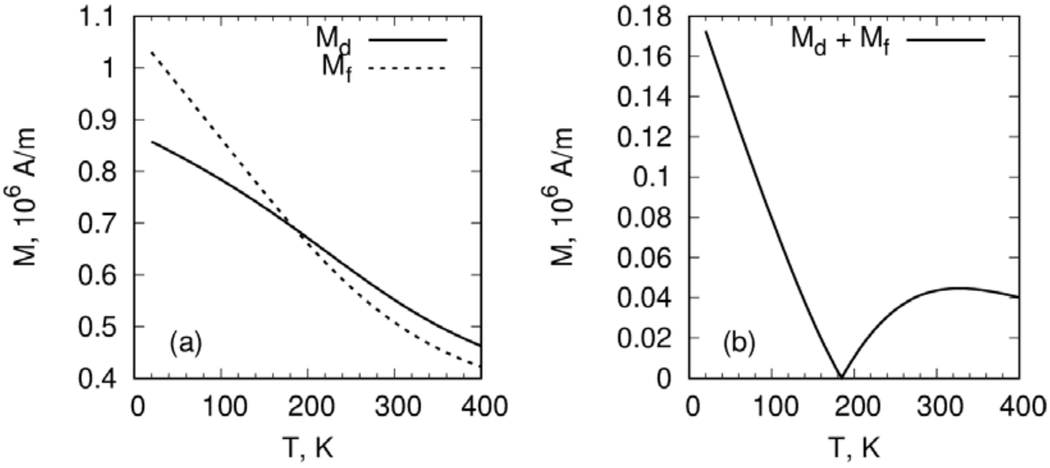

Fig. 1 (a) — Calculated magnetization dependencies on temperature for f- and d-sublattices in absence of external magnetic field; (b) — a dependence of the total magnetization on temperature, showing the presence of the compensation point.

The suggested model allows to describe the magnetic phases and phase transitions in amorphous ferrimagnet in external magnetic field for different temperatures and RE ions concentrations. For instance, for 70% of RE ions in $Gd_{0.7}(FeCo)_{0.3}$ alloy the suggested model shows the presence of compensation point, when the magnetizations of f- and d-sublattices becomes equal, which leads to vanishing of spontaneous magnetization as it is shown in Fig. 1. We present results of impact of sperimagnetic structure on critical temperatures and magnetic fields, which affects displacement of lines on phase diagrams.

Investigation of new magnetic phases and peculiarities of phase transitions in GdFeCo alloys, especially in the vicinity of the compensations point, are important for possible applications in magnetic recording and spintronics, and for development of theoretical and experimental understanding of these materials. The presented model are of interest for discovery of equilibrium and metastable states in amorphous ferrimagnets of RE-TM type.

This work is supported by the Russian Science Foundation (project 17-12-01333).

References

[1] C.D. Stanciu, F. Hansteen, A.V. Kimel, A. Kirilyuk, A. Tsukamoto, A. Itoh, and Th. Rasing, *Phys. Rev. Lett.* 99, 047601 (2007).
[2] V.V. Yurlov, K.A. Zvezdin, P.N. Skirdkov, A.K. Zvezdin, *Phys. Rev. B* 103, 134442 (2021).
[3] M.D. Davydova, K.A. Zvezdin, J. Becker, A.V. Kimel, and A.K. Zvezdin, *Phys. Rev. B* 100 (6), 064409 (2019).
[4] G.V. Sayko, S.N. Utochkin, A.K. Zvezdin, *JMMM* 113 (1-3), 194-200 (1992).

Antiferromagnets with random vacancies and substitutional spins on triangular lattice

F.D. Timkovskii, A.V. Syromyatnikov

Konstantinov Petersburg Nuclear Physics Institute of National Research Centre «Kurchatov Institute», Gatchina, Russia

Corresponding Author's Email: philippinho@yandex.ru

We discuss theoretically static and dynamical properties of XY and Heisenberg antiferromagnets on the triangular lattice with random vacancies and substitutional spins. It is shown that the distortion of 120^0 magnetic order produced by a single defect is described by electrostatic equations for a field of an electrically neutral complex of six charges located around the impurity. The first finite term in the multipole expansion of this field is the octupole moment which decays as $1/r^3$ with the distance r. The linearity of equations allows to describe analytically the distortion of the long-range magnetic order at a small concentration c of defects. We obtain analytically renormalization of the elastic neutron scattering cross section and the magnon spectrum $\varepsilon_{\mathbf{k}}$ in the leading order in c. We find that the scattering on impurities renormalizes weakly the bare spectrum $\varepsilon_{\mathbf{k}} \propto k$ at $k \gg \sqrt{c}$. However the renormalization is substantial of the long-wavelength magnon spectrum at $k \ll \sqrt{c}$: $\varepsilon_{\mathbf{k}} \propto \sqrt{c/\ln(1/k)}$ at $k \to 0$ and there is a parametrically large region in which magnons with not too small momenta are overdamped and localized. This strong modification of the long-wavelength spectrum leads to the stabilization of the slightly distorted magnetic long-range order at $T < T_N \sim S^2 J/\ln(1/c)$ and to the considerable change in the density of states and in the specific heat. The overdamped modes arise also in quasi-2D spin systems on a stacked triangular lattice.

Low-temperature transition in non-centrosymmetric CoGe: the influence of the quadrupole transition on the occurrence of an incommensurate phase

A.V. Tsvyashchenko[1,2], V.A. Sidorov[1,2], A.V. Nikolaev[3], Seung-Ho Baek[4], T. Klimczuk[5] and F. Ronning[6]

[1] *Vereshchagin Institute for High Pressure Physics, RAS, Moscow, Troitsk, Russia*
[2] *Lebedev Physical Institute, RAS, Moscow, Russia*
[3] *Skobeltsyn Institute of Nuclear Physics MSU, Moscow, Russia*
[3] *Changwon National University, Gyeongsangnam-do, Republic of Korea*
[4] *Faculty of Applied Physics and Mathematics, Gdansk University of Technology, Gdansk, Poland*
[5] *Los Alamos National Laboratory, MPA-CMMS, Los Alamos, New Mexico, USA*

Corresponding Author's Email: tsvyash@hppi.troitsk.ru

The B20 phases of MnGe, CoGe and RhGe are metastable requiring high pressure and temperature for their synthesis [1,2]. The CoGe is a semimetal and the magnetic susceptibility measurements showed that CoGe is a Pauli paramagnet [3]. Another characteristic feature of the band structure of CoGe is the Dirac cone with a flat band at the Γ point of the Brillouin zone near E_F [4].

The specific heat measurements on CoGe were published in two papers [2,5], earlier. But a weak peak of the specific heat between 13.4 K and 13.9 K was missed in these publications (See Fig.1). The NMR measurements also exhibit anomalous behavior around 13.5 K (See Fig.2).

We argue that the T = 13.7 K heat capacity anomaly found experimentally in CoGe can be attributed to a quadrupolar phase transition to a modulated (incommensurate) phase. The heat capacity peak and other anomalies of NMR measurements are caused by a (second order) transition which is soften because the Lifshitz condition is not fulfilled and the transformation to a commensurate phase is not possible.

A.V.T.and V.A.S. acknowledge the support of their experimental work Russian Science Foundation: (Grant No. 17-12-01050).

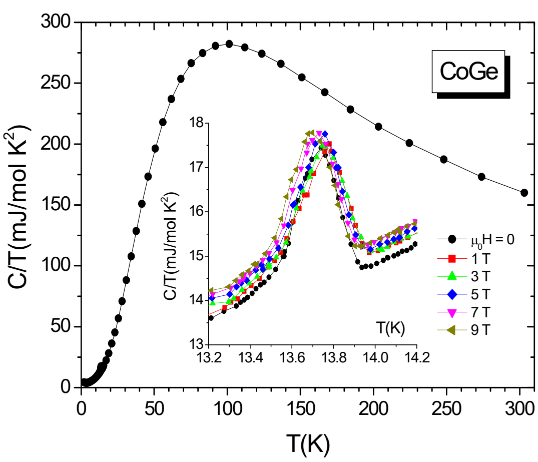

Fig.1

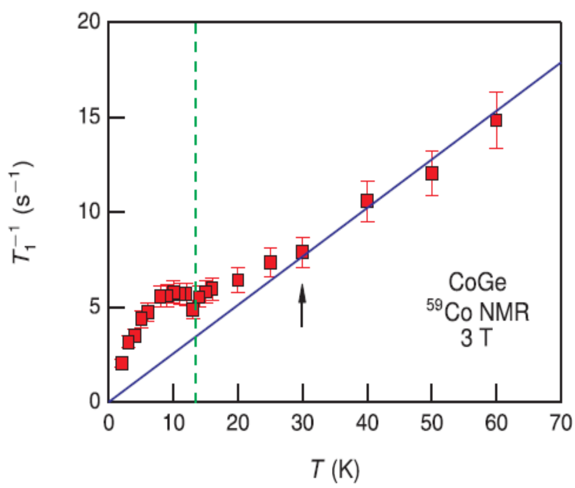

Fig.2

References

[1] V.I. Larchev, S.V. Popova, J. Less-Common Met. 87, 53 (1982).

[2] H. Takizawa, T. Sato. T. Endo, and M. Shimada, J. Solid State Chem. 73, 40 (1988).
[3] A.V. Tsvyashchenko, V.A. Sidorov, et al., Solid State Phenomena 190, 225 (2012).
[4] N. Kanazawa, Y. Onose, Y. Shiomi, S. Ishiwata, and Y. Tokura, Appl. Phys. Lett. 100, 093902 (2012).
[5] J.F. DiTusa, S.B. Zhang, K. Yamaura, Y. Xiong, et. al., Phys. Rev. B 90, 144404 (2014).

Phase competition in anisotropic frustrated antiferromagnets

O.I. Utesov[1,2,3], A.V. Syromyatnikov[1]

[1] *Konstantinov Petersburg Nuclear Physics Institute of National Research Centre «Kurchatov Institute», Gatchina, Russia*
[2] *St. Petersburg School of Physics, Mathematics, and Computer Science, HSE University, St. Petersburg, Russia*
[3] *St. Petersburg State University, St. Petersburg, Russia*

Corresponding Author's Email: utiosov@gmail.com

Multiferroics of spin-origin [1] attract significant attention now. The possibility to realize cross-control between magnetism and electricity in such compounds paves the way to many desirable applications. There are three main mechanisms of ferroelectricity of spin origin: exchange-striction mechanism, inverse Dzyaloshinskii-Moriya (DM) mechanism, and spin-dependent p-d hybridization mechanism [1]. Noncollinear helical spin ordering induced, e.g., by frustration is indispensable for the second and the third mechanisms. Moreover, in frustrated helimagnets interplay between small anisotropic interactions and magnetic field determine the plane where spins rotate and, thus, the electric polarization direction.

In the present report, we consider sequences of phase transitions in frustrated centrosymmetric antiferromagnets with biaxial anisotropy or dipolar forces. We suppose that the exchange interaction has only two incommensurate minima **k** and –**k**, so only single-modulated magnetic structures are allowed. Using the smallness of anisotropic interaction, we analytically derive expressions for the fields of phase transitions, which can be observed at low temperatures in the considered model.

First, we address small magnetic fields (much smaller than the saturation field) oriented along the easy axis. In regular anisotropic antiferromagnet one has conventional spin-flop phase transition [2] (see Fig. 1(a)), where collinear antiferromagnetic ordering (AF) is substituted by canted AF structure (CAF). In the helimagnet with small biaxial anisotropy or dipolar forces spiral plane flop takes place [3] (see Fig. 1(b)), where helicoid with spins rotating in the easy plane (YZ) "jumps" into conical XY structure. However, if the anisotropy is moderate, the collinear AF ordering can have lower energy at zero field, than the YZ one (see Ref. [4] for the details). In such a case, three scenarios of phase transition involving commensurate and incommensurate magnetic structures can be observed in our model, depending on its parameters. The scenario shown in Fig. 1(c) can be considered as the spin-flop with an intermediate helicoid phase. The two others ((d) and (e)) show the possibility to have a conical magnetic structure under magnetic field increase when starting from the collinear AF one. Importantly, the scenario shown in Fig. 1(e) was observed in Ref. [6] experimentally.

Second, we consider the high magnetic fields domain near the saturation field, where all spins are aligned along the field (SAT phase, see Fig. 2). In usual antiferromagnets, there is one simple transition from the CAF to SAT structure (Fig. 2(a)). We show (see Ref. [5] for the details), that if there is no competition with commensurate structures, then the conical XY phase is unstable towards the transition to the FAN phase at the field, lower than the saturation one. The reason for that instability is the anisotropy in the spiral plane, perpendicular to the external field. We derive an analytical expression for this field, where Ising-type phase transition restoring chiral symmetry takes place. So, in this case, the scenario shown in Fig, 2(b) can be observed. When there is a competition with commensurate spin ordering, scenarios which are shown in Fig. 2(c) and Fig. 2(d) can be observed. Importantly, the FAN phase always emerges before saturation.

We test our theory by comparing its predictions with the numerical results of Ref. [7], where the authors introduced the model with biaxial anisotropy and frustrated Heisenberg exchange in order to describe complicated $MnWO_4$ phase diagram. We find that our approach allows describing analytically all five magnetic field-induced phase transitions for the field along the easy axis (the sequence of phase transitions is the combination of the one shown in Fig. 1(c) at weak fields and the one shown in Fig. 2(c) at strong fields), and two transitions for the field along the middle axis, see Fig. 2(d). Moreover, corresponding critical fields are in good quantitative agreement with the obtained numerically in Ref. [7] values.

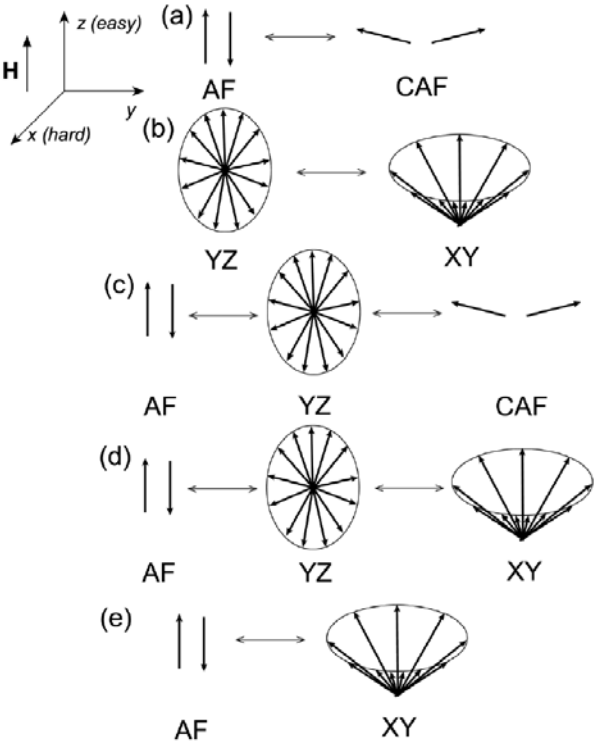

Fig.1 Sequences of phase transitions in frustrated antiferromagnet with biaxial anisotropy or dipolar forces at weak magnetic fields.

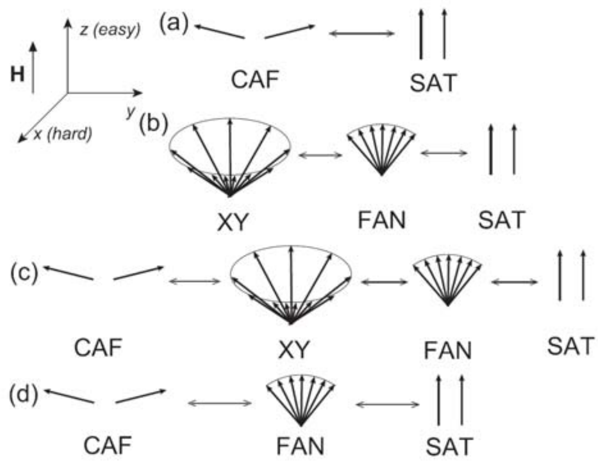

Fig.2 Sequences of phase transitions at strong magnetic fields near the saturation field.

The reported study was funded by RFBR according to the research project 18-02-00706.

References

[1] Y. Tokura, S. Seki, and N. Nagaosa, Rep. Prog. Phys. 77, 076501 (2014), and references therein.
[2] L. Neel, Ann. Phys. 11, 232 (1936).
[3] O.I. Utesov and A.V. Syromyatnikov, Phys. Rev. B 98, 184406 (2018).
[4] O.I. Utesov and A.V. Syromyatnikov, Phys. Rev. B 99, 054439 (2019).
[5] O.I. Utesov and A.V. Syromyatnikov, Jour. Mag. Mag. Mater. 527, 167732 (2021).
[6] J. Lass, et. al., Phys. Rev. B 101, 054415 (2020).
[7] M.V. Gvozdikova, T. Ziman, and M.E. Zhitomirsky, Phys. Rev. B 94, 020406(R) (2016).

PARTICIPANTS

NAME	PAGES
IVANOV Alexander	–
ISHITO Kyosuke	97
KA Mouhamadou Bamba	–
KATSUMOTO Hiroshi	98
KAZUKI Ohishi	–
KISHINE Junichiro	26
KOPLAK Oksana	81
KOUSAKA Yusuke	–
KRASNORUSSKY Vladimir	42
KUMAWAT Kishor Kumar	–
LALIENA Victor	58
LIKHOLETOVA Elena	–
LIN Shizeng	99
MAGNITSKAYA Maria	100
MALEEVA Ekaterina	–
MASELL Jan	57
MINEEV Vladimir	17
MOSKVIN Alexander	–
NEMYTOVA Olga	102
NIGMATULLINA Evgeniya	–
OKUMURA Shun	104
OSORIO Santiago Antonio	65
OVCHINNIKOV Alexander	29
OVSIANIKOV Alexander	–
PARDO Miguel	106
PAPPAS Catherine	21
PIKUL Md. Abu Jafar	108
PSHENAY-SEVERIN Dmitry	83
PSHENICHNAIA Angelina	–
PSHENICHNYI Kirill	–
PYATAKOV Alexander	77
SADOVNIKOV Alexander	109
SADYKOV Ravil	–
SALAMATIN Denis	39